



Microfacies, Carbon and Oxygen Isotopes of the
Late Archean Stromatolitic Carbonate Platform of
the Kaapvaal Craton, South Africa:
Implications for Changes in Paleo-environment

Dissertation
der Fakultät für Geowissenschaften
der Ludwig-Maximilians-Universität München

Vorgelegt von
Baiquan Xu

München, Juni 2011

Erstgutachter: Prof. Dr. Wladyslaw Altermann

Zweitgutachter: PD. Dr. Christoph Mayr

Tag der mündl. Prüfung : 14.12.2011

ACKNOWLEDGEMENTS

I am indebted to many people for their long-lasting support and encouragement which were invaluable for the successful completion of this thesis. Here, I would like to express my gratitude to all those people who gave me the possibility to complete this thesis and to a great number of good things have happened to me during the past years.

Firstly, I would like to take this opportunity to thank the organization who provided scientific and financial support to make this work possible. I am grateful to the China Scholarship Council (CSC) for financially supporting my doctoral research at Ludwig-Maximilians University München, between 2007 and 2011.

I am deeply indebted to my supervisor Prof. Dr. Wladyslaw Altermann for: the opportunity to work on the Ghaap Group carbonates in South Africa and the money to do so; the freedom to follow my scientific curiosity and allowing my interests to shape the direction of this research; innumerable discussions, stimulating suggestions and encouragement that helped me develop the ideas presented here and writing of this thesis; encouraging participation in other research projects including the field work in various Archean carbonate platforms; actively promoting my work to the geological community at large.

Thanks to Dr. Christoph Mayr for: the kind helps to finish all the geochemical measurements in Geo-Bio-Lab of LMU; the discussions and suggestions to develop my interpretation on the geochemical data.

Thanks to Dr. Michaela Frei for her kind helps to solve all the problems in my daily life in Germany.

This thesis is dedicated to the people of University of Pretoria and the farmers in Griqualand West, South Africa, especially to the family of Jan and Sybil Visagie, who showed me the importance of human dignity and facilitated the field trip.

I also extend my sincere thanks to various colleagues who work and study in the geological department of LMU. Special thanks to Prof. Dr. Robert Marschik, Prof. Dr. Anke Friedrich, Simon Kübler, Markus Hoffmann, Ramona Baran, Alexander Heyng, Markus Oehlerich, Franziska Häuser, Karin Hessinger and Dr. Ing. Amir Abolghasem. They helped me to confront all the difficulties of life in Munich and give me good suggestions and discussions on my research work.

Thanks to my friends Dai Jiqiang, Dong Lu, Gao Lu, Chen Zhao, Harry Baer and Ma Xiaoguang who gave me their help and time in listening to me and encouraged me to fulfil my studies here in Munich.

Finally, I would like to give my special thanks to Prof. Dr. Yang Fengjie, my parents and my wife Wang Lin whose patient and thoughtfulness enabled me to complete this work.

ABSTRACT

Precambrian stromatolites record the origin and occurrence of life. The interpretation and understanding about these ancient rocks are mostly focused on the studies of morphological expression of stromatolites, carbonate petrology and fossils investigation. It is important to use these approaches for the reconstruction of sedimentary facies and environmental conditions, and geochemical investigation in carbonate rocks, especially for the stable isotopes (C and O), can best record the valuable information about the evolution and characteristics of life and chemical composition of ancient seawater and atmosphere. This study is confined to late Archean carbonate rocks, associated with abundant stromatolites occurrences in the Ghaap Group, South Africa. Based on the microscopic observation of selected carbonate samples, C and O isotopic compositions of carbonate rocks have been examined for the sedimentary facies comparison and paleo-environmental reconstruction.

The well-preserved, abundant stromatolitic carbonates in the Griqualand West Basin of South Africa represent a wide range of depositional environments from subtidal to supratidal platform. Despite much work has been done in the Ghaap Group carbonate rocks (Beukes, 1987; Altermann and Siegfried, 1997; Altermann and Nelson, 1998; Sumner and Grotzinger, 2004; Sumner and Beukes, 2006; Schröder et al., 2006; Simonson et al., 2009; Schröder et al., 2009), stable isotopic studies, such as carbon and oxygen, are still scarce (Fischer et al., 2009; Frauenstein et al., 2009). The present study extends previous work by assembling geochemical and stratigraphic data for the entire Ghaap Group and focuses on the microfacies observation and stable isotopic (C and O) analyses of microbial community precipitations in carbonate environments. Sedimentary facies changes are documented both by field and microscopic observations of carbonate rocks, which are then, correlated to the stable isotopes data ($\delta^{13}\text{C}$ and $\delta^{18}\text{O}$ values). It offers a new type of carbon and oxygen isotope analysis on the carbonate rocks from Ghaap Plateau sub-basin.

The Ghaap Group in South Africa persisted for >100 myr from 2642 ± 3 Ma to at least 2516 ± 4 Ma and comprised tidal flat and shallow marine deposits followed by sub-tidal carbonates. The carbonates were deposited in a basin transgressing from southwest to the northeast for a distance of over 400 km, with abundant stromatolites. The transgression trend has changed the depositional conditions with time, including water depth, sediment influx and mixing with meteoric water as recognised in field observations of lateral and vertical facies changes and of altering stromatolite morphology, and from microfacies studies on thin sections.

In this study, carbonate samples were collected from the 3600-m deep Kathu borehole core, but at stratigraphic intervals, where intrusive rocks and tectonic structures disturbed the stratigraphic sequence; samples were taken from other boreholes including Lime Acres, Finsch, YSKOR GH6/7 and Hotazel cores, for comparison studies and environmental constrain. For each sample, two main analysis points were drilled into the dark matter (organic C-rich) and light matter (carbonate C-rich), corresponding to the thin section description. C and O isotopes were measured in the different (micro)facies, in order to establish whether they follow stratigraphic and depositional changes. The reported values of $\delta^{13}\text{C}$ for Ghaap Group carbonate rocks are consistently at the order of $-0.5 \pm 1\text{‰}$ while the $\delta^{18}\text{O}$ values range between -15‰ and -5‰ VPDB.

A $+0.5\text{‰}$ shift in the mean $\delta^{13}\text{C}$ values is presented in the carbonate samples from deep subtidal water conditions to intertidal water conditions. Supratidal carbonate displays a wide range of $\delta^{13}\text{C}$ values, which indicate heavier post-depositional alteration of interaction among different carbon reservoirs than the deeper water environments (intertidal to deep subtidal environment). Two stratigraphic profiles of Ghaap Group carbonate rocks are obtained for $\delta^{13}\text{C}$ and $\delta^{18}\text{O}$ values.

For the $\delta^{13}\text{C}$ values, stratigraphic profile shows a fluctuated carbon isotopic composition and slightly negative than Phanerozoic carbonate rocks. The $\delta^{13}\text{C}$ values display a continuously increasing trend upward (from about -0.9‰ to about

0‰) from the base to the top formations of Campbellrand Subgroup carbonate rocks, which is attributed to the increasing microbial activity and productivity in the Ghaap Group carbonate deposition. A large $\delta^{13}\text{C}$ values excursion (from about -7‰ to about -0‰) is observed in the transition from the siliciclastic and less carbonate deposits of Schmidtsdrif Subgroup to the abundant stromatolitic carbonate deposits of Campbellrand Subgroup. The strongly negative ^{13}C isotopic composition of carbonate rocks of the Schmidtsdrif Subgroup indicates that these carbonate rocks were deposited in relatively ^{13}C -depleted seawater. The ^{13}C -depleted seawater was presumably caused by extensively earlier volcanic and tectonic activities, which finally changed the composition of seawater more depleted in ^{13}C than the modern seawater.

Comparing to the Phanerozoic oxygen composition (-6‰ to 0‰), our results show low $\delta^{18}\text{O}$ values (from about -15‰ to about -6‰). This could be caused by elevated temperature or post-depositional equilibration with meteoric and/or diagenetic fluids. Cross-plot of $\delta^{18}\text{O}$ and $\delta^{13}\text{C}$ values shows lack of co-variance and is characterized by a wide spread of $\delta^{18}\text{O}$ values, combined with a narrow range of $\delta^{13}\text{C}$ values. The observed $\delta^{18}\text{O}$ values (\sim -10‰) in the Campbellrand Subgroup are in the range of previously reported Neoproterozoic values and therefore reflect the primary (or near primary) isotope signature of these carbonate rocks. Alternatively, the oxygen isotope values (lower than -10‰ both in the basal Schmidtsdrif Subgroup and the upper Campbellrand Subgroup) are thought to be influenced by elevated deep burial temperature and isotopic exchange with diagenetic fluids in the course of post-depositional alteration. Further studies are needed to disentangle these potential effects.

LIST OF FIGURES

Figure 1.1: Geological map of the three Archean basins on the Kaapvaal Craton of southern African.	6
Figure 1.2: The geological map of the Griqualand West Basin of the Transvaal Supergroup, and the location of the Kathu borehole northwest of the Maremane Dome.	8
Figure 2.1: Interbasinal comparison of formations of the Ghaap and Chuniespoort (Transvaal sub-basin) Groups.	13
Figure 2.2: View of Vryburg quartzite at Westerberg.	16
Figure 4.1: The photographs of Group A show examples of the open space structure stromatolites.	38
Figure 4.2: The photographs of Group B show examples of the columnar stromatolites.	39
Figure 4.3: The photographs of Group C show examples of the contorted, finely laminated microbial mats.	39
Figure 4.4: Open space structure stromatolites in the intertidal to supratidal microfacies assemblage.	41
Figure 4.5: Columnar stromatolites and inter-columnar space, formed in the shallow subtidal to intertidal microfacies assemblage.	44
Figure 4.6: Contorted, fine microbial mats of the deep subtidal microfacies assemblage.	48

Figure 5.1: Selected environmental factors and their influence on carbonate $\delta^{13}\text{C}$ values.	54
Figure 5.2: Stratigraphic profiles of carbonate $\delta^{13}\text{C}_{\text{carb}}$ and $\delta^{13}\text{C}_{\text{org}}$ values through the Ghaap Group from the Kathu borehole, South Africa.	57
Figure 5.3: Selected environmental factors and their influence on carbonate $\delta^{18}\text{O}$ values.	58
Figure 5.4: Stratigraphic profile of carbonate $\delta^{18}\text{O}$ values through the Ghaap Group from the Kathu borehole, South Africa.	60
Figure 6.1: The photographs of open space structure stromatolites in thin sections.	70
Figure 6.2: The photographs of columnar stromatolites in thin sections.	72
Figure 6.3: The photographs of contorted, finely laminated microbial mats in thin sections.	74
Figure 6.4: Ranges of $\delta^{13}\text{C}$ values for the three lithofacies studies.	77
Figure 6.5: Crossplot of $\delta^{13}\text{C}$ and $\delta^{18}\text{O}$ values for the three lithofacies studies.	78
Figure 6.6: Crossplot of $\delta^{13}\text{C}$ and $\delta^{18}\text{O}$ values for carbonate rocks of the Ghaap Group.	80
Figure 6.7: Secular trends of $\delta^{18}\text{O}$ values in sedimentary carbonate rocks.	86

Figure 6.8: Histograms of compiled carbonate $\delta^{18}\text{O}$ values for different geological age group.

87

LIST OF TABLES

Table 2.1: Stratigraphic subdivision of the Schmidtsdrif and Campbellrand Subgroups in the Kathu borehole.	17
Table 3.1: List of samples for isotopic analyses in this study.	30
Table 3.2: List of the samples from the Kathu borehole chosen according to the observation of three morphological stromatolite facies realms.	31
Table 6.1: $\delta^{13}\text{C}$ and $\delta^{18}\text{O}$ values of the open space structures dominated carbonate rocks.	70
Table 6.2: $\delta^{13}\text{C}$ and $\delta^{18}\text{O}$ values in the columnar stromatolite dominated carbonate rocks.	71
Table 6.3: $\delta^{13}\text{C}$ and $\delta^{18}\text{O}$ values in the finely laminated microbial mats dominated carbonate rocks.	74

LIST OF CONTENTS

1. Introduction	1
1.1 Previous Work	4
1.2 Methods	7
1.3 Aim and Scope	10
2. Stratigraphy	11
2.1 Geological Background	12
2.2 Stratigraphy	14
2.2.1 Basal Schmidtsdrif Subgroup siliciclastic sediments	14
2.2.2 Campbellrand Subgroup carbonate sediments	17
2.2.3 Asbestos Hills Subgroup Iron Formations	22
3. Microfacies, Isotopic Methodology and Sample Selection	23
3.1 Microfacies of Carbonate Rocks	24
3.2 Isotopes (C and O) of Carbonate Rocks	25
3.2.1 Carbon isotopes	26
3.2.2 Oxygen isotopes	28
3.3 Sample Selection and Preparation of Carbonate Rocks	29
4. Microfacies of Carbonate Rocks in the Ghaap Group	35
4.1 Microbialite Morphology	36
4.1.1 Intertidal to supratidal microfacies assemblage ----Open space structure-dominated	39

4.1.2 Shallow subtidal to intertidal microfacies assemblage	
---Columnar stromatolites-dominated	43
4.1.3 Deep subtidal microfacies assemblage	
---Finely laminated microbial mat-dominated	46
5. Stratigraphic Variations of Carbon and Oxygen	
Isotopes in the Ghaap Group Carbonates	51
5.1 Carbon Isotopes	53
5.1.1 Carbon isotopes in the general geological processes	53
5.1.2 Carbon isotopes in the Ghaap Group carbonate rocks	56
5.2 Oxygen Isotopes	57
5.2.1 Oxygen isotopes in the sedimentary processes	57
5.2.2 Oxygen isotopes in the Ghaap Group carbonate rocks	59
5.3 Carbon and Oxygen Isotopic Variations in the Ghaap	
Group Carbonates	61
5.4 Stratigraphic Variation of Carbonate C and O	
Isotopes in the Ghaap Group Carbonate Rocks	62
6. Relationship between Microfacies Observation	
and Isotopic Analyses	67
6.1 Carbon and Oxygen Isotopes Variation in	
Campbellrand Subgroup Carbonate Rocks	69
6.1.1 Intertidal to supratidal carbonates dominated by open	
space structures	69
6.1.2 Shallow subtidal to intertidal carbonates dominated by	
columnar stromatolites	71

6.1.3 Deep subtidal carbonates dominated by finely laminated microbial mats	73
6.2 Carbon Isotopes and Water Depth	75
6.2.1 Carbon isotopes of microbialite types	75
6.2.2 Interpretation of carbonate isotope variations	78
6.3 Carbon and Oxygen Isotopes and Sedimentary Facies	79
6.4 Discussion	82
6.4.1 Isotopes (C and O) and water depth	82
6.4.2 Isotopes (C and O) and sedimentary facies	83
6.4.3 Late Archean environment and carbonate chemistry	84
7. Conclusions	91
8. References	96
Appendix	113

INTRODUCTION

1 Introduction

The rocks of Southern Africa preserve over 3600 million years of Earth history (Johnson et al., 2006) and supply an enormous mineral wealth to the entire world. The late Archean to earliest Paleoproterozoic Ghaap Group, which is the subject of the present thesis, is a thick succession of platform carbonates, rich in microbial components and covered by iron formations. The lower Ghaap Group is one of the earliest well-preserved major carbonate platforms in Earth history (Beukes, 1987). Successive stromatolitic carbonate platforms were developed in Griqualand West basin of South Africa between approximately 2640 Ma and 2516 Ma (Eriksson and Altermann, 1998). These carbonate rocks record significant environmental, geochemical and biological changes and provide valuable information for the studies of ancient atmosphere and ocean.

Abundant earliest life evidence is preserved in these marine carbonates (Altermann and Schopf, 1995; Altermann, 2008). The primary mineralogy of Archean and Proterozoic carbonate rocks reflects the paleo-bio-ecology and carbonate saturation state of seawater (Veizer et al., 1992a; Sumner and Grotzinger, 2004; Polteau et al., 2006; Fischer et al., 2009) and the morphology of Archean stromatolites records the energetic conditions of the environment (Klein et al., 1987; Altermann and Siegfried, 1997; Kazmierczak and Altermann, 2002; Altermann, 2008). The geochemistry supplies evidence to the once existed equilibriums among biology, sea floor hydrothermal activity, carbonate precipitation and weathering of old crust (e.g. Veizer and Compston, 1976; Garde, 1979; Veizer et al., 1990), and stable isotope elements including carbon and oxygen, can be used primarily to define depositional or diagenetic environments (e.g. Kaufman and Knoll, 1995; Des Marais, 2001; Fischer et al., 2009). Research on the Neoproterozoic carbonate rocks of the Ghaap Group, is helpful for the reconstruction of sedimentary environments and the interaction between ancient atmosphere and ocean.

Carbonate precipitation is involved in an extensive interaction among biological, chemical and physical processes of the oceans. Because oxygen is reactive and easily forms many oxides with other elements; the content of free oxygen can directly

influence various surficial geochemical processes of weathering, ion transportation in water, isotopic exchanges between atmosphere and ocean. The Archean Earth is thought to contain less free oxygen and more CO₂ than the modern Earth (Holland, 1984; Kasting, 2001; Ono et al., 2003; Bekker et al., 2004; Ohmoto et al., 2006; Ono et al., 2006). Cyanobacteria are the only evident life, which conducted photosynthesis and produced free oxygen in Archean time. Thus, the marine biogenic carbonate preservation during the late Archean would be significantly different from later periods (Proterozoic and Phanerozoic) because the oxidation state of surface ocean was changing (Grotzinger and Kasting, 1993; Grotzinger and Knoll, 1999) by the progressively increases of O₂ accumulation in ocean water (Voegelin et al., 2010; Kendall et al., 2010).

Three main questions are involved in the studies of the late Archean carbonate rocks:

(1) Which chemical and biological processes acted during the late Archean carbonate deposition?

(2) How are these various processes recorded in the well-preserved Ghaap Group carbonate successions?

(3) How do they differ from later and modern processes?

The Transvaal epeiric sea covered an area of in excess of 600 000 km² (Beukes, 1987). The late Archean to Paleoproterozoic Transvaal Supergroup, of which the Ghaap Group, constitutes the lower part, in Griqualand West, was developed within three structural basins on the Kaapvaal Craton of southern Africa: the Transvaal and Griqualand West Basins in South Africa and the Kanye Basin in Botswana (Figure 1.1) (Johnson et al., 2006). The Griqualand West basin comprises two stromatolitic carbonate successions which are located in the Ghaap Plateau sub-basin, in the north of the Griquatown fault, and in the Prieska sub-basin, in the south of the Griquatown fault.

Based on the depositional facies studies of the paleo-environment, of stromatolite morphology (Beukes, 1987; Altermann and Siegfried, 1997; Eriksson and Altermann, 1998), and of interbedded volcanic rocks and their available radiometric age data (Walraven and Martini, 1995; Altermann, 1996; Altermann and Nelson, 1998), the Ghaap Group preserved in the Griqualand West Basin of South Africa is subdivided into two subgroups and several formations among these two subgroups. The lower Schmidtsdrif Subgroup at the base of the Ghaap Group, consists of three formations, which are the basal Vryburg Formation, the middle Boomplaas Formation and the overlying Lokammona Formation. The conformably following Campbellrand Subgroup comprises seven formations of the Monteville, Reivilo, Fairfield, Klipfontein, Papkuil, Klippan, Kogelbeen and Gamohaam Formations, from the bottom to the top, all displaying abundant stromatolites.

Carbonate deposition started during the lowermost Vryburg Formation of underlying, mainly siliciclastic Schmidtsdrif Subgroup and ended at the uppermost Gamohaam Formation of the overlying Campbellrand Subgroup. The depositional facies of these carbonate rocks represent a wide range of depositional environments from deep subtidal to supratidal platform. These rocks had persisted for at least 100 million years, from 2642 ± 3 Ma (Walraven and Martini, 1995) to 2516 ± 4 Ma (Altermann and Nelson, 1998) and provide a research opportunity for the evolution of early microbial life and the mechanisms of Archean carbonate deposition.

1.1 Previous Work

The Archean – Proterozoic boundary is one of the most important markers in geological history, probably subsequent to the large-scale oxidation of the ocean-atmosphere system (Shaw, 2008). The timing of the transition from a widely anoxic to oxic world is highly controversial (e.g. Holland, 1984; Holland and Beukes, 1990; Kasting, 2001; Ono et al., 2003; Bekker et al., 2004; Kasting and Howard, 2006; Ohmoto et al., 2006; Ono et al., 2006; Godfrey and Falkowski, 2009; Knoll and Beukes, 2009; Simonson et al., 2009). The increasing O₂ accumulation in both atmosphere and surface ocean changed the redox state of atmosphere and ocean

which probably consumed the organic carbon in carbonate rocks, and finally changed the isotopic composition of seawater and carbonate rocks.

The earliest studies of the Precambrian carbonate and Banded Iron Formation successions in South Africa can be traced back to 1896, and mainly concentrated on the mineral exploration (Atherstone, 1896; Brown, 1896; Wilson, 1896). In the later studies, many geologists become more and more interested in the sedimentary rocks (Hatch, 1904; Rogers, 1933) and in the sedimentary structures in the carbonates (Young, 1928, 1934; Sharpe, 1949; Winter, 1963). Young (1933) initially described the stromatolites preserved in carbonate rocks and pointed out the similarities between the different carbonate sub-basins of South Africa.

Detailed studies on both modern and ancient carbonate depositional systems have been developed since the 1970's by Visser and Grobler (1972) in the Cape Province, and by Truswell and Eriksson (1972, 1975), Button (1973) and Eriksson (1977) in the Transvaal Province. These publications presented the first intensive stratigraphic research and established the regional stratigraphy and interpretation of depositional environments (Eriksson, 1972; Button, 1973; Eriksson et al., 1975, 1976; Beukes, 1977, 1980).

Various discussions on the basin geometry and depositional environments of the Neoproterozoic to Paleoproterozoic carbonate successions in South Africa followed after the initial work by Beukes (1977; 1987). The Transvaal Supergroup, which was deposited also within the Griqualand West Basin, shows a several thousand meters thick pile of strata (Eriksson et al., 2006) and has been extensively deformed along the basin margins, during several events of folding, with stacking thrust packages between >2500 Ma and 1100 Ma (Altermann and Hålbich, 1990, 1991; Eriksson et al., 2006). Towards basin interior, the rocks are relatively undeformed and underwent low to very low grade metamorphism which is reflected by the illite crystallinity (Altermann et al., 1992; Altermann, 1997).

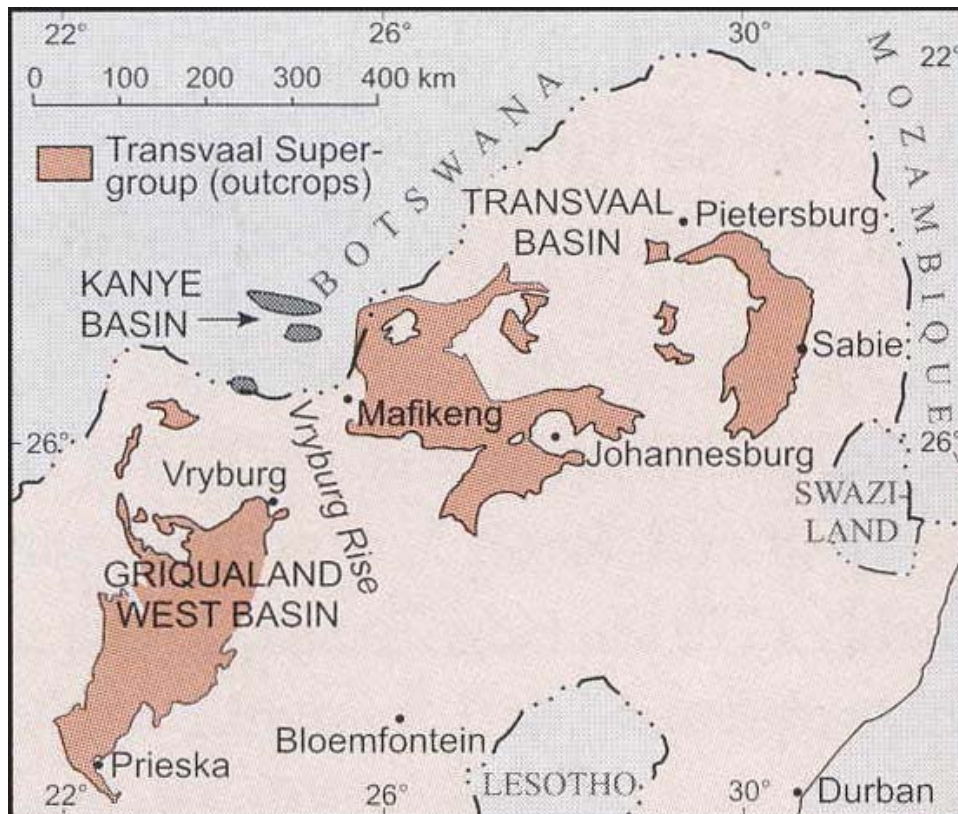


Figure 1.1 Geological map of the three Archean sub-basins on the Kaapvaal Craton of southern African. (Johnson et al., 2006).

Truswell and Eriksson (1973) firstly proposed a tidal flat model for the entire Transvaal carbonates, which is characterized by giant domal subtidal stromatolites. Clendenin (1989) developed a model of three broad facies belts in Kaapvaal Craton: distal shallow basin, subtidal periplatform and peritidal flats. This model also suggested five episodes of transgression and regression under the influence of syndepositional extensional tectonics, caused largely by thermal subsidence.

Altermann and Herbig (1991) suggested a peritidal origin for the laminated “rhythmites” of the Prieska facies, which were previously interpreted by Beukes (1987) as basinal. The detailed drill core studies of the Kathu borehole, Ghaap Plateau facies, by Altermann and Siegfried (1997) suggested that the depositional conditions have been of shelf to subtidal character during Schmidtsdrif Subgroup. Subsequent to the deposition of Schmidtsdrif Subgroup, a shallowing-up conditions of tidal-flats prevailed and were characterized by several transgression-regression episodes.

Paleo-environmental studies (Klein and Beukes, 1989; Beukes et al., 1990; Altermann and Siegfried, 1997; Altermann and Nelson, 1998; Eriksson and Altermann, 1998) imply that widespread microbial communities involved in carbonate precipitation were developed on a tectonically stable Kaapvaal craton (Altermann and Nelson, 1996).

Stable isotope studies became more frequent after the initial work by Beukes et al. (1990) and Veizer et al. (1992a), which recorded the “normal marine” carbonate $\delta^{13}\text{C}$ signatures in Campbellrand Subgroup carbonates. Shields and Veizer (2002) reported ubiquitous samples with $\delta^{13}\text{C}$ values of around 0‰ (PDB) in Precambrian marine carbonate rocks. The concepts of isotope stratigraphy become more and more popular in geological studies of the Campbellrand Subgroup (Schröder et al., 2006; Wille et al., 2007; Frauenstein et al., 2009; Godfrey and Falkowski, 2009; Kendall et al., 2010; Voegelin et al., 2010). Other studies on stable isotopes mainly concentrate on the mechanisms of carbonate precipitation, and conditions and evolution of the Precambrian atmosphere and seawater.

1.2 Methods

This thesis extends previous work by adding new and assembling previously published geochemical and stratigraphic data for the entire Campbellrand Subgroup and Schmidtsdrif Subgroup and focuses on the microfacies observation and stable isotopic (C and O) analyses of precipitates of microbial communities in carbonate environments. Temporal facies changes are documented by field and microscopic observations, which are correlated to the isotopic indicators of changes in geochemical cycles in ocean and atmosphere.

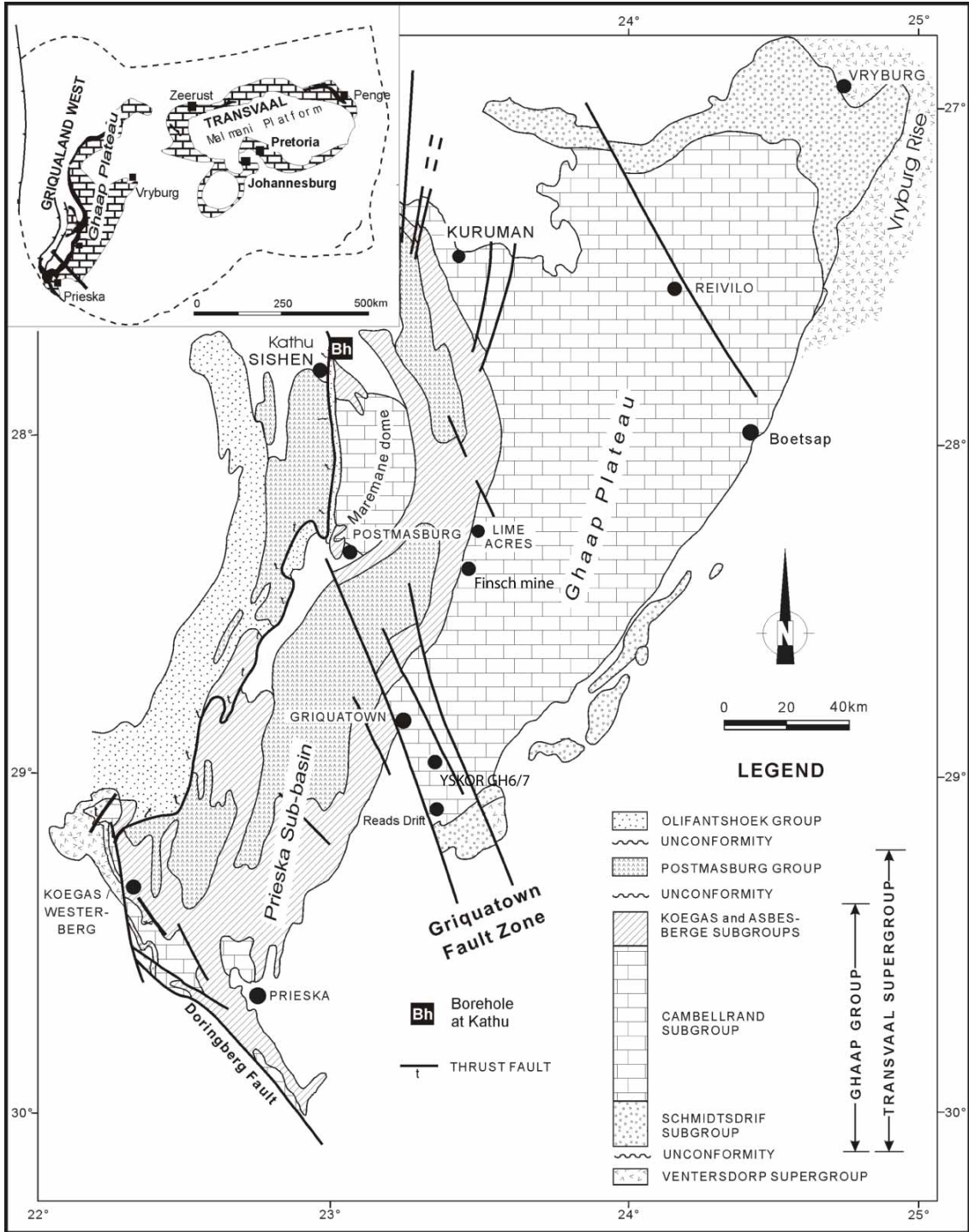


Figure 1.2 The geological map of the Griqualand West Basin of the Transvaal Supergroup, and the location of the Kathu borehole northwest of the Maremane Dome.

Most of the newly described carbonate rocks were samples from the 3600-m deep Kathu borehole core, but at stratigraphic intervals, where intrusive rocks and tectonic structures disturbed the stratigraphic sequence; samples were taken from other

boreholes. The Kathu borehole is located on the farm SACHA 468, west of Kathu village (Figure 1.2). The borehole was drilled in 1988 and it provides a unique and continuous section through the poorly exposed Schmidtsdrif and Campbellrand Subgroups. Ghaap Group rocks were first penetrated at 325.4 m from the surface, being covered by the Permo-Carboniferous Dwyka Formation (Karoo) and Tertiary Kalahari Group deposits (Altermann and Siegfried, 1997). Supplementary carbonate samples were collected from Lime Acres, Finsch Diamond Mine, YSKOR GH6/7 borehole and Hotazel cores, for comparison studies and environmental constrain. Radiometric constraints of the Ghaap Group define a chronostratigraphic framework for the carbonate successions of Schmidtsdrif and Campbellrand Subgroups (Walraven and Martini, 1995; Altermann and Siegfried, 1997; Altermann and Nelson, 1998).

All the samples were prepared as 5×5 cm and 2.5×5 cm petrographic thin sections for the detailed petrographic description, including morphology of stromatolites, petrology of sediments between laminations, shape and size of stromatolitic columns and diagenetic overprints. The samples usually display some sort of lamination of more or less strongly differing dark and pale laminae. For each sample, two main analysis points were drilled into the dark matter laminae (organic-rich) and light matter laminae (carbonate-rich) of each sample, corresponding to the thin section description. Samples were drilled with a diamond coated micro-drill for 0.5 mg and 5 mg respectively for $\delta^{13}\text{C}_{\text{carb}}$ and $\delta^{13}\text{C}_{\text{org}}$, and weighed into septum vials. Standard stable isotopic techniques of $\delta^{13}\text{C}_{\text{org}}$ (‰, VPDB), $\delta^{13}\text{C}_{\text{carb}}$ (‰, VPDB) and $\delta^{18}\text{O}$ (‰, VPDB) were used in the laboratory of GeoBio-Center in LMU München. The values are reported in the conventional delta notation:

$$\delta^{13}\text{C}_{\text{sample}} = \left\{ \left[\frac{(^{13}\text{C}/^{12}\text{C})_{\text{sample}}}{(^{13}\text{C}/^{12}\text{C})_{\text{reference}}} \right] - 1 \right\} \times 10^3 \text{ and}$$

$$\delta^{18}\text{O}_{\text{sample}} = \left\{ \left[\frac{(^{18}\text{O}/^{16}\text{O})_{\text{sample}}}{(^{18}\text{O}/^{16}\text{O})_{\text{reference}}} \right] - 1 \right\} \times 10^3$$

with respect to the Vienna Pee Dee Belemnite (VPDB). The $\delta^{13}\text{C}_{\text{org}}$, $\delta^{13}\text{C}_{\text{carb}}$ and $\delta^{18}\text{O}$ system was calibrated with NBS18, NBS19 and a lab-internal carbonate standard. The reproducibility of the method was $\pm 0.1\%$. The $\delta^{13}\text{C}_{\text{org}}$ system was calibrated with NBS18, NBS19 and a lab-internal carbonate standard and the reproducibility of the method was $\pm 0.1\%$.

1.3 Aim and Scope

Unweathered, fresh rock, drill core carbonate samples were selected from the entire stratigraphic succession of the Ghaap Group in South Africa, as representative samples for the major formations and facies described (Altermann and Siegfried, 1997; Altermann and Nelson, 1998). It is expected within this thesis, to contribute to the understanding of the relationships between the stable isotopic signatures and macro- to microscopic bio-sedimentary lamination morphologies, reflecting the depositional conditions of these Neoproterozoic carbonate rocks, and further, to elucidate the evolution of the early biosphere, atmosphere and oceans.

The first step of this study is to document the changes in carbonate microfacies which were interpreted from macro- and microscopic observation. By combining thin section descriptions, previous microfacies studies and stromatolite morphologies, a possible depositional depth and environmental variation of different microbial mats and stromatolites was proposed for the main three distinguished morphological types of stromatolitic lamination, which are intertidal to supratidal fenestral stromatolites, shallow subtidal to intertidal columnar stromatolites and deep subtidal finely laminated microbial mats. Then, the microscopic observation was correlated to the isotopic variations measured in the entire carbonate rocks succession of the Ghaap Group.

Finally, stratigraphic profiles of carbonate $\delta^{13}\text{C}_{\text{carb}}$, $\delta^{13}\text{C}_{\text{org}}$ and $\delta^{18}\text{O}$ were obtained through the entire Ghaap Group in the Kathu borehole of South Africa. Combining the microfacies observation with the isotopic analysis offers a new insight to the paleo-environmental settings of the Ghaap Group sedimentary deposits.

STRATIGRAPHY

2. Stratigraphy

2.1 Geological Background

The Ghaap Group in South Africa is the basal group and an important part of the Transvaal Supergroup, for the abundance of microbial carbonate deposits. It comprises of a lower, mixed siliciclastic-chemical sedimentary rock unit (Schmidtsdrif Subgroup), overlain by shallow marine to tidal flat carbonates (Campbellrand Subgroup) and further upward, by shelf-deposited iron formations (BIFs of the Asbestos Hills Subgroup). The Ghaap Group preserves a continuous facies transition from a transgressional conglomerate deposited on the underlying Ventersdorp Subgroup, to an intratidal to shallow shelf, to deep shelf depositional environments (Beukes, 1987; Altermann and Herbig, 1991; Altermann and Nelson, 1998; Knoll and Beukes, 2009). The sedimentary rocks were deposited in a basin transgressing from southwest to the northeast for a distance of over 400 km (Figure 1.2) (Altermann and Wotherspoon, 1995; Altermann and Siegfried, 1997). They represent one of the oldest recorded and well-preserved carbonate platforms on Earth, containing abundant stromatolites in sedimentary facies that range from deep subtidal to supratidal (Altermann and Wotherspoon, 1995; Sumner and Beukes, 2006; Knoll and Beukes, 2009).

The Kathu borehole in the Northern Cape Province (Figure 1.2) provides a continuous stratigraphic column of the Ghaap Plateau carbonate succession. The drilling depth of Kathu borehole is 3672.05 m from the surface. It is firstly reached the Ghaap Group rocks at the depth of 325.4 m in the drill core. The Ghaap Group, above that depth, is covered by the Permo-Carboniferous Dwyka Formation (Karoo) and Tertiary Kalahari Group deposits (Altermann and Siegfried, 1997). Thus, a continuous section of c. 3100 m of Ghaap Group sedimentary rocks (excluding an intrusive dyke of c. 250 m thickness, comp. Table 1), is recorded in the core of this drill hole. This was surprising at the time of the drilling, as a total thickness of only c. 2000 m was assumed for the Ghaap Group rocks (comp. Altermann and Siegfried, 1997). The base of the Transvaal Supergroup was however not reached in the drill core and also, the uppermost few tens of metres of the Campbellrand Subgroup (Gamohaan

Formation) are missing in the record due to the Permo-Carboniferous erosional surface.

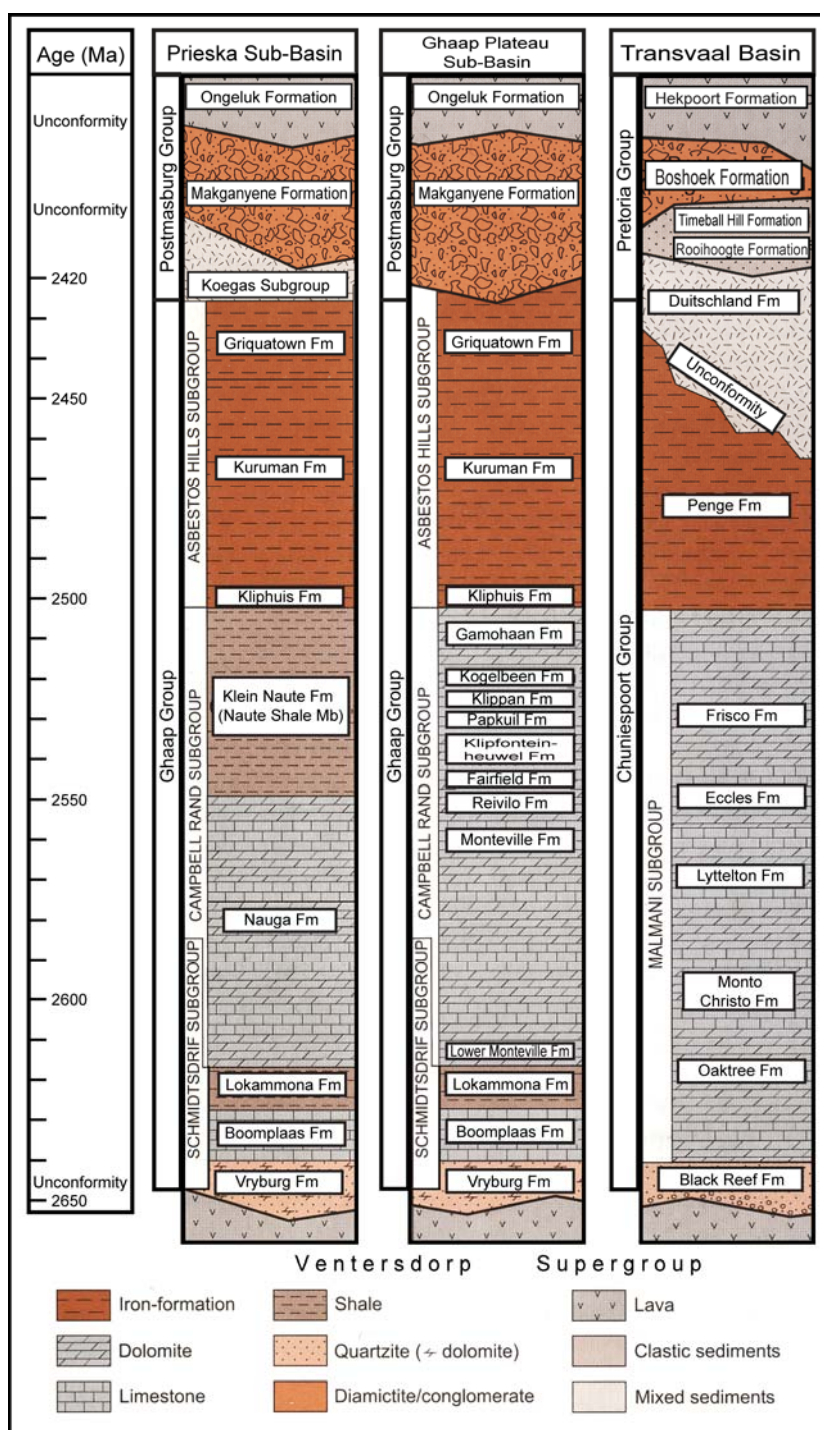


Figure 2.1 Interbasinal comparison of formations of the Ghaap and Chuniespoort (Transvaal sub-basin) Groups. In Griqualand West (Prieska and Ghaap Plateau sub-basins) and Transvaal areas, the geological ages are radiometric ages (dating of zircons in tuffs

intercalated with carbonates). Note that the vertical scale is not the thickness but the time of deposition, e.g. the Naute Shales are in reality much thinner than the Gamohaam Formation. Modified after Altermann and Nelson, 1998.

The Ghaap Group succession in the Kathu borehole core nevertheless comprises eight formations of the Campbellrand Subgroup encompassing tidal flat and shallow marine stromatolitic carbonate deposit, which are followed by deep subtidal carbonates, present only in the uppermost, thin Gamohaam Formation. The changes of lithology were interpreted as the second-order transgression-regression cycles for the Ghaap Plateau area (Altermann and Nelson, 1998). Generally the basal Schmidtsdrif Subgroup consists of siliciclastic sediments, carbonate oolites, stromatolitic carbonates and minor lava flows. The following Campbellrand Subgroup conformably overlies the Schmidtsdrif Subgroup with the subtidal, deeper water Monteville Formation and intertidal carbonates of the successively following remaining seven carbonate formations (see below). However in the Kathu drill core, the facies development differs partly strongly from this scenario (Altermann and Siegfried, 1997).

2.2 Stratigraphy

The Ghaap Group in Griqualand West Basin is subdivided into the Prieska sub-basin and Ghaap Plateau sub-basin, according to their different sedimentary facies development at different times of deposition. The two sub-basins are separated by the NW-SE striking Griquatown fault zone. Both lay unconformably on the 2.7 Ga volcano-sedimentary Ventersdorp Supergroup and are conformably overlain by BIF deposits of the Asbestos Hills Subgroup, deposited at c. 2500 Ma (Figure 2.1). The Ghaap Group in the Ghaap Plateau Sub-basin is subdivided into the Schmidtsdrif, Campbellrand and Asbestos Hills Subgroups. Its sedimentation persisted for > 200 Ma from c. 2642 ± 3 Ma (Walraven and Martini, 1995) to c. 2432 ± 31 Ma (Trendall et al., 1990).

2.2.1 Basal Schmidtsdrif Subgroup siliciclastic sediments

The base of the Ghaap Group consists of the Schmidtsdrif Subgroup. The Schmidtsdrif Subgroup is similar in the Prieska and Ghaap Plateau sub-basin. The deposition of Schmidtsdrif Subgroup is dated at 2642 ± 3 Ma (zircon age for the Vryburg lavas below the Schmidtsdrif Subgroup on the Ghaap Plateau – Walraven and Martini, 1995; Altermann, 1996). Three formations making up the Schmidtsdrif Subgroup attain a maximum thickness of 275 m on the Ghaap Plateau, but are much thicker in the Prieska sub-basin and in the Kathu borehole core (Beukes, 1979; Altermann and Siegfried, 1997).

At the base of the Schmidtsdrif Subgroup, the Vryburg Formation is interpreted as fluvial to marginal marine deposits (Beukes, 1987). The overlying Boomplaas Formation consists of interlayered dolomite, stromatolites, shale and limestones, while the Lokammona Formation covering the Boomplaas Formation consists of dolomite, shale, chert nodules, and sandstone layers. Rocks of the Schmidtsdrif Subgroup record the initial flooding of the craton and the establishment of mixed carbonate-siliciclastic ramps (Schröder et al., 2006) that pass upward to a carbonate platform.

Vryburg Formation

The Vryburg Formation, at the base of the Schmidtsdrif Subgroup, lies unconformably on the Ventersdorp Supergroup. The rocks consist of conglomerates, shales, quartzites and lesser carbonates. A basaltic to andesitic amygdaloidal lavas is intercalated in places (Beukes, 1983; Altermann and Siegfried, 1997). Beukes (1979, 1986) interpreted the sedimentary environment as fluvial to marginal marine deposits, however, for the Kathu borehole, it has been interpreted by Altermann and Siegfried (1997) as a much deeper environment, of chiefly shallow shelf fine grained, chiefly siliciclastic and carbonate-clastic deposits. In the Kathu borehole, the contact to the Ventersdorp is not exposed and thus of unknown nature. The entire Vryburg Formation was estimated to be approximately 100 m thick in outcrop (SACS, 1980), but is at least 230 m thick in the Kathu borehole (Altermann and Siegfried, 1997) and comprises abundant dolarenites and quartzites.



Figure 2.2 View of Vryburg quartzite at Westerberg.

Boomplaas Formation

The Boomplaas Formation consists in outcrops of platform carbonates with well preserved stromatolites, carbonate sands and oolites. Altermann and Siegfried (1997) interpreted the normally graded-bedded oolite sands of the Kathu borehole as transported down slope and not *in situ*, and consequently deposited in a deeper subtidal environment, as also represented by the abundance of shales and the lack of large domal stromatolites in the drillcore of Kathu. The Boomplaas Formation was estimated to be up to 100 m thick in the surface outcrops (Beukes, 1979, 1983), but consists of 185 m of shale and carbonate rocks in the Kathu borehole (Altermann and Siegfried, 1997).

Table 2.1 Stratigraphic subdivision of the Schmidtsdrif and Campbellrand Subgroups in the Kathu borehole. Lithology and facies interpretation for each formation are summarized after Altermann and Siegfried, 1997.

Subgroup	Depth from surface in m	Formation	Lithology	Facies	
Campbellrand	325	Gamohaam	Dwyka tillite		
	392		Columnar stromatolites, various bioherms and laminites	Subtidal, shallow platform	
		Kogelbeen	Fenestral laminites, domal to columnar stromatolites	Subtidal to intertidal platform	
	922	Dyke intrusion			
	1205	Klippan	Brecciated stromatolites, silicified microbial laminites	Subtidal, shelf-lagoon	
	1235	Papkuil	Columnar stromatolites, fenestral carbonates with shale intercalation	Subtidal to intertidal platform	
	1478	KlipfonteinHeuwels	Domal stromatolites, dolomites and microbial laminites	Subtidal to intertidal	
	1615		Fairfield	Clastic laminites, fenestral columnar stromatolites	Shallow subtidal platform
	1765	Reivilo	Various bioherms, fenestral and columnar stromatolites, stratiform laminites	Subtidal to intertidal platform	
	2615	Monteville	Fenestral and columnar stromatolites, oolite sands and tuffite	Deep platform to wave agitated subtidal	
Schmidtsdrif	3155	Lokammona	Shales with graded tuff beds, carbonate breccias	Deep platform	
	3210	Boomplaas	Shales with graded oolite beds	Deep platform	
	3395	Vryburg	Shales and quartzites, carbonates with microbial lamination	Deep platform	
	3672				

Lokammona Formation

The Lokammona Formation, uppermost of the Schmidtsdrif Subgroup comprises predominantly shales with graded tuff beds, carbonates and carbonate breccias, abundant BIF-like chert nodules and dolomite intercalations. The thickness and lithology of the Lokammona Formation in the Kathu borehole are consistent with the outcrop description. In the drill core, the deposition of Lokammona Formation reaches a thickness of 55 m. The formation is interpreted as a transgressive deposit over the Boomplaas platform in both outcrop and Kathu drill-core (Beukes, 1979; Altermann and Siegfried, 1997).

2.2.2 Campbellrand Subgroup carbonate sediments

The Campbellrand Subgroup follows conformably on the Lokammona Formation of the Schmidtsdrif Subgroup. It consists of a series of carbonate platform sequences

(Monteville, Reivilo, Fairfield, Klipfontein, Papkuil, Klippan, Kogelbeen and Gamohaans Formations) and is overlain by thick units of banded iron formation belonging to the Asbestos Hills Subgroup.

Table 2.1 shows the thickness of each of these formations in the Kathu borehole. In the Griqualand West Basin, the deposition of Campbellrand Subgroup is subdivided into two sub-basins of Prieska and Ghaap Plateau, with different sedimentary histories (compared above). The Kathu borehole penetrated the Ghaap Plateau sub-basin (Figure 2.1), where the Campbellrand Subgroup was estimated to be about 1600 m thick (Beukes, 1980; SACS, 1980), but is at least 2500 m thick in the borehole of Kathu, with the uppermost Gamohaans Formation being partially eroded and covered by the Dwyka glaciation (Altermann and Siegfried, 1997).

The lowermost Monteville Formation in the Kathu borehole essentially consists of stromatolitic carbonates and shales (Altermann and Siegfried, 1997), and the remaining formations consist of sometimes cherty, light grey stromatolitic dolomite and the dark grey chert-free stromatolitic carbonates (Beukes, 1987; Altermann and Siegfried, 1997). The Campbellrand Subgroup carbonate rocks were deposited in a basin transgressing from southwest to the northeast for a distance of over 400 km. The subgroup records an aggradational, rimmed stromatolitic carbonate platform (Schröder et al., 2009) or a westwards inclined carbonate ramp (Altermann and Herbig, 1991; Altermann and Wotherspoon, 1995; Altermann and Nelson, 1998), of interbedded microbialites, stromatolites and re-sedimented carbonates deposited in the deeper platform or ramp margin.

Monteville Formation

The basal 200-m-thick Monteville Formation consists of giant stromatolitic domes, columnar stromatolites, fine-grained clastic carbonates, intercalated shales and siltstones. It was interpreted as a shelf deposit by Beukes (1987) and reinterpreted by Altermann and Herbig (1991) as a shallow marine deposit for the Kathu borehole, where it is approximately 540 m thick. The boundary between Monteville and Reivilo Formations is defined at 2615 m depth of the Kathu drill core, at the greenish, marly

tuffite bed (Altermann and Siegfried, 1997). The appearance of stromatolitic carbonates and intercalated shales suggested that the entire Monteville Formation records a shallowing-upward cycle over the Lokammona Formation, of the Schmidtsdrif Subgroup, which is superimposed on smaller transgressive-regressive cycles (Altermann and Siegfried, 1997).

Reivilo Formation

The Reivilo Formation comprises the largest part of the Campbellrand Subgroup and reaches a thickness of up to 900 m in surface outcrops. In the Kathu borehole, the Reivilo Formation is occupied by an 850-meter-thick carbonate sequence, starting at 2615 m depth with columnar stromatolites and ending at 1765 m depth with cryptic microbial laminates and cross-bedded dolarenites marking the beginning of the overlying Fairfield Formation. It consists of carbonates with giant stromatolitic domes and columnar stromatolites, fenestral facies, thin intercalated oolitic beds. The thin shale intercalations (Altermann and Siegfried, 1997) and the uppermost BIF-like intercalations (Beukes, 1987) reveal a renewed transgressive phase superimposed on smaller shallowing-upward cycles. Giant stromatolitic domes and columnar stromatolites indicate that the depositional paleo-environment of the Reivilo Formation was of platform conditions ranging from deeper subtidal to intertidal.

Fairfield Formation

The succeeding Fairfield Formation is made up of lower clastic laminated carbonate beds, passing upward into columnar stromatolites, microbial laminates and fenestrated stromatolitic facies. The facies cycles are duplicated for three, and in some places, four times within the 120-135 m thick Fairfield Formation (Beukes, 1980). The entire Fairfield Formation represents repeated shallowing upward cycles. In the Kathu borehole, the deposition of Fairfield Formation starts at 1765 m depth with pelletal wackestones-and-dolarenites and terminates at 1615 m above the shale bed below the chert layer at the base of the Klipfontein Heuwel Formation (Altermann and Siegfried, 1997). The lithological change from earlier carbonate-clastics to stromatolitic carbonates reflects changes of hydrodynamic condition and reveals that

the entire depositional paleoenvironment of Fairfield Formation was mostly shallow subtidal (Altermann and Siegfried, 1997).

Klipfontein-Heuwel Formation

The following Klipfontein-Heuwel Formation comprises platform carbonates with domal stromatolites, stratiform microbial laminates, and becomes increasingly silicified upwards. Abundant drusy quartz crystallites are presented in the fenestral dolomites. The formation starts with silicified, spaced and domal stromatolites at the depth of 1615 m in the Kathu borehole and continues through a silicified chert zone, where the last chert layer defines the top of the Klipfontein-Heuwel Formation at 1478 m depth. Thus, the entire Klipfontein-Heuwel Formation is 137 m thick in the Kathu borehole. The similarities of stromatolite morphology and carbonate petrography imply that the depositional paleoenvironment has not change significantly, comparing to the preceding Fairfield Formation, which is suggested as the shallow subtidal carbonate platform (Altermann and Siegfried, 1997).

Papkuil Formation

The Papkuil Formation consists of laminoid fenestral mats and columnar stromatolites in the lower part, which is covered by columnar stromatolites with oolite beds and dolarenite intercalations, and end with intercalations of columnar stromatolites, clastic laminated dolmicrites and sapropelic carbonates in the upper part. Silicification is very common in the deposits of the whole Papkuil Formation which is approximately 250 m thick in the Kathu borehole. The depositional paleoenvironment of Papkuil Formation is of subtidal carbonate platform facies (Altermann and Siegfried, 1997), as the underlying Klipfontein-Heuwel and Fairfield Formations. Altermann and Siegfried (1997) suggested that shallowing upward cycles, reaching from subtidal to intertidal facies, make up the deposition of Papkuil Formation, marked by the repeated occurrences of laminoid, fenestrated carbonates and columnar stromatolites with coarse intraclastic sediments.

Klippan Formation

The Klippan Formation starts with a few centimetre-high domal stromatolites, passing upward into silicified, coarse crystalline microbial laminates with drusy quartz concentrations. The Klippan Formation is only 20 m thick in outcrop. In the Kathu borehole, it starts at 1235 m depth with marl and dark carbonaceous dolmicrites and extends up to a thick talc layer at 1205 m depth, which marks the intrusion of a thick dyke masking the top of this formation (Table 2.1). The dark and organic-rich marls and dolmicrites with carbonate intraclasts infer that the depositional paleo-environment was deeper than in the underlying Papkuil Formation. Thus, this formation marks a further transgression over the carbonate platform.

Kogelbeen Formation

The Kogelbeen Formation consists of over 300 m thick carbonate succession, and increases to 445 m thick in the Kathu borehole, represented by varying dolomites, limestones and cherts. It starts with laminoid, fenestrated limestones and locally developed columnar stromatolites with oolitic beds, followed by cycles of domal to columnar stromatolites and silicified laminates, which in turn are overlain by a thick sequence of laminates with abundant chert replacement. Note that an over 300 m thick dolerite intruded between the Kogelbeen Formation and the underlying Klippan Formation in the Kathu borehole (Table 2.1). The Kogelbeen Formation possesses the largest variety of stromatolitic microstructures of all the formations in the Kathu Campbellrand Subgroup drill core (Altermann and Siegfried, 1997). Hence, the depositional paleoenvironment is inferred to be entirely of shallow subtidal to intertidal carbonate platform conditions.

Gamohaam Formation

The Gamohaam Formation of the uppermost Campbellrand Subgroup is occupied by finely laminated microbial mats, domal to columnar stromatolites, sapropelic carbonates and dolarenites. It is covered by the succeeding shales (Naute Formation) and BIFs of the Asbestos Hills Subgroup (Beukes, 1980; Altermann and Wotherspoon, 1995). The Gamohaam Formation is not fully preserved in the Kathu borehole. It starts at 392m depth with large columnar stromatolites, tabular domes and laminates (Altermann and Siegfried, 1997), followed by 67 m thick succession of stromatolitic

carbonates. The Phanerozoic Dwyka Formation unconformably overlies the partly eroded Neoproterozoic strata (Altermann and Siegfried, 1997). The depositional paleoenvironment of the Gamohaam Formation is interpreted as shallow subtidal with a deepening-upward tendency (Altermann and Siegfried, 1997) that is transitional to the transgressing; overlying shale and BIF deposits (Beukes, 1980).

2.2.3 Asbestos Hills Subgroup Iron Formations

The Asbestos Hills Subgroup conformably follows on the Campbellrand Subgroup, and was subdivided by Beukes (1983) into a lower orthochemical rhythmically banded Kuruman Iron Formation and an upper, allochemical, clastic-textured and shallow-water Griquatown Iron Formation. Beukes (1983) suggested that the lithological transition from the underlying Campbellrand Subgroup carbonate to the overlying Asbestos Hills Subgroup BIF-deposition is due to a major marine transgression and associated sea level rise. Subsidence led to the drowning of the stromatolitic platform. Finally, in the entire basin, chemical, iron-rich silica-banded iron formations were deposited (Eriksson and Altermann, 1998). The Kuruman Iron Formation consists mainly of banded iron formation deposits that record the deeper shelf environment. This environment becomes shallower upward with the clastic-textured Griquatown Iron Formation. The mixed siliciclastic and Fe-rich chemical deposits of the Koegas Subgroup overlying the Asbestos Hills Subgroup BIF are only preserved in the south-western Prieska sub-basin and indicate further shallowing-upward conditions (Beukes, 1983).

**MICROFACIES, ISOTOPIC
METHODOLOGY AND SAMPLE
SELECTION**

3. Microfacies, Isotopic Methodology and Sample Selection

3.1 Microfacies of Carbonate Rocks

The term “microfacies” was originally suggested and defined from petrographic and paleontological characteristics that were studied in thin sections (Brown, 1943). Today, based on new techniques, microfacies study involves more subjects such as the comparison of element concentration and composition in modern and ancient carbonates, the concepts on defining facies models, the course of carbonate sedimentation through geological time and the biological controls on carbonate sedimentation (Flügel, 2004).

More than 90% of the carbonate rocks found in modern sedimentary environments are of biological origin (Moore, 1997). Distribution and frequency of most carbonates are strongly controlled by environmental factors that are favourable for the growth of carbonate-producing organisms, such as water temperature, salinity, light availability and sedimentary influx (Flügel, 2004). Thus, carbonate rocks deposited in Ghaap Group are discussed here, in this thesis, using microfacies and isotopic analysis, in order to find the relationship between microscopic observations and isotopic signatures in late Archean carbonate environments.

The influence of microbial activity on the morphology and preservation of stromatolitic carbonates has been controversially discussed in the studies of Precambrian carbonate rocks (i.e. Eriksson and Altermann, 1998; Sumner and Grotzinger, 2004; Altermann et al., 2006; Altermann, 2008; Schröder et al., 2009). Today, a general agreement on this topic exists, whereby the complex interaction between biological and environmental processes is understood to constrain the morphology and preservation degrees of biogenic carbonate deposits, rather than only biological influence (Grotzinger and Knoll, 1999; Riding and Awramik, 2000; Awramik and Grey, 2005; Altermann, 2008). The Campbellrand Subgroup platform exhibits remarkable carbonate rocks with variable stromatolitic morphologies that

provide a unique opportunity to study their growth mechanisms and the interactions between biological and environmental processes.

The least altered carbonate minerals and stromatolitic laminae were selected for this thesis, constituting 40 rock samples with primary textures such as stromatolite lamina etc. In order to ensure the correct stratigraphic order and continuity, which is sometimes difficult in the field and in order to concentrate on a possible complete stratigraphic record, the Kathu borehole core was chosen for this work, as sampled by W. Altermann in 1990-1995 (Altermann and Siegfried, 1997).

3.2 Isotopes (C and O) of Carbonate Rocks

Stable isotope studies of carbon ($\delta^{13}\text{C}$) and oxygen ($\delta^{18}\text{O}$) in ancient carbonate rocks have been used primarily to define depositional or diagenetic environments. Such isotopic tracers have been increasingly studied from Precambrian rocks (Kaufman and Knoll, 1995; Des Marais, 2001; Fischer et al., 2009). The carbon isotope ratios of marine carbonate rocks are extremely useful for the reconstruction of ancient environmental changes. The oxygen isotope compositions of carbonate rocks are controlled by the $\delta^{18}\text{O}_w$ of the surrounding seawater, and normally is a function of temperature (Veizer and Hoefs, 1976). Oxygen isotope ratios are mainly used here to constrain the diagenetic process and estimate the average seawater temperature of carbonate formation.

Stratigraphic records of the stable isotope composition of carbon in Precambrian carbonate-rich sedimentary successions have been widely used as proxies for paleo-environmental reconstruction (Kaufman et al., 1990; Klein and Beukes, 1993; Klein and Beukes, 1989; Condie et al., 2001; Tsikos et al., 2003). Most of the carbonates from marine depositional environment have a $\delta^{13}\text{C}$ value of $0 \pm 2\text{‰}$ vs. the Pee Dee Belemnite standard, whereas fresh water has a ^{13}C -depleted carbon isotope value (Veizer and Hoefs, 1976; Veizer et al., 1992b; Des Marais, 2001; Shields and Veizer, 2002; Hoefs, 2009).

Oxygen isotopes in marine carbonate rocks are commonly temperature-dependent. Since Urey (1947) firstly proposed the theoretical basis for using the $\delta^{18}\text{O}$ values in carbonate minerals as a paleo-temperature signature, oxygen isotopic composition in marine carbonate has been widely used to calculate the paleo-temperatures (Craig, 1965; Burdett et al., 1990; Winter and Knauth, 1992; Robert and Chaussidon, 2006). Carbonates precipitated from seawater at high temperatures are usually more ^{18}O -depleted than those precipitated at lower temperatures (Friedman and O'Neil, 1977; Kim and O'Neil, 1997; Kim et al., 2007). In the Precambrian, the temperature and salinity of the seawater are thought to be the major environmental variables relevant for microbial evolution (Knauth, 2005). Oxygen isotope results from carbonates and early diagenetic cherts in Archean time are greatly arguable (Veizer and Hoefs, 1976; Shields and Veizer, 2002; Knauth and Lowe, 2003; Knauth, 2005; Kasting et al., 2006); the distinguished depleted values of $\delta^{18}\text{O}$ indicate that the surface ocean temperatures were possibly on the order of $60 \pm 20^\circ\text{C}$ throughout the Precambrian. Thus, microbes in Archean time, which have formed abundant stromatolites, are thought to have inhabited a marine environment with a relatively high temperature.

3.2.1 Carbon isotopes

Carbon has two naturally occurring stable isotopes: ^{12}C and ^{13}C . The ^{12}C constitutes 98.90% of natural carbon, and ^{13}C makes up almost the entire remaining 1.10%. Because the mass of ^{13}C is 8.36% greater than that of ^{12}C , the C isotopic fractionation, which is caused by a variety of chemical, physical and biological processes in nature, will lead to the differences in $\delta^{13}\text{C}$ values (as defined below) among carbon reservoirs. Carbon is commonly stored in sedimentary rocks as inorganic carbonate minerals and organic remains, and in the earth interior as carbon dioxide and methane. Over 99% of carbon in the lithosphere is preserved in the sedimentary rocks and their metamorphic equivalents (Schidlowski, 1995). The carbon isotopic composition of carbonate minerals depends on the environmental conditions and biological activity during their formation, thus isotopic analyses of carbon can reveal the information on the

physical, chemical and biological processes, in which the carbon isotopes were preserved.

The $\delta^{13}\text{C}$ measurements are commonly reported as

$$(\delta^{13}\text{C}_{\text{sample}} = \left\{ \frac{(^{13}\text{C}/^{12}\text{C})_{\text{sample}}}{(^{13}\text{C}/^{12}\text{C})_{\text{reference}}} - 1 \right\} \times 10^3$$

with respect to the widely used artificial international standard “Vienna Pee Dee Belemnite” (V-PDB) composed after the natural standard of a belemnite from the Pee Dee Formation.

Carbon in sediments and sedimentary rocks occurs as either carbonate carbon (C_{carb}) or organic carbon (C_{org}). Carbonate carbon (C_{carb}) is mainly deposited in the form of calcite, dolomite or aragonite that precipitates actively or bio-induced by organisms as oxidized carbon, and of inorganically precipitated carbonate crystals in the water column, on the sea floor or as inter-grain cements during diagenesis. Organic carbon (C_{org}) is the carbon of biogenic origin deposited in sediments as reduced carbon. Microbial organisms possess numerous mechanisms for assimilation of inorganic carbon (i.e. carboxylation), with typical isotope fractionation, which strongly favors the lighter isotope ^{12}C . The C_{org} is thus ^{12}C -enriched relative to the inorganic C compounds, and normally around -25‰ versus V-PDB (Kump and Arthur, 1999; Des Marais, 2001), due to the biological fractionation. Especially for the late Archean, isotopic fractionation associated with cyanobacterial photosynthesis for production of organic carbon is estimated at about -26‰ (Preuss et al., 1989). Organisms having RubisCO as the key enzyme of the Calvin cycle preferentially use ^{12}C over ^{13}C for the fixation of CO_2 and dissolved bicarbonate (HCO_3^-) in microbial mats with a distinguishable ^{13}C isotope effect (Roeske and O’Leary, 1984).

Therefore, organic carbon is isotopically lighter than the surrounding dissolved inorganic carbon in seawater. In the previous studies of marine carbonate minerals, typical $\delta^{13}\text{C}_{\text{carb}}$ values of seawater were suggested to be approximately at 0‰

(Clayton and Degens, 1959; Keith and Weber, 1964; Ripperdan, 2001) through the geological time.

3.2.2 Oxygen isotopes

Oxygen has three naturally occurring stable isotopes with atomic mass numbers of 16, 17 and 18 (^{16}O , ^{17}O and ^{18}O), which show relative proportions of 99.76%, 0.04% and 0.2% respectively (IAPWS, 2002). Because ^{17}O is less abundant than ^{18}O in nature, the ratio of $^{18}\text{O}/^{16}\text{O}$ is normally used in water, carbonate sediments and organic matter, as oxygen isotope ratio. The oxygen isotope composition of carbonate precipitated in aquatic systems depends on the temperature and isotopic composition of the host water (Veizer and Hoefs, 1976; Kasting et al., 2006). $\delta^{18}\text{O}$ values of carbonates are usually decreasing with increasing temperature and decreasing salinity, thus the variations in their $\delta^{18}\text{O}$ values are commonly used in reconstructing paleo-climatic fluctuations, paleo-geographic evolution and diagenetic degrees (Burdett et al., 1990; Veizer et al., 1999; Kasting et al., 2006).

The $\delta^{18}\text{O}$ values are reported as

$$\delta^{18}\text{O}_{\text{sample}} = \left\{ \frac{(^{18}\text{O}/^{16}\text{O})_{\text{sample}}}{(^{18}\text{O}/^{16}\text{O})_{\text{reference}}} - 1 \right\} \times 10^3$$

with respect to the international standard Vienna Pee Dee Belemnite (V-PDB) for carbonate rocks (CaCO_3) while another international standard is commonly used for water samples (H_2O), the Standard Mean Ocean Water (SMOW). Because the oxygen isotopic analyses of water are usually reported as SMOW standard values for paleo-temperature calculation, a conversion of $\delta^{18}\text{O}$ values from the carbonate V-PDB scale to the water SMOW scale have been calculated according to Hoefs (2009) (Equation 3.1).

$$\delta^{18}\text{O}_{\text{V-PDB}} = 0.97002 \times \delta^{18}\text{O}_{\text{SMOW}} - 29.98 \quad \text{(Equation 3.1)}$$

The fractionation of oxygen isotopes is strongly dependent on temperature of the seawater. Although post-depositional alteration can affect the $\delta^{18}\text{O}$ values, the

oxygen isotopic composition of carbonate rocks in many cases offers a possibility to evaluate the ancient seawater temperature trends. Much controversy is concentrated on the history of surface temperature and diagenetic overprints on the original isotope composition of seawater through Earth history, especially in the Phanerozoic. Only few such studies are concerned with Precambrian marine carbonate rocks. The few available oxygen isotope data are compiled by Veizer and Hoefs (1976), Shields and Veizer (2002), Knauth (2005) and Kasting et al. (2006) from marine carbonate rocks and early diagenetic cherts suggesting one of the following:

The $\delta^{18}\text{O}$ values were more depleted in most of the Precambrian carbonate rocks than those of Phanerozoic

(1) because of the more frequent post-depositional exchanges between ancient carbonate minerals and meteoric water (Killingley, 1983; Fairchild and Kennedy, 2007).

(2) because of higher rates of recrystallization and dolomitization of these more ancient carbonate minerals (Reinhold, 1998; Fu et al., 2006).

(3) because of the intensively deep burial diagenesis in ancient carbonate minerals (Choquette and James, 1987; Mabrouk et al., 2006).

(4) because the average temperatures of Precambrian seawater were essentially higher than at present (Karhu and Epstein, 1986; Knauth and Lowe, 2003).

(5) because they represented the isotopic composition of ancient seawater where the carbonate mineral precipitated from (Knauth and Epstein, 1976; Kasting et al., 2006; Kasting and Howard, 2006).

3.3 Sample Selection

Table 3.1 List of samples for isotopic analyses in this study. Most of these samples were collected from the Kathu borehole except for the samples of GAS1-558, WA91-41, WA91-43, WA92-6 and WA95-26.

Subgroup	Formation	Thickness(m)	Sample No.	Lithology	Location and depth in the core
Campbellrand	Gamohaam	100	GAS1-558	Contorted microbial mats	Hotazel core 558m
			WA92-60	Contorted microbial mats	Kathu core 336m
			WA92-57	Contorted microbial mats	Kathu core 341m
			WA92-56	Conophytions	Kathu core 358m
			WA92-55	Bio-clastic dolarenite	Kathu core 368m
			WA92-54	Tuff	Kathu core 372m
			WA92-53	Bio-clastic dolarenite	Kathu core 372m
	Kogelbeen	445	WA91-41	Laminated stromatolites	Lime Acres
			WA91-43	Fenestral stromatolites	Lime Acres
			WA92-6	Chert	Finsch Mine
			WA92-45	Columnar stromatolites	Kathu core 540m
			WA92-43	Chert breccia	Kathu core 587m
			WA92-38	Columnar stromatolites	Kathu core 822m
			WA92-37	Columnar LLH stromatolites	Kathu core 847m
	WA92-35	Metamorphic stromatolites	Kathu core 855m		
	Klippan	20	WA92-32	Birds eyes carbonates	Kathu core 1232m
	Papkuil	243	WA92-34	Columnar stromatolites	Kathu core 1357m
			WA95-26	Laminated stromatolites	YSKOR GH6/7 102m
	Klipfontein Heuwels	137	WA92-31	Chert seams	Kathu core 1502m
			WA92-28	Finger-like columnar stromatolites	Kathu core 1553m
			WA92-27	Algal laminites	Kathu core 1553m
			WA92-25	Recrystallized wavy laminites	Kathu core 1611m
	Fairfield	150	WA92-24	Chert	Kathu core 1644m
			WA92-21	Columnar stromatolites	Kathu core 1693m
			WA92-20	Laminated bio-clastic carbonates	Kathu core 1769m
	Reivilo	850	WA92-19	Laminated bio-clastic carbonates	Kathu core 1803m
			WA91-63	Fenestral stromatolites	Kathu core 2090m
			WA91-62	Laminated microbial carbonates	Kathu core 2130m
			WA91-60	Breccia stromatolites	Kathu core 2280m
			WA91-57	Laminated microbial mats	Kathu core 2547m
	Monteville	540	WA91-56	Pelletal carbonates	Kathu core 2638m
			WA91-55	Bifurcating stromatolites	Kathu core 2685m
WA91-54			Columnar stromatolites	Kathu core 2796m	
WA91-52			Recrystallized carbonates	Kathu core 2892m	
Schmidtsdrif	Lokammona	55	WA91-51	Laminated micrite	Kathu core 3199m
	Boomplaas	185	WA91-50	Gray and black micrite	Kathu core 3242m
			WA91-49	Irregular laminated micrite	Kathu core 3327m
	Vryburg	230	WA91-48	Oolites	Kathu core 3586m
			WA91-47	Mottled micrite	Kathu core 3647m
			WA91-46	Silicified micrite	Kathu core 3656m

Table 3.2 List of the samples from the Kathu borehole chosen according to the observation of three morphological stromatolite facies realms. All these samples were previously listed and their depth recorded by Altermann and Siegfried, 1997. Formations, which are not represented in this collection, did not contain samples sufficiently unaltered by post-depositional processes.

Subgroup	Formation	Thickness (m)	Columnar stromatolites	Fenestral stromatolites	Finely laminated microbial mats	Sample No.
Campbellrand	Gamohaam	108			4	92-56, 92-57, 92-60, GAS1-558
	Kogelbeen	445	3	3		91-41, 91-43, 92-43, 92-45, 92-37, 92-38
	Klippan	20		1		92-32
	Papkuil	243	1			92-34
	Klipfontein	137		1		92-28
	Fairfield	150	1	1		92-21, 92-24
	Reivilo	850	1	1		91-60, 91-63
	Monteville	540	1	1		91-052, 91-55

In this study, 40 samples were selected (Table 3.1) through the entire Ghaap Group section of the Kathu core and few other localities in South Africa, Griqualand West. The investigations were focused on microfacies and isotopic (carbon and oxygen) analyses. Because there were not enough suitable samples for the isotopic analyses available from some stratigraphic formations of Ghaap Group, samples of GAS1-558 (from Hotazel drill core, 558m), WA91-41 (from Lime Acres), WA91-43 (from Lime Acres), WA92-6 (from Finsch) and WA95-26 (from YSKOR GH6/7, 102m) were collected for completing the carbonate isotopic analysis of the entire Ghaap Group. The sample GAS1-558 is stratigraphically equivalent to the Gamohaam Formation samples in Kathu borehole, samples of WA91-41, WA91-43 and WA92-6 are stratigraphically equivalent to the Kogelbeen Formation samples in Kathu borehole, sample WA95-26 is stratigraphically equivalent to the Papkuil Formation samples in Kathu borehole.

As the processes that formed the carbonate carbon and organic carbon have different isotope fractionations, there is a characteristic difference in their $\delta^{13}\text{C}$ values. Two points for each sample have been drilled, one in dark laminae

(organic-rich matter) and one in the light colored laminae (carbonate-rich matter). Each sample was drilled with a diamond coated micro-drill for 0.5 mg of sample and weighed into septum vials. All the samples for the C_{carb} measurement were put into a block and heated to 72°C and then flushed with Helium with a COMBIPAL (CTC Analytics) sampling device. Afterwards, 103% phosphoric acid was added with a syringe to the sample. After at least 3 hours of equilibration, the evolved CO_2 gas was sampled and purified in a GasBench II (Thermo-Finnigan) and thereafter isotopically analyzed with an isotope ratio mass spectrometer (DeltaPlus, Thermo-Finnigan).

For organic carbon isotope analyses, a pre-treatment following Mayr et al. (2005) was employed on the samples to remove carbonates. Homogenized sediment-samples were heated in water bath at 50°C, in the presence of hydrochloric acid (5%) for 6 hours, thereafter rinsed with de-ionized water until neutral pH. The decalcified samples were thoroughly dried and then weighed into tin capsules and combusted in an elemental analyzer (NC2500, Carlo Erba, Italy) at 1080°C, in the presence of excess oxygen. After reduction of nitrogen oxide and excess oxygen by passing over copper wires at 650°C and trapping of water vapour with $\text{Mg}(\text{ClO}_4)_2$, the remaining gases N_2 and CO_2 were separated in a GC column at 45°C. N_2 and CO_2 were passed successively via a ConFloII interface into the isotope ratio-mass spectrometer (Delta Plus, Thermo-Finnigan) and isotopically analyzed. Carbon and nitrogen contents were determined from the peak area vs. sample weight ratio of each individual sample and calibrated with elemental standards (Cyclohexanone-2,4-dinitrophenylhydrazone $\text{C}_{12}\text{H}_{14}\text{N}_4\text{O}_4$ and Atropine $\text{C}_{17}\text{H}_{23}\text{NO}_3$, Thermo Quest, Italy). A lab-internal organic standard (Peptone) was used for final isotopic calibrations. Typical analytical precision was 0.1‰ for both $\delta^{13}\text{C}$ and $\delta^{15}\text{N}$ (one standard deviation). All element concentrations given are weight percentages relative to dry weight. The system was calibrated with NBS18, NBS19 and a lab-internal carbonate standard. The reproducibility was $\pm 0.1\%$. All the samples collected for the isotopic analysis are listed in Table 3.1, according to the stratigraphic succession and the depth in Kathu drill-hole.

Three main stromatolite facies with distinct morphology are present in the Campbellrand platform deposits, namely deep subtidal fine laminated microbial mats, intertidal columnar stromatolites and supratidal open space structured, laminated carbonate (Altermann and Herbig, 1991; Altermann, 2008). Twenty samples were selected for microscopic analysis (Table. 3.2) from these facies. Initially, thin sections of micritic, fenestral, columnar, laminated and stromatolitic carbonates were evaluated petrographically for grain size, degree of recrystallization, authigenic and detrital components, stylolites, veins and silicification alteration, which may be associated with post-depositional deep burial diagenesis.

MICROFACIES OF CARBONATE ROCKS IN THE GHAAP GROUP

4. Microfacies of Carbonate Rocks in the Ghaap Group

Carbonate rock deposits in the late Archean Ghaap Group, South Africa, are chiefly composed of microbialites and stromatolites of different morphologies (Truswell and Eriksson, 1972, 1975; Beukes, 1979, 1980, 1987; Altermann, 2008). Dolomites and limestones of various non stromatolitic facies, like oolites and edgewise conglomerates with interbedded marls, carbonate arenites and siliciclastic sediments (Altermann and Wotherspoon, 1995; Altermann and Siegfried, 1997) also occur in abundance. Stromatolites and the carbonate sediments in their direct neighbourhood can be used for facies analysis. The morphology of stromatolites often shows vertically changing growth patterns as an expression of laterally migrating facies changes. The assemblage of these carbonate rocks implies a diversely depositional paleoenvironments that developed on the late Archean platform in South Africa (Altermann, 2008).

4.1 Microbialite Morphology

Microbial processes, such as photosynthesis, cyanobacterial calcification and decomposition of organic matter, directly or indirectly influenced and controlled the carbonate precipitation by repeatedly accretive growth of microbial communities. Microbial calcification is associated with the rise of alkalinity which is caused by the photosynthetic up-take of CO_2 and/or HCO_3^- , and leads to the calcification of mucilaginous sheaths (Flügel, 2004; Kazmierczak et al., 2004). The nucleation of carbonate minerals can be enhanced or inhibited by the up-taking activity of HCO_3^- by microbial communities. Microbial communities, trap and bind the surrounding sedimentary grains, and form the complex structures of stromatolites through their microbial growth and secretion or precipitation of various mineral nuclei. These microbial activity leads to distinct microbial textures in carbonate rocks that provide valuable information for the reconstruction of ancient depositional environment of these carbonates (Altermann, 2004, 2008).

After the formation of nuclei of minerals by microorganisms, possible biochemical degradation, early and deep burial alteration can occur. Although the organic degradation and deep burial tend to destroy the organic fabrics, calcium carbonate

and silica (chert) may permineralize cyanobacterial cells and sheaths below the growth surface of stromatolitic communities and preserve their morphology (Wright and Altermann, 2000).

The variations in stromatolitic morphology suggest that possible environmental changes, including sea level fluctuations, wave and current disturbance, occurred during and/or after the carbonate deposition.

Carbonate rocks discussed in the present thesis were grouped into different environmental realms, according to the macro and micro facies expression of their stromatolitic morphology (Figure 4.1, 4.2 and 4.3).

Three types of microbial carbonates have been recognized due to the morphology of stromatolites and associated sedimentary structures and microfacies: (1) Open space structure stromatolites (Group A in figure. 4.1) show fenestrae-rich, undulating microbial laminae. Common stylolites, parallel to each other and often sub-parallel to lamination originated during the deep burial diagenesis. The truncation surfaces and fenestral structures in this type of fenestral stromatolites are interpreted as evidence of shallow water realm, ranging from intertidal to supratidal and lagoonal facies (Beukes, 1987; Altermann, 2008). (2) Columnar stromatolites (Group B in figure. 4.2) display continuous lamination with trapped microbial mat clasts, sparitic and pelletal sediment grains between the laminated columns. It was suggested that these carbonate rocks were deposited in a subtidal to intertidal, shallow marine environment (Altermann and Herbig, 1991; Altermann, 2008). (3) Densely laminated microbial mats (Group C in figure. 4.3) with delicate morphology of the microbialites, lack of scouring evidence and absence of clastic carbonate but displaying sometimes contorted microbial mats, were grouped into a deep subtidal and/or sub-wave base depositional environment (Sumner, 1997; Altermann, 2008).

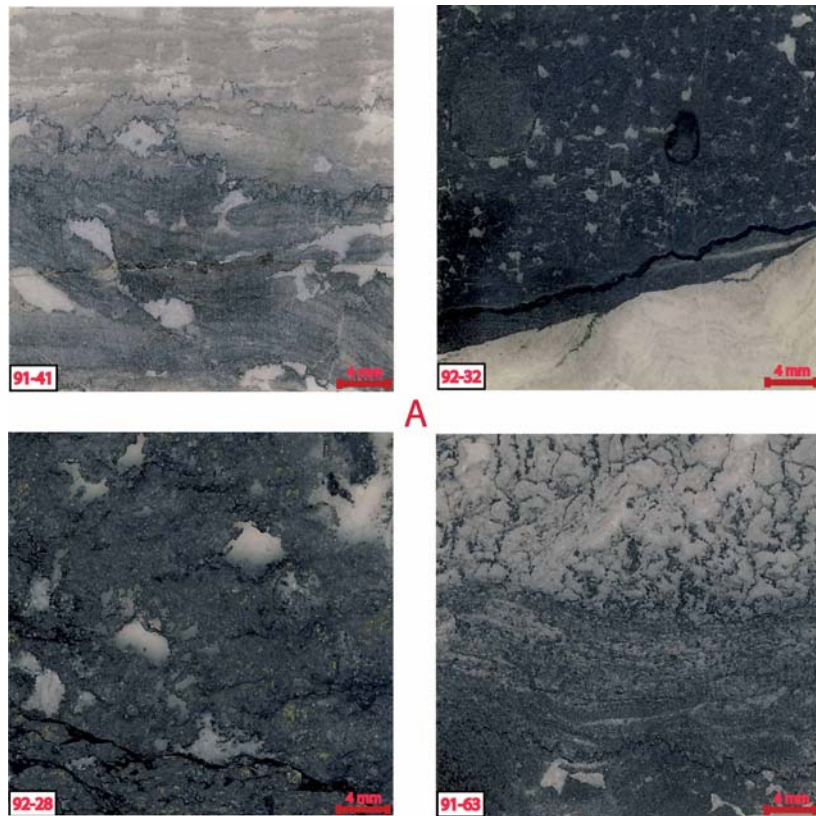


Figure 4.1 The photographs of Group A show examples of the open space structure stromatolites. Sample numbers are given in the left bottom of the photographs and the scale bar in red colour is of 4 mm, right lower corner.

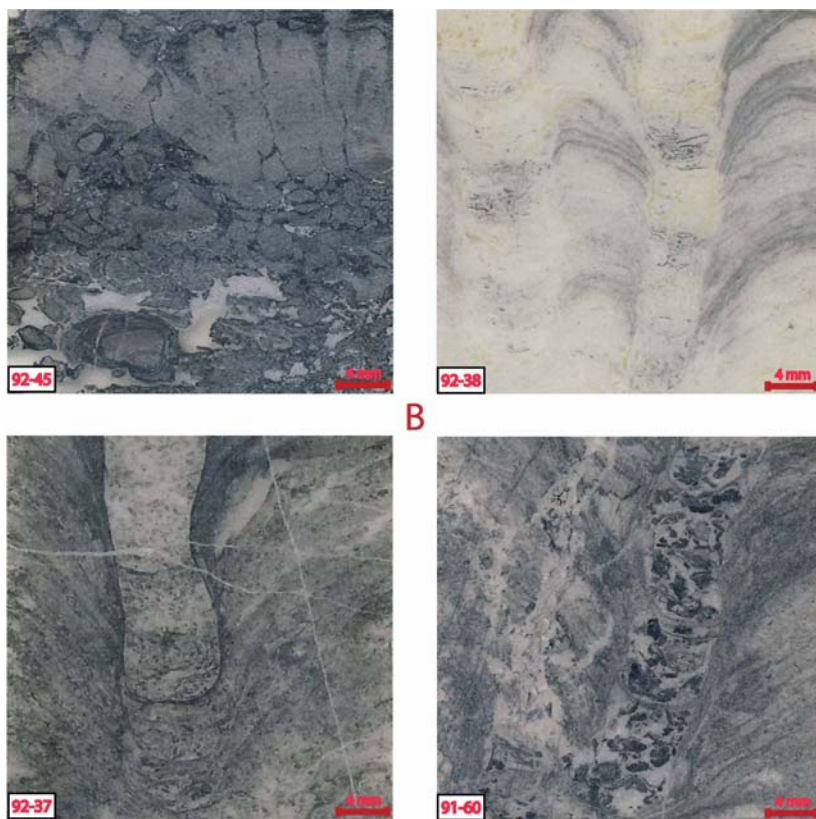


Figure 4.2 The photographs of Group B show examples of the columnar stromatolites. Sample numbers are given in the left bottom of the photographs and the scale bar in red colour is of 4 mm, right lower corner.

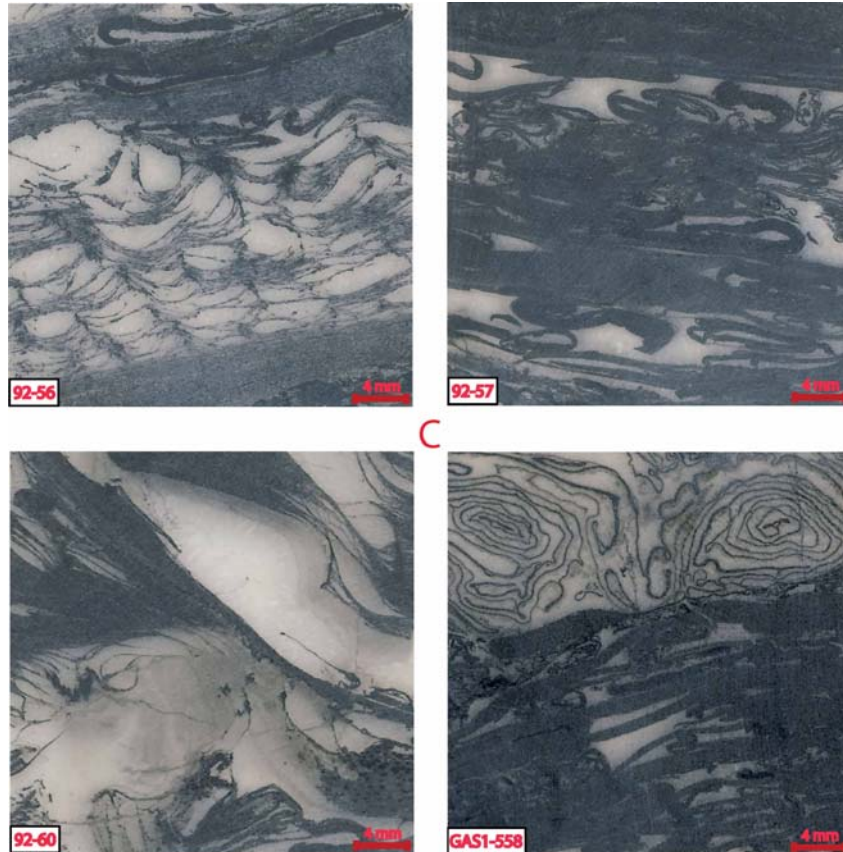


Figure 4.3 The photographs of Group C show examples of the contorted, finely laminated microbial mats. Sample numbers are given in the left bottom of the photographs and the scale bar in red colour is of 4 mm, right lower corner.

4.1.1 Intertidal to supratidal microfacies assemblage

----- Open space structure-dominated

The samples in this type of carbonate rocks show fenestrae-rich fabrics in the undulating laminae and microbial mats. The fenestral laminite microfacies consist of light grey or dark, laminated and mm-scale-layers of limestone with stylolites arranged sub-parallel to the laminations. The laterally discontinuous and altered stylolites, which are parallel to these laminates, indicate that these rocks had experienced somewhat deep burial diagenesis of pressure dissolution. This type of diagenesis probably preferentially affected particularly this facies, because of possible presence

of evaporitic minerals and because of higher porosity and thus compactibility. The cavities are filled with white spary calcite which is attributed to early diagenesis (Flügel, 2004), but also by dog tooth like calcites or are sometimes followed by idiomorph second generation quartz cements, filling the remaining space in the voids. The voids among the laminates imply that gas bubbles, which were produced by the degradation of organic matter, once existent in the microbial laminae or by photosynthesis. The voids are conspicuous constituents of the limestones and form characteristic fabrics, some of which resemble blind windows within a dark wall. The abundance of fenestral structures in carbonate rocks suggest a shallow water realm ranging from intertidal to supratidal depositional facies and lagoon facies (Beukes, 1987).

In this study, fenestral fabrics consist of laminoid fenestrae (0.5 – 2 mm high) and irregularly formed and distributed fenestrae (5 mm – 10 mm diameter). The cavities in microbial matrix and laminations vary from <1 mm to 10 mm in diameter, and are diagenetically filled with fibrous to equant calcite cements, quartz, and/or with internal sediment.

In **A**, mm-sized cavities are infilled with micritic limestones (arrow a). The microfracture (arrow b) cuts the centre of cavity and is filled with blocky calcite. In **B**, the outline of the cavities is lined with dark microbial laminates (arrow). The **C** and **D** show organic-rich microbial bindstones with birds eyes. The < 1 mm - scale voids are horizontally elongated and are filled with carbonate cements. In **E**, mm-sized, rounded and spar-filled voids (arrow a) are associated with microbial remains (arrow b). **F** is an enlargement of the microbial laminates with dark dolomites. In **G** and **H**, the laminates pass upward into netlike fenestral frames. Late diagenetic blocky calcite (arrow a), arranged in between dark laminated layers (arrow b) is shown in **H**. The dark irregular net delineates recrystallization boundaries along which organic matter was enriched. The carbonate minerals were subsequently altered and partly micritized or recrystallized, evidencing a complicated multiphase alteration of these samples.

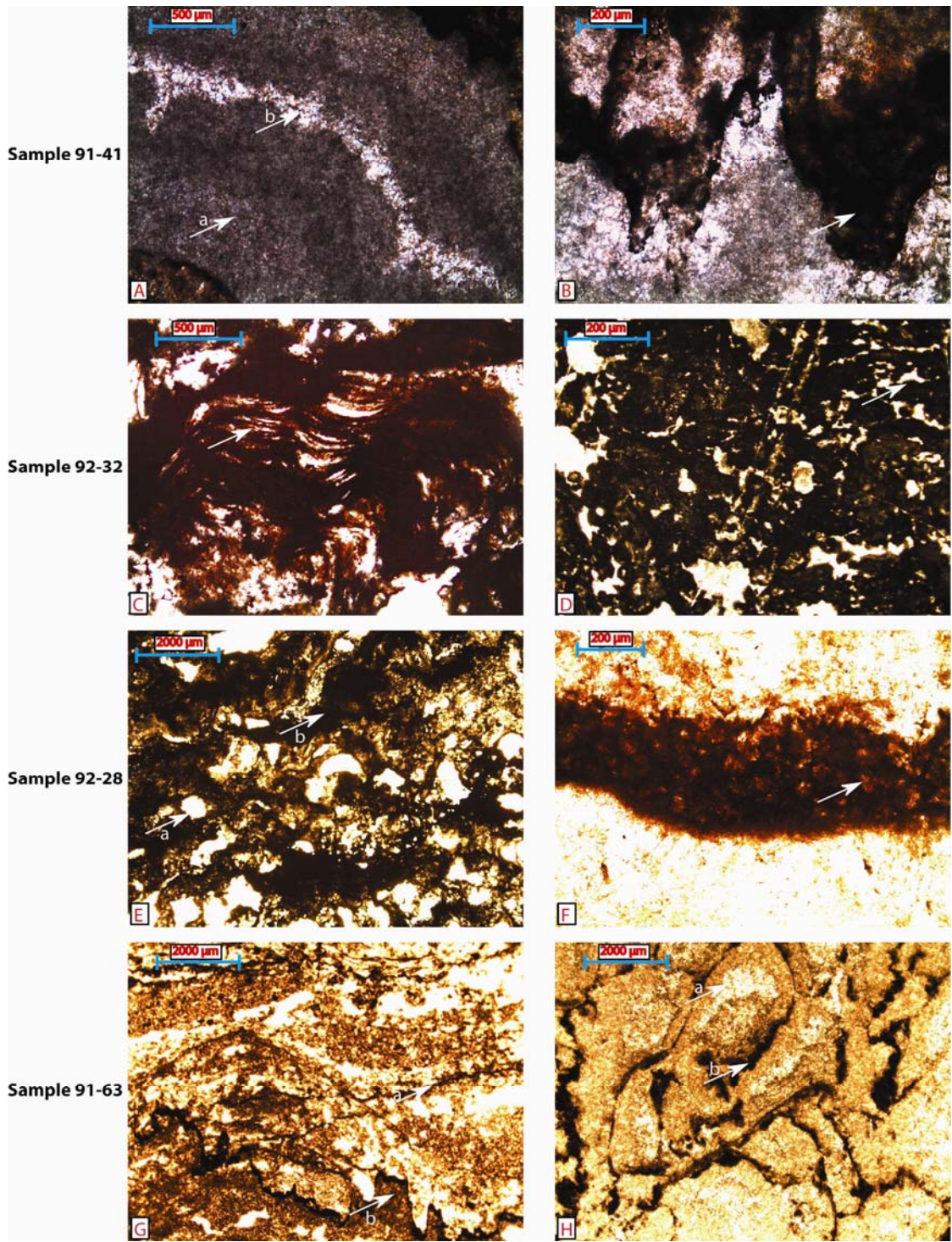


Figure 4.4 Open space structure stromatolites in the intertidal to supratidal microfacies assemblage. The morphology is highly affected by sedimentation in shallow water and the post-depositional diagenesis and recrystallization. Stylolites and microbial mats can be recognized in the thin section. (A) Enlargement of fenestrae in the thin section of sample 91-41. Note the centre of cavities may be cut by linear microfractures. Recrystallization seams paralleling the lamination and altering the cavities are present as well (arrow b). (B) The cavity is outlined with microbial laminates (arrow). (C) Microbial mats

(arrow) are locally recognized in the thin section of sample 92-32. (D) Laterally elongated open spaces within microbial laminates (arrow). (E) Rounded open spaces (arrow a) within microbial laminates (arrow b) in the thin section of sample 92-28. (F) Enlargement of microbial laminates in E. (G) Laterally linked microbial laminates (arrow a) and stylolites (arrow b) in the bottom thin section of sample 91-63. (H) Irregularly shaped, net-like fenestral frames (arrow b) were filled with blocky re-precipitate calcite (arrow a) at the top of thin section of sample 91-63.

Interpretation of Microfacies Assemblage

Open space structures and fenestral fabrics are usually formed in shallow, near-coast supratidal and upper intertidal environments (Flügel, 2004). The fenestral fabrics, which formed in tidal flat, are generally thought to be attributed to diagenetic processes, associated with the degradation of the microbial mats (Hofmann et al., 1980).

Laminoid fenestrae are probably formed by wetting and drying of carbonate mud in supratidal settings (Shinn, 1968; Flügel, 2004) and/or drying of the microbial mats and their adjacent sediments in intertidal to supratidal settings (Logan, 1974). Irregular fenestrae are probably formed by desiccation/lithification in frequently exposed sediments and/or during burial of pustular microbial mats in tidal flats.

The voids in the samples of figure 4.4, which are filled with micritic and blocky calcite, indicate re-precipitation of calcite minerals during diagenesis. The observed stylolites among the microbial mats suggest deep burial diagenesis (pressure dissolution) after the carbonate formation. As the fenestrae are mostly associated with the microbial laminates and organic-rich microbial remains (Figure 4.4), it is suggested that these fenestrae are the preferential sites of gas accumulation. The gas bubbles are possibly originated from microbial decay and/or oxidation within the microbial mats.

The samples shown in Figure 4.4 were selected from the Reivilo, Klipfontein Heuwels, Klippan and Kogelbeen Formations. Grover and Read (1978) suggested that tidal flat sedimentation should keep pace with contemporary subsidence or sea level rise so that the depositional surface remained in tidal/supratidal zones for long

periods, causing complex overprinting of fenestral fabrics. Such a model was also proposed for the Neoproterozoic carbonates of parts of the Nauga Formation, investigated by Altermann and Herbig (1991). The presence of fenestral fabric in this microfacies assemblage in several formations indicates that tidal-flat facies of the middle Campbellrand Subgroup is widespread.

4.1.2 Shallow subtidal to intertidal microfacies assemblage

----- Columnar stromatolite-dominated

The columnar stromatolites show continuous and regular updoming laminae, which are vertically followed by intervals of irregular lamination, with different colour and minerals. The stromatolites, in thin sections, show parallel and divergent bifurcating columns, solitary columns and sporadically, laterally linked columns with vertically equal width or upward widening club-shape (Altermann, 2008). Microbial laminations within the columns are clearly recognized by alternating dark organic matter-rich and pale micrites. Sediment between the columns and within the lamination is usually of sparitic and stromatolitic debris, sometimes also of micritic limestone. Bifurcating and parallel, laterally linked columnar stromatolites show upward widening or vertically equal width of columns in Figure 4.5. The width of columns varies from millimetre to centimetre. Spaces between columns are filled with fine-grained carbonates constituting, stromatolitic debris, pellets and micritic limestone.

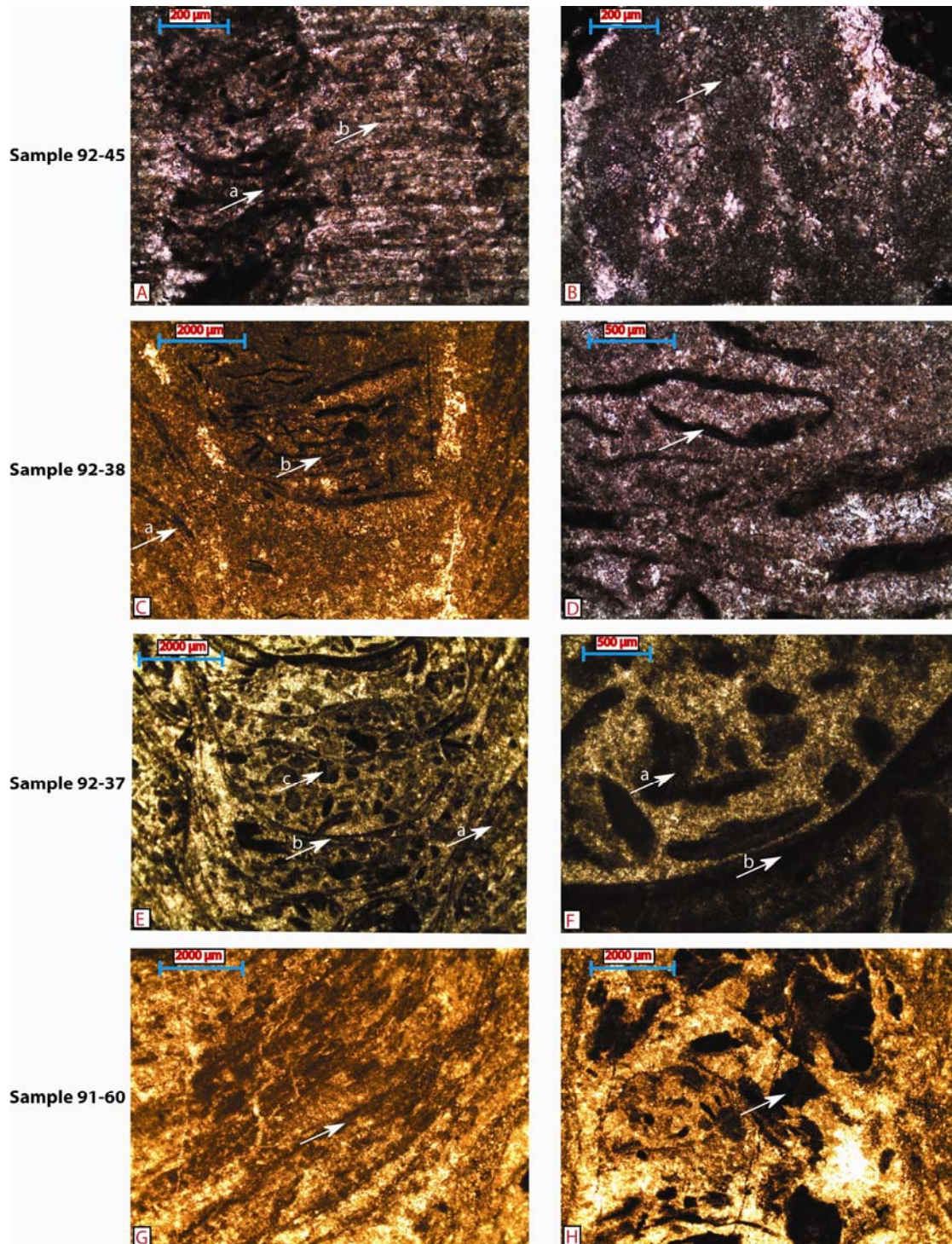


Figure 4.5 Columnar stromatolites and inter-columnar space, formed in the shallow subtidal to intertidal microfacies assemblage. The morphology is highly affected by the sediment input and trapping and binding activity. Microbial and mechanical trapping and binding of sediment are very common in the formation of the columnar stromatolites. (A) Enlargement of extremely fine lamination of organic matter (arrow a) and recrystallized calcite (arrow b) in the thin section of sample 92-45. (B) Micritic limestone (arrow) between the columns, white speckles are recrystallized, neosparitic parts spots. (C) Microbial laminates (arrow a) of the columnar stromatolites and sediment (arrow b) trapped

between the columns in the thin section of sample 92-38. (D) Enlargement of the stromatolitic debris between the columns. (E) Stromatolitic debris trapped between the columns (arrow c) and within the columnar laminae (edge of the column) (arrow a). Laterally linked stromatolites (arrow b) are shown in the thin section of sample 92-37. (F) Enlargement of the stromatolitic debris (arrow a) between the columns and laterally linked lamina between two columns of stromatolites (arrow b). (G) Microbial lamination (arrow) of the columnar stromatolites in the thin section of sample 91-60. (H) Microbial remains trapped between the columns (arrow).

In this group, columnar stromatolites show fine upward updoming laminations in the interior of each column and sporadically laterally linked, bowl-shaped laminations overgrowing the accumulated detritus between columns (Figure. 4.5). In **A** and **B**, the dark lamination is rich in organic-matter and light lamination is of recrystallized calcite. Partly laterally linked stromatolites are shown in the thin section of sample 92-45. Very fine micritic limestone is shown between the columns. Sediment trapping and binding columnar stromatolites and microbial debris with sediments between columns are shown in **C** and **D** of sample 92-38. In **E** and **F**, microbial lamination (arrow a) constitutes the walled columns in sample 92-37. The walls of columns are constrained by remnant organic matter (arrow b) from microbialite overgrowth. Between the interlinked lamina, clastic carbonate debris of pellets (arrow c) is concentrated. The pellets also delineate and are bound along the column rims, where they are overgrown by the next lamina generation, stabilizing the pellets on the steep rims. In **G** and **H** of sample 91-60, microbialite debris is visible in the space between laterally linked stromatolitic columns, as in sample 92-37 but with more abundant micrite in between (partly recrystallized to neosparite).

Interpretation of Microfacies Assemblage

Columnar stromatolites were abundant and widespread in the Precambrian but are rare in modern marine environments (Awramik and Riding, 1988). Columnar forms represent more than a half of morphological forms, described from Precambrian stromatolite assemblages (Raaben, 2006), and usually formed in shallow subtidal to intertidal marine environment. Columnar stromatolites of various morphologies are preserved in the entire Campbellrand Subgroup carbonate platform.

The samples described above show both optically oriented crystals and clastic grains preserved within the columns which implies a combination of directly precipitated and trapped origin for the grains constituting of these stromatolites (Sumner, 1997; Grotzinger and Knoll, 1999; Altermann, 2008). The various sediments are trapped and bound or precipitated by the growth of microbial mats. The varying morphology of columnar stromatolites and the sediment between and within the columns, represent an extensive variety of depositional paleo-environments within the Ghaap Group carbonate platform. The change in infilling microbialitic clasts, sparitic and pelletal grains between columns, indicates an agitated wave and/or current action between the columnar bioherms and biostromes. Variations in the overall morphology of laminations are probably due to the changes in influx of detrital micrite and carbonate sand, scouring of strong currents, mat growth and precipitation within the mats.

The samples in figure 4.5 are mainly selected from the Reivilo and Kogelbeen Formations. The various columnar stromatolites of the Ghaap Group represent shallow water, wave-agitated facies for the carbonate deposition, ranging from shallow subtidal to intertidal for this microfacies assemblage.

4.1.3 Deep subtidal microfacies assemblage

----- Finely laminated microbial mat-dominated

The samples in figure 4.6 are from the Gamohaan Formation, and show fine laminated microbial mats, conical, microbial supports between the laminae, and voids filled with pure carbonate cement but barren of matrix between the sub-vertical supports and the sub-horizontal laminae. Regular layers of soft sediment deformation and brecciation are very common in these microbialites, and usually terminate each growth cycle of several cm thicknesses. After deposition of some detrital material on the contorted and interrupted lamina, a new growth cycle starts with a sharp boundary. The finely laminated microbial mats display contorted lamination with light, fibrous and blocky calcite cements. Dark microbial mats are mainly finely and smoothly, flat laminated, sometimes also eroded and rolled up by wave and/or currents. The deformation is visibly in soft sediment. Little to no very fine siliciclastic sediment

occurs in these carbonate rocks, besides at the end of each growth cycle (Sumner, 1997; Altermann, 2008). The contorted and slumped microbial lamination strings show generally only a weak compaction, remaining of high curvature, with laminae not broken and preserving empty space, later filled with blocky calcite during diagenesis. Anhedral and microsparitic dolomite crystals penetrate into the dark microbial laminae and the space between the laminae. This type of mat growth and sedimentation is typical for the upper parts of the Gamohaán Formation carbonate rocks.

In this study, finely laminated microbial mats consist of dark and contorted laminations, with voids between the contorted lamina, filled with blocky calcite, and of coiled structures of microbial laminae. In **A**, cusped microbial mats (arrow a) are encased in calcite crystallized in voids between the lamina (arrow b) in the thin section of sample 92-56. The cusped form of the laminae is interrupted by regularly spaced columnar, conical supports as described by Sumner and Grotzinger (2004) and Altermann (2008). In-between the lamina and supports the calcite must be of diagenetic origin. No sediment trapping is evident. Any detrital sediment grains are absent from such voids closed between the lamina. The lamination is mostly not updoming but rather dish-shaped. In **B**, contorted dark laminae (arrow b) separate the previously water-filled, now calcite filled, voids between the laminae strings and the upper fine laminated microbial mats (arrow a). In **C**, contorted finely laminated microbial mats (arrow b) cemented by blocky and equant radial calcite (arrow a), are visible in the thin section of sample 92-57. **D** shows an enlargement of the dark and light intercalations of fine microbial mats. All above details of the figures evidence absent of trapping and binding of sediment in this facies. In **E** and **F**, contorted fine microbial mats, as described above, are shown in the thin section of sample 92-60. Fine laminated microbial mats with mat parallel recrystallization seams are visible in the thin section. In **G**, microbialites exhibit coiled, dark laminae on the top of finely laminated microbial mats in the thin section of sample GAS1-558. Similar structures were described from outcrops of the upper Gamohaán Formation and from the upper Nauga Formation of the Prieska facies (Altermann and Nelson, 1998; Altermann, 2008). The **H** shows an enlargement of the single coiled dark lamina. The microbial laminations are inter-layered with light laminae of fibrous and blocky calcite.

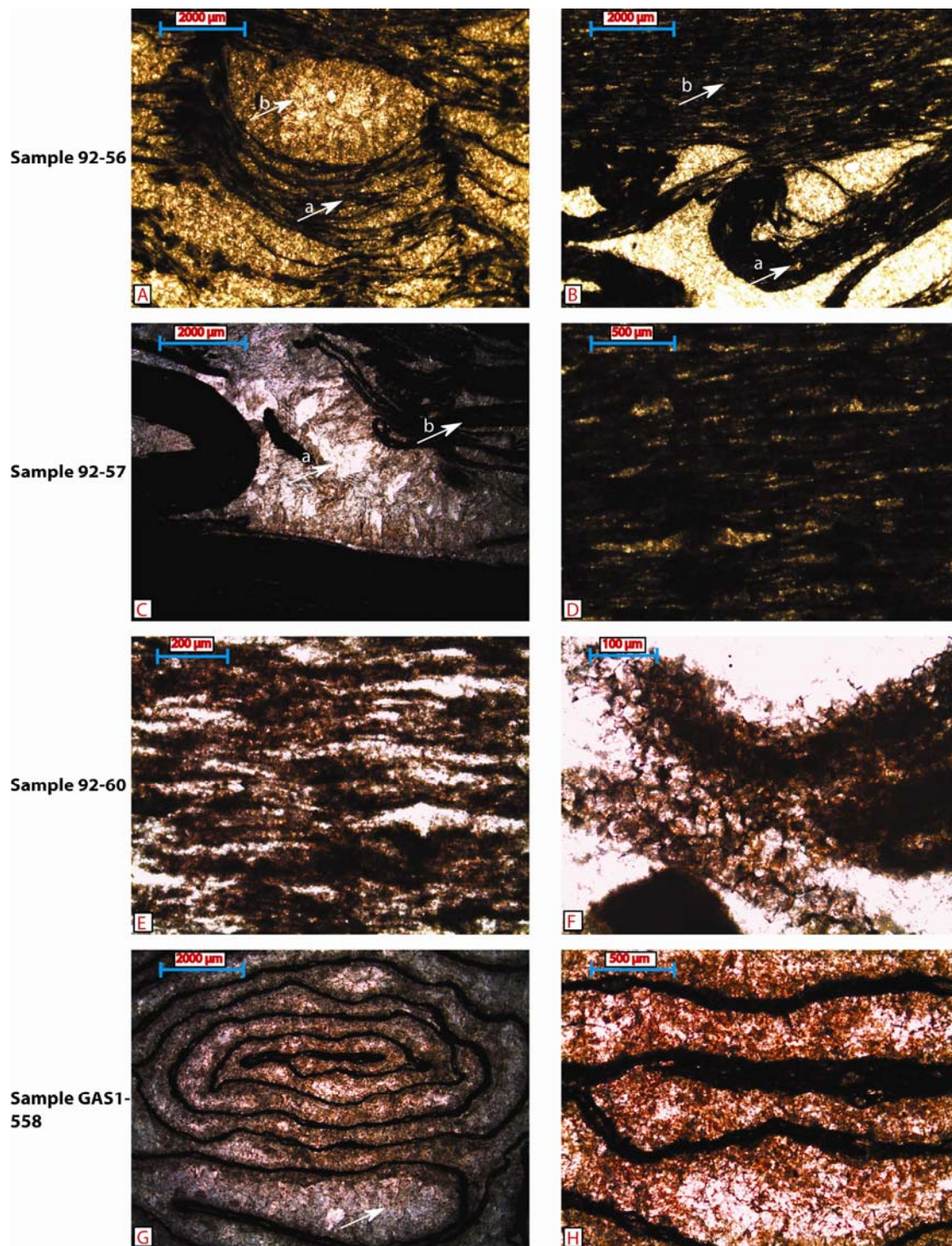


Figure 4.6 Contorted, fine microbial mats of the deep subtidal microfacies assemblage. (A) The dark microbial mats (arrow a) are encased in light calcite (arrow b) in the thin section of sample 92-56. (B) The fine laminated microbial mats (arrow a) on the top of contorted lamination (arrow b). (C) Blocky and equant radial calcite (arrow a) cemented between the convoluted fine laminated microbial mats (arrow b) in the thin section of 92-57. (D) Enlargement of dark and light laminations in the fine microbial mats. (E) Finely laminated microbial mats with mat parallel recrystallization seams in the thin section of 92-60.

(F) Enlargement of recrystallized carbonate minerals. (G) Coiled organic-rich dark laminae on the top of the convoluted finely laminated microbialites in the thin section of sample GAS1-558. (H) Enlargement of the coiled dark lamina. The coiled laminae are inter-layered with light laminae of fibrous and blocky calcite.

Interpretation of Microfacies Assemblage

The fine laminated microbial mats are usually formed in a relatively deep water environment with lower water energy. The folded and rolled up structures of dark, microbial laminae suggest that they were flexible, cohesive and unmineralized before and/or during their deformation. The preservation of voids between little compressed and slump-generated folds in microbial mats implies an early cementation and lithification before compaction. Well preserved laminae are typically several, to 15 μm thick. The thick contorted microbial mats indicate the copious growth of microbial communities and the high burial rate of organic matter during carbonate deposition, thorough lithification however must have significantly preceded burial and compaction.

Many mechanisms can control the formation of microbial laminae. The laminations are usually interpreted as the periodical response of the microbial community to the microbial growth and its surrounded environment. Among these fine laminations, the soft-sediment disruptions are preferentially interpreted as the effects of wave, episodic currents and/or storm events (Wright and Altermann, 2000; Sumner and Grotzinger, 2004). The voids, within the microbial mats, increase their size and become more irregular in their shape, upward within the beds. This may be the result of gas bubbles, which are generated by organic degradation and accumulating preferentially and increasingly in the upper parts of the unconsolidated mat layers (Wright and Altermann, 2000). However because the cavities between the lamina are mostly not updoming, this explanation is somewhat questionable. An alternative explanation would be that the mats grew preferentially at the apices of the conical supports as tufted mat and then linked laterally enclosing large cavities between the lamination. Because of the absolute lack of sediment trapped in the depressions of the cavities and in the laminae, the conditions of growth must have been very stable lacking suspension. The successive enlargement of cavities upward eventually leads

to a mat of low stability that resulted in slumping, triggered by storm waves or current. This is evident also from accumulations of detritus of mud and carbonate pellets on top of such slumped horizons (comp. Altermann, 2008). The continuous, rolled up laminae on top of the convoluted laminae are somewhat flattened by compaction. The laminae of the microbial mats are unbroken and filled with cements but not completely collapsed. This may indicate that the space between organic strands was water-filled and the sediment brought by storm event was more compactable and less rapidly lithified than the undisturbed mat (Wright and Altermann, 2000).

The sample GAS1-558 was collected from 558m depth of Hotazel core and the other samples were all selected only from the Gamohaam Formation in Kathu borehole core. A 100 m thick section of the Gamohaam Formation in Kathu borehole consists exclusively of calcite in stromatolites and contorted mats (e.g. Altermann and Nelson, 1998). The delicate morphology of the microbialites, the lack of evidence for scouring beside of the directly slumped horizons, and the absence of clastic carbonate between the laminae, suggest a deep subtidal, sub-fair-wave-base depositional environment for these microbialite forms in the Gamohaam Formation. However, Gandin et al. (2005) interpreted the upper part of this facies of the Gamohaam Formation as “vanished evaporites” and shallow water environment with evaporate precipitation within microbial mats and laminates. The subsequent dissolution, and/or solid, ductile flowing of recrystallizing evaporitic sulphate minerals, caused the collapse and slumping, whereby the evaporitic minerals were subsequently replaced by carbonate in the upper Gamohaam Formation.

STRATIGRAPHIC VARIATIONS OF
CARBON AND OXYGEN
ISOTOPES IN THE GHAAP
GROUP CARBONATES

5. Stratigraphic Variations of Carbon and Oxygen Isotopes in the Ghaap Group Carbonates

The principal difference of the sedimentary environments between modern and Precambrian lies in the variability of rates and intensities of the processes, including weathering, erosion, transport, deposition, lithification and diagenesis (Wright and Altermann, 2000; Eriksson et al., 2005). Numerous important geological events have been identified in the global geological evolution during the Precambrian (Eriksson et al., 2004). The activity of oxygenic photosynthesis was possibly promoted by the emergence of large continents and extensive shallow-marine environments around the continents, because photosynthetic life can not inhabit the sea tens of meters below the surface (Berkner and Marshall, 1965). The oxygen produced by the biological photosynthesis was firstly consumed by oxygenation of reduced minerals (e.g. Fe^{2+}) in seawater (e.g. Walker, 1979), and subsequently it increasingly accumulated in the atmosphere (Komiya et al., 2008). Additionally, independently of photosynthetic activity, the major growth of continental crust and the consequent enhanced sediment deposition in the oceans, caused possibly a continuous rise of $p\text{O}_2$ in the Precambrian atmosphere from c. 3.5 Ga on (Des Marais, 1994, 1997; Godderis and Veizer, 2000).

Numerous studies (Holland, 1984; Farquhar et al., 2000; Kasting, 2001; Pavlov et al., 2001; Ono et al., 2003; Canfield, 2005; Ohmoto et al., 2006; Ono et al., 2006; Kendall et al., 2010; Voegelin et al., 2010) have been focused on the concentration and evolution of free oxygen in the atmosphere and ocean, and suggest a progressing, pervasive increase of free oxygen in the late Archean shallow water domain. Since oxygen is produced by photosynthesis, next to other non-biological processes of minor importance, the physical and chemical properties of seawater, marine oxidation-reduction states, mineral formations and cycling of elements within the oceans varied as the results of different marine chemical reactions with progressing evolution and oxygen levels. Carbonate precipitation depends on the composition of seawater and a variety of the above factors (T, DIC, $p\text{CO}_2$, pH), thus changes in these factors may be reflected in the mechanisms of carbonate precipitation. The Campbellrand Subgroup carbonate rocks, associated with abundant stromatolites,

record the evolution of life involved in the carbonate deposition and thus, the cycles of C and O isotopes in the Precambrian atmosphere and ocean.

Studies of $\delta^{18}\text{O}$ values in carbonate rocks through geological time show a continuously increasing trend and have a biggest shift in the Phanerozoic (Veizer and Hoefs, 1976; Kasting et al., 2006). The depleted $\delta^{18}\text{O}$ values observed in most Precambrian marine carbonate rocks indicated that carbonate rocks formed during this time preserved the isotopic signature of ancient seawater, and not only the post-depositional conditions (Lohmann and Walker, 1989; Burdett et al., 1990; Shields et al., 2003; Kasting et al., 2006). Studies on carbonate $\delta^{13}\text{C}$ values (Veizer and Hoefs, 1976; Schidlowski et al., 1983; Des Marais, 2001; Knauth and Kennedy, 2009) through geological time, suggest that marine carbonate $\delta^{13}\text{C}$ values are relatively stable through the last 3.5-billion-year geological history with a variation within $\pm 3\text{‰}$. Large excursions in carbonate $\delta^{13}\text{C}$ values are only confined to great events in the stratigraphic record such as mass extinctions, global glacial epochs and periods of enhanced evolutionary radiation.

Stratigraphic variations in the carbon and oxygen isotopic composition of Ghaap Group marine carbonate and organic matter are observed here for the reconstruction of paleo-environment and refining of stratigraphic interpretation.

5.1 Carbon Isotopes

5.1.1 Carbon isotopes in the general geological processes

The isotopic composition of C in marine carbonate rocks through Earth history depends on several factors like biological productivity, decomposition of organic carbon and preservation of organic carbon (Figure 5.1). Previous studies of carbonate isotopes in the Griqualand West basin rocks of around 2.5 Ga indicate that the $\delta^{13}\text{C}_{\text{carb}}$ values are slightly less ^{13}C -enriched than modern values (Veizer et al., 1990; Watanabe et al., 1997; Ripperdan, 2001; Frauenstein et al., 2009). Furthermore, carbon isotopic values from the lower Ghaap Group imply that carbonate carbon experienced a positive excursion during this time.

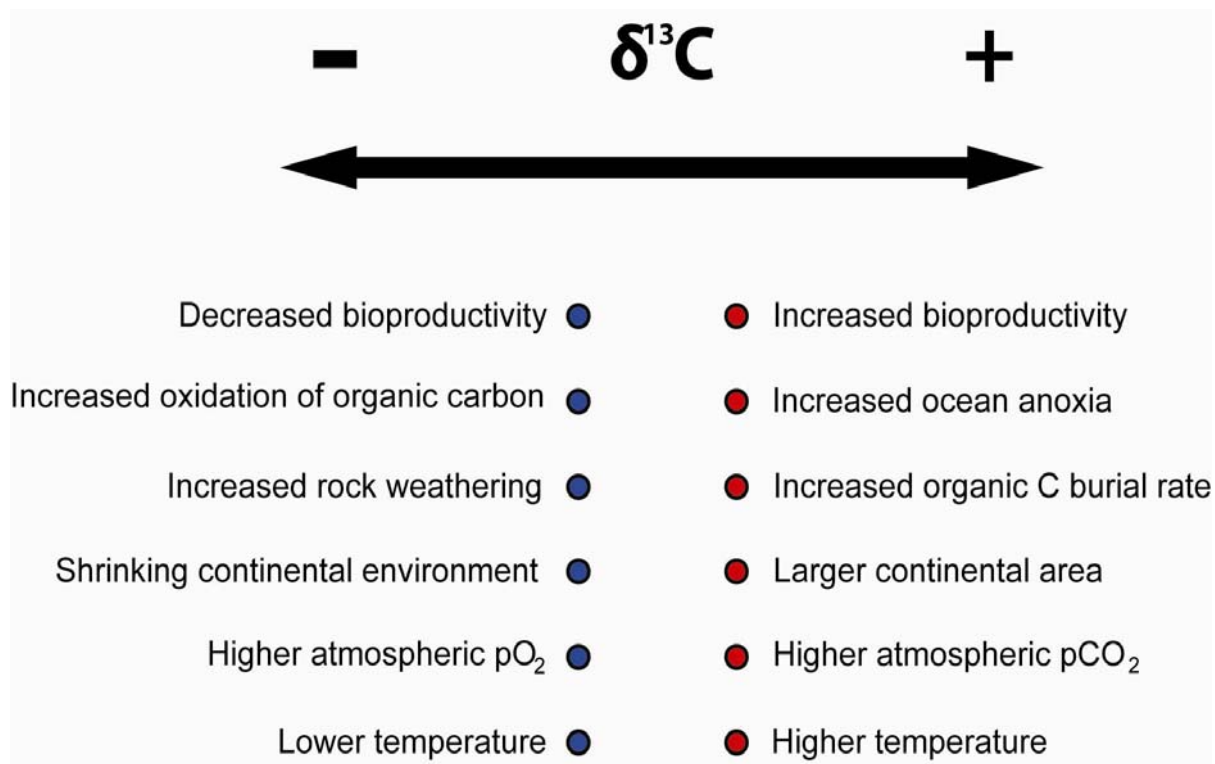


Figure 5.1 Selected environmental factors and their influence on carbonate $\delta^{13}\text{C}$ values (Condie et al., 2001; Des Marais, 2001; Faure and Mensing, 2005; Allègre, 2008; Hoefs, 2009).

The fractionation of carbon isotopes employs mainly two different mechanisms: (1) Exchange of carbon isotopes in the system of $\text{CO}_2 + \text{HCO}_3^-$ causes marine carbonate relatively enriched in ^{13}C . In the system of $\text{CO}_2 + \text{CH}_4$, which is affected by volcanic out-degassing, exchange of carbon isotopes causes marine carbonate relatively depleted in ^{13}C (2) The dynamic effect in the photosynthesis process, enriches the ^{12}C in organisms and their remains and ^{13}C is depleted in organic-rich marine carbonates and in organic carbon. Among the impact factors on carbon composition in marine carbonate (Figure 5.1), organic oxidation and relative burial are the most important influences on the $\delta^{13}\text{C}$ values.

When abundant organic carbon is rapidly buried, the uptake of light carbon (^{12}C) by organisms will cause a high concentration of ^{12}C in the sediments and in the living biosphere, and thus a relatively increased concentration of ^{13}C dissolved in seawater. Subsequently, this phenomenon increases the $\delta^{13}\text{C}$ values in carbonate rocks precipitated from this sea water. Because sea-level rises provide favorable conditions

for sedimentary burial of organic carbon through enhanced sediment accumulation; therefore, organic matter can survive the post-depositional decomposition and sink below the boundary of Surface Ocean where water is still oxidized. Considering that over 99% of the primary carbon productivity is rapidly oxidized in the surface ocean (Sundquist, 1985), the burial rates of marine organic carbon are apparently controlled by the seawater depth and then reflected by the $\delta^{13}\text{C}$ values of carbonate rocks.

Because temperature has a relatively small effect on carbon isotope fractionation, the variations in $\delta^{13}\text{C}$ values of carbonate minerals most commonly reflect the primary isotopic composition of the dissolved inorganic carbon of the solution from which they precipitated, independently of later burial history (Hoefs, 2009). Accordingly, fluctuations in $\delta^{13}\text{C}$ values of marine carbonate rocks represent secular variations of $\delta^{13}\text{C}$ in ocean water and are indicators of tectonic, climatic, oceanographic and evolutionary changes that influence the carbon cycling (Des Marais, 1994; Condie et al., 2001; Des Marais, 2001).

Another factor that can affect the fractionation of C in marine environment is the metamorphic and volcanic flux of CO_2 . Original mantle values for $\delta^{13}\text{C}$ are estimated to be approximately -5‰ (Kump and Arthur, 1999; Condie et al., 2001; Des Marais, 2001) which is less ^{13}C enriched than the normal carbonate $\delta^{13}\text{C}$ values. Condie (2001) and Condie et al. (2001) have suggested that during a mantle plume event, the ratio of $\delta^{13}\text{C}_{\text{org}}$ to $\delta^{13}\text{C}_{\text{carb}}$ is controlled by hydrothermal fluxes on the seafloor, volcanic outgassing, anoxia, and ocean currents. As the rate of organic carbon burial increases, there should exist a corresponding increase in the value of $\delta^{13}\text{C}_{\text{carb}}$. Kump and Arthur (1999) experimentally determined that periods of increased volcanic activity have a larger effect on organic carbon than on carbonate carbon isotopes. The increase of pCO_2 in the atmosphere, caused by the extensive volcanic eruptions, increases the available amount of carbon dioxide (Dissolved Inorganic Carbon or DIC) for marine photosynthetic organisms through the exchange between ocean water and atmosphere. This leads to an increase in the burial of anomalously light organic matter and to sedimentation of anomalously heavy carbonate carbon counterparts.

Carbonate rocks record the isotopic composition of Dissolved Inorganic Carbon (DIC) in sea water, from which they precipitate, with an offset of 1‰, due to thermodynamic isotopic equilibrium (Morse and Mackenzie, 1990). In the late Archean stromatolitic carbonate environments, the isotopic composition of DIC was strongly influenced by the distribution, concentration and transportation of DIC between the microbial communities and the surrounding water (Sumner and Grotzinger, 2004). Thus, we can use the $\delta^{13}\text{C}_{\text{carb}}$ values as reliable indicators of the DIC isotope ratios in early Earth environments. Several factors control the $\delta^{13}\text{C}_{\text{org}}$ isotopic composition of sedimentary organic matter, including source effects (isotopic composition of the DIC), kinetic and equilibrium isotope effects associated with the C assimilation. When the isotopic composition of the C source is recorded in the $\delta^{13}\text{C}_{\text{carb}}$, the difference between $\delta^{13}\text{C}_{\text{carb}}$ and $\delta^{13}\text{C}_{\text{org}}$ ($\Delta\delta^{13}\text{C}_{\text{org-carb}} = \delta^{13}\text{C}_{\text{org}} - \delta^{13}\text{C}_{\text{carb}}$) reflects the C cycling between the atmosphere and ocean during this period and usually is used as a valuable proxy for evolution of life (Thomazo et al., 2009).

5.1.2 Carbon isotopes in the Ghaap Group carbonate rocks

The carbon isotopic composition of the Ghaap Group carbonates reveals a distinctive pattern. The $\delta^{13}\text{C}$ values are highly fluctuating, but in general, they are slightly negative and show an increasing trend from the lower to upper stratigraphic levels. Although the determined stratigraphic variations in carbon isotope composition of late Archean carbonate rocks show a generally increasing trend in $\delta^{13}\text{C}_{\text{carb}}$ values through the entire stratigraphic succession (Figure 5.2), they fluctuate significantly in time. The markedly higher fluctuation of $\delta^{13}\text{C}$ values during the middle Campbellrand Subgroup succession indicates that the depositional environment was generally a tidal flat ranging from deep subtidal to supratidal, which is in accordance with the interpretation from outcrop and microfacies (Altermann and Siegfried, 1997; Altermann and Nelson, 1998). A $\delta^{13}\text{C}_{\text{carb}}$ excursion (from around -7‰ to around -0‰, in Figure 5.2) has been found between the Schmidtsdrif Subgroup and Campbellrand Subgroup. The $\delta^{13}\text{C}_{\text{org}}$ values (-38‰ to -20‰) show a typical range of isotopic composition of organic C reservoir in most organic-rich sediments of different ages from 3.5 Ga to 2.0 Ga, which could be used as the evidence of the kinetic effects of

carbon assimilation pathways and proxy for life in sedimentary rocks (Klein et al., 1987; Thomazo et al., 2009).

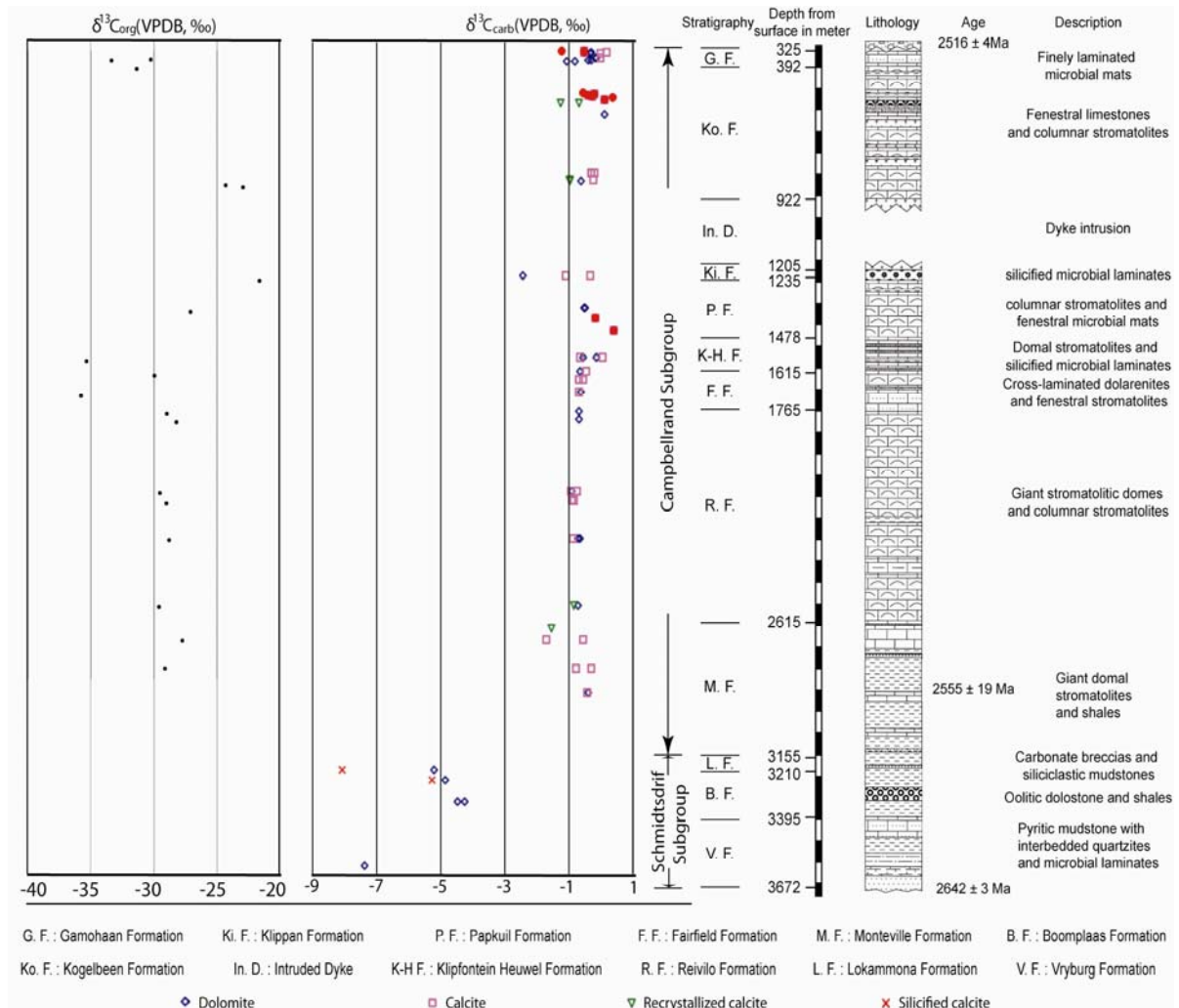


Figure 5.2 Stratigraphic profiles of carbonate $\delta^{13}\text{C}_{\text{carb}}$ and $\delta^{13}\text{C}_{\text{org}}$ values through the Ghaap Group from the Kathu borehole, South Africa. The sedimentological descriptions are based on Altermann and Siegfried (1997) and Altermann and Nelson (1998). Dates of 2555 ± 11 Ma and 2516 ± 4 Ma are from Altermann and Nelson, 1998; the date of 2642 ± 3 Ma is from Walraven and Martini, 1995. Five samples (Table 3.1) were collected from other drill cores because of unavailability of suitable material for analysis in the Kathu borehole and are colored in red for comparison.

5.2 Oxygen Isotopes

5.2.1 Oxygen isotopes in the sedimentary processes

The oxygen isotopic composition in marine carbonate rocks is attributed to the temperature and the $\delta^{18}\text{O}$ values of the surrounding seawater where the carbonate formed. Compared to the largely immobile carbon isotopic compositions of marine

carbonate rocks, the $\delta^{18}\text{O}$ values can be easily changed by various post-depositional diagenetic modification processes, including the interaction between carbonate rocks and meteoric and/or hydrothermal fluids, recrystallization-and-dolomitization and deep burial diagenesis (Veizer and Hoefs, 1976; Allan and Matthews, 1982; Killingley, 1983; Choquette and James, 1987; Rollinson, 1993). Selected factors that can change the oxygen isotopic composition in marine carbonate rocks are shown in Figure 5.3.

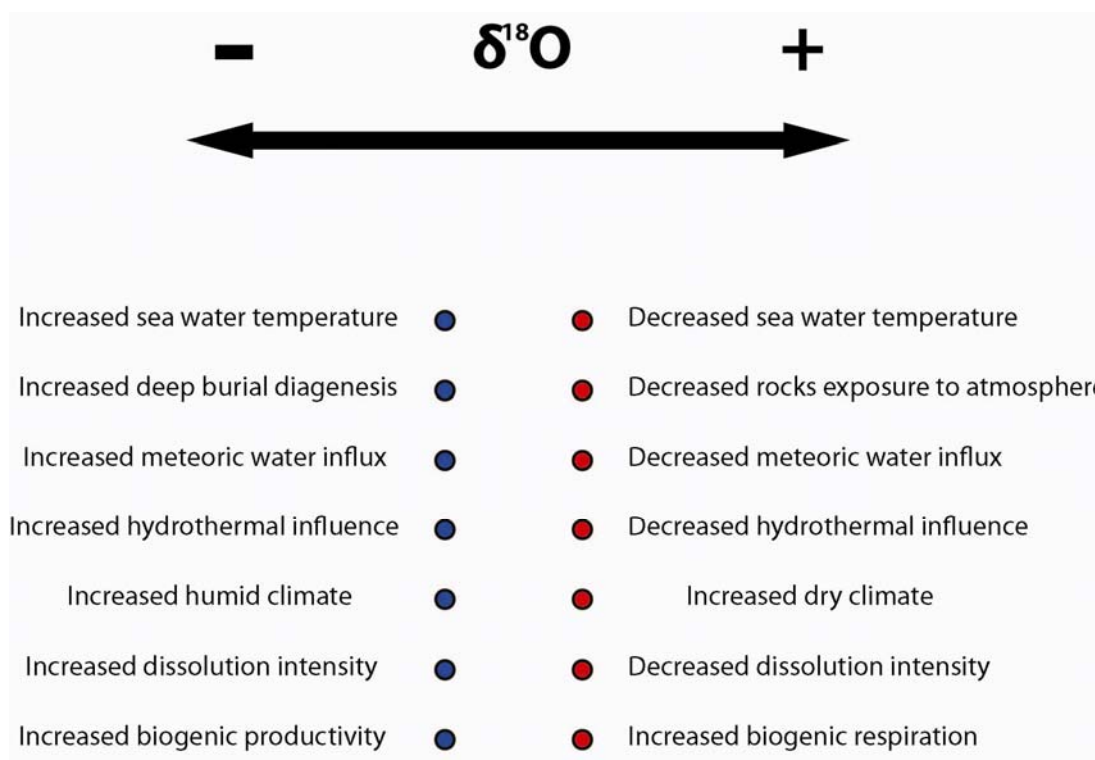


Figure 5.3 Selected environmental factors and their influence on carbonate $\delta^{18}\text{O}$ values (Condie et al., 2001; Des Marais, 2001; Faure and Mensing, 2005; Allègre, 2008; Hoefs, 2009).

Because of relatively large effects of temperature on oxygen isotope fractionation in seawater (O'Neil et al., 1969; Friedman and O'Neil, 1977; Kim and O'Neil, 1997; Kim et al., 2007), variations in $\delta^{18}\text{O}$ values of carbonate minerals most commonly reflect the changes in original seawater temperature or the temperature of diagenesis. Fractionation of oxygen isotopes between carbonate and water is highly temperature dependent, not only during sedimentation (precipitation from watery solutions) but also during diagenesis and metamorphism, as a function of temperature (over the temperature range 0 – 500 °C, O'Neil et al., 1969). Based on the work of Friedman

and O'Neil (1977), Kim and O'Neil (1997) and Kim et al., (2007), T (temperature of the seawater) in Kelvin can be calculated from the below equation 5.1.

$$10^3 \ln \alpha_{\text{Cc-H}_2\text{O}} = 18.03 (10^3 T^{-1}) - 32.42 \quad \text{(Equation 5.1)}$$

After the formation of carbonate rocks, later water influx will have additional effects on their oxygen isotopic composition, because of the intensive exchanges between carbonate minerals and e.g. meteoric, formational and/or metamorphic water. Thus, measurements of the oxygen isotopic composition of marine carbonate rocks can serve as indicators of the seawater temperature and of post-depositional diagenetic processes. The $\delta^{18}\text{O}$ values of individual depositional and diagenetic carbonate components were used to constrain the diagenetic environments and the extent of diagenetic modifications in this thesis.

5.2.2 Oxygen isotopes in the Ghaap Group carbonate rocks

Determined stratigraphic variations in oxygen isotope composition are shown in Figure 5.4. The Ghaap Group carbonate rocks reveal a distinctive $\delta^{18}\text{O}$ values pattern: $\delta^{18}\text{O}$ values of marine carbonates have an increasing trend upward in the lower formations up to the Papkuil Formation, and then display a decreasing trend upward from the upper Papkuil Formation to Gamohaam Formation (Figure 5.4). The $\delta^{18}\text{O}$ values are, in general, depleted but mostly in a narrow range between -8‰ to -10‰.

The Schmidtsdrif Subgroup shows a depleted $\delta^{18}\text{O}$ values range, from -13.4‰ to -11.5‰, while the younger Campbellrand Subgroup displays on average “heavier” and wider ranged $\delta^{18}\text{O}$ values of -15.9‰ to -5.0‰, but mostly within the range of -10‰ to -6‰. Two trends of $\delta^{18}\text{O}$ values can be traced from the Schmidtsdrif Subgroup to the Papkuil Formation of Campbellrand Subgroup (increasing from -13‰ to -8‰) and from the beginning of Papkuil Formation to Gamohaam Formation (decreasing from -7‰ to -12‰).

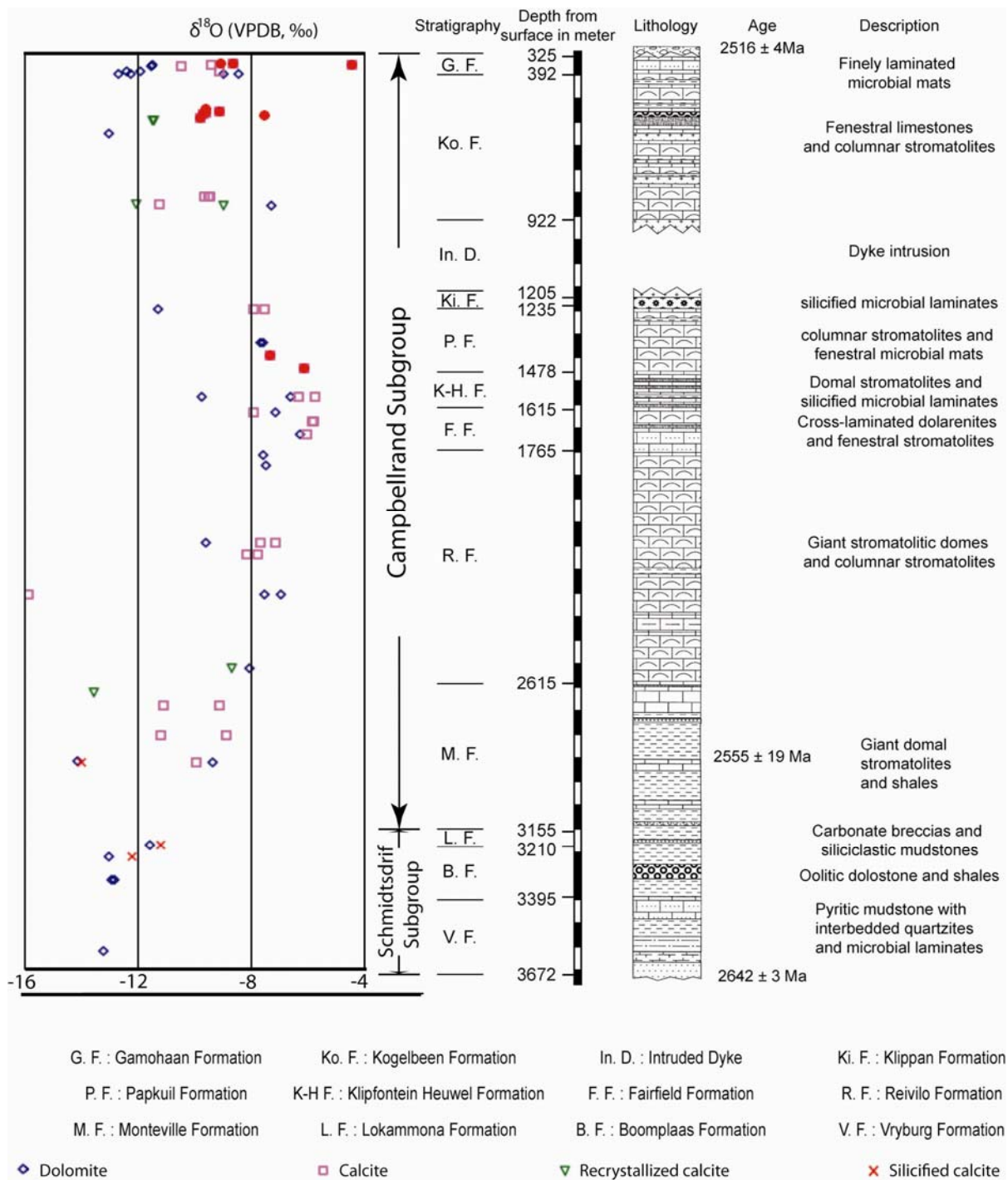


Figure 5.4 Stratigraphic profile of carbonate $\delta^{18}\text{O}$ values through the Ghaap Group from the Kathu borehole, South Africa. The sedimentary description is based on Altermann and Siegfried (1997) and Altermann and Nelson (1998). Dates of 2555 ± 11 Ma and 2516 ± 4 Ma are from Altermann and Nelson, 1998; the date of 2642 ± 3 Ma is from Walraven and Martini, 1995. Not all the measurements are measured on Kathu core samples: five samples were collected from other drill cores because of unavailability of suitable material for analysis in the Kathu borehole, and are colored in red for comparisons.

5.3 Carbon and Oxygen Isotopic Variations in the Ghaap Group Carbonates

In this study, carbon and oxygen isotopes have been measured for $\delta^{13}\text{C}_{\text{carb}}$, $\delta^{13}\text{C}_{\text{org}}$ and $\delta^{18}\text{O}$ values for the entire Ghaap Group as represented in the Kathu borehole (Figure 5.2, 5.4). Different amounts of samples were taken from different formations of the Ghaap Group according to the thickness of each formation in order to produce a representative study.

The isotopic composition of Ghaap Group carbonate rocks investigated herein, ranges from -7.3‰ to +0.4‰ for $\delta^{13}\text{C}_{\text{carb}}$ and from -21.6‰ to -38.6‰ for $\delta^{13}\text{C}_{\text{org}}$ respectively (Figure 5.2). These results largely correspond to the results published by others (Veizer et al., 1992a; Fischer et al., 2009; Frauenstein et al., 2009; Voegelin et al., 2010). The stratigraphically older Schmidtsdrif Subgroup at the base of the Ghaap Group, shows lower $\delta^{13}\text{C}_{\text{carb}}$ values, ranging from -7.3‰ to -4.2‰, while the younger Campbellrand Subgroup shows normal marine carbonate $\delta^{13}\text{C}_{\text{carb}}$ value ranges of -2.4‰ to +0.4‰. The Campbellrand Subgroup carbonates display a fluctuation in $\delta^{13}\text{C}_{\text{org}}$ values from -21.6‰ to -38.6‰ but generally show a decreasing trend upward from around -29‰ to -38‰ except for the sudden increase in both Klippan and Kogelbeen Formations which are respectively, underlying and overlying the thick dyke intrusion. The increases of $\delta^{13}\text{C}_{\text{org}}$ values are suggested that light ^{12}C (CH_4 and CO_2) is lost during metamorphism by thermal decomposition of sedimentary organic matter (Hunt, 1995; Des Marais, 2001).

The oxygen isotope compositions of Ghaap Group carbonate rocks ranges from -15.9‰ to -5.0‰ (Figure 5.4). The observed $\delta^{18}\text{O}$ values show a depletion of around -10‰ on average when compared to the Phanerozoic marine carbonate rocks, but are largely consistent with the results for the Precambrian, as published by others (Veizer et al., 1992a; Fischer et al., 2009; Frauenstein et al., 2009). The low oxygen isotope values of Ghaap Group carbonate rocks are thought to be influenced by isotopic exchange with meteoric and hydrothermal fluids in the course of diagenesis. Further studies are needed to disentangle these potential effects.

5.4 Stratigraphic Variation of Carbonate C and O Isotopes in the Ghaap Group Carbonate Rocks

Stable isotope analysis in marine carbonates including C and O isotopes were measured in this study. Based on the interpretation of microfacies studies, the co-variations between carbon and oxygen isotopic system during the late Archean Ghaap Group carbonate deposition provide key information not only on the microbial participation of the carbonate deposits, but also on the geochemical cycling of carbon and oxygen isotopes on the early Earth's surface.

The Neoproterozoic marine carbonates may record a higher CaCO_3 saturation state of Neoproterozoic sea water (Sumner and Grotzinger, 2004). Carbonate crystal growth rates would be faster compared with sediment influx rates in the supersaturated sea water with respect to calcite. The high CaCO_3 saturation in seawater implies that limited early diagenetic alteration in the well-preserved Ghaap Group carbonate rocks. The observed oxygen isotopic composition of investigated carbonate rocks of South Africa is essentially related to the properties of ancient seawater and post-depositional diagenesis. The temperature of Archean surface ocean water was suggested to have been at least 60°C (Knauth and Lowe, 2003; Knauth, 2005; Kasting et al., 2006; Robert and Chaussidon, 2006). The hypothetical high ocean surface temperature will lead to a higher water vapour concentration in the early atmosphere, which reduces the evaporation of water from the surface seawater to the atmosphere. Therefore, the lower oxygen isotopic composition implies that evaporation is not significant in the late Archean marine carbonate deposition.

Comparing to the Phanerozoic oxygen composition, late Archean carbonates of South Africa show anomalously low $\delta^{18}\text{O}$ values. The oxygen isotopic composition of the entire Ghaap Group is characterised by most consistent $\delta^{18}\text{O}$ values (varying between -7‰ to -10‰ , averaging -8‰), whereas values for the Schmidtsdrif Subgroup are consistently close to -13‰ . It was suggested by Kaufman and Knoll (1995) and Xiao et al. (1997) that samples with $\delta^{18}\text{O}$ values $< -5\text{‰}$ are probably altered and $< -10\text{‰}$ are not applicable for stratigraphic analysis because of post depositional alteration. Here, I apply the $\delta^{18}\text{O}$ values for interpretation of facies and

diagenetic conditions, independently of the age, although two stratigraphic trends are clearly visible. The question whether the $\delta^{18}\text{O}$ values are applicable for stratigraphic correlation across basins, is not relevant in this discussion.

The microbial carbonates, preserved in the Campbellrand Subgroup, have “normal marine” $\delta^{13}\text{C}$ values of essentially 0‰ versus the PDB standard (Beukes et al., 1990; Veizer et al., 1992a). Samples collected from the Kathu borehole show typical marine carbonate $\delta^{13}\text{C}$ values range from -2.4‰ to +0.4‰ in accordance with other published values (Karhu and Holland, 1996; Sreenivas et al., 2001; Des Marais, 2001; Thomazo et al., 2009; Frauenstein et al., 2009). The oxygen isotopic composition is slightly depleted in ^{18}O (-15.9 to -5.0‰) but consistent with most late Archean to Paleoproterozoic marine carbonates (Veizer et al., 1990, 1992b; Des Marais, 2001; Frauenstein et al., 2009). The $\delta^{13}\text{C}$ and $\delta^{18}\text{O}$ values are plotted in figure 5.2 and 5.4 according to the stratigraphic order. The $\delta^{13}\text{C}$ values display an increasing trend with the stratigraphy while the $\delta^{18}\text{O}$ values show an increasing trend upward, only in the lower depositional sequence, up to the Papkuil Formation and a decreasing trend upward above the Papkuil Formation. Both $\delta^{13}\text{C}$ and $\delta^{18}\text{O}$ values show systematic variations with the developing stratigraphic succession. However, there is no systematic co-variation between $\delta^{13}\text{C}$ and $\delta^{18}\text{O}$ values. The lack of such co-variation suggests that post-depositional alteration on these microbial carbonate is not significant (Allan and Matthews, 1982).

The increase of $\delta^{13}\text{C}_{\text{carb}}$ values upward for the Campbellrand Subgroup, shown in Figure 5.2, is interpreted as progressive reflecting the increasing microbial activity and productivity (oxygen-producing photosynthesis) that took up ^{12}C from the seawater and left the ^{13}C to form more ^{13}C -enriched carbonate minerals formed from seawater DIC. The strongly negative ^{13}C isotopic composition of carbonate rocks of the Schmidtsdrif Subgroup indicates lower burial rates of organic carbon and lower microbial productivity and/or these carbonate rocks were possibly strongly affected by the effects of an earlier volcanic outgassing that changed the composition of seawater toward more depleted in ^{13}C than the modern seawater. As the transgression over the 2.7 Ga Ventersdorp Supergroup rocks began during the upper Campbellrand

Subgroup, microbial life began to flourish and the deposition of carbonate rocks and burial of organic matter prevailed. The fluctuation of carbon isotopes in the Campbellrand Subgroup implies that transgression-regression processes have influenced the carbonate deposition by variation of environmental conditions such as water energy, sediment influx and currents or storm events, as described from facies interpretation by Beukes (1987), Altermann and Herbig (1991), Altermann and Nelson (1998).

The $\delta^{13}\text{C}_{\text{carb}}$ excursion between the Schmidtsdrif Subgroup and Campbellrand Subgroup (from around -7‰ to around -0‰ , in Figure 5.2) probably implies that the depositional paleo-environment has changed in the Ghaap Plateau sub-basin because of continuous subsidence and growth of abundant and voluminous microbial mats. The facies change from the lower siliciclastic-carbonate Schmidtsdrif Subgroup to the upper stromatolitic Campbellrand Subgroup clearly demonstrates this environmental change. No results of the $\delta^{13}\text{C}_{\text{org}}$ values in the lower Schmidtsdrif Subgroup are because of low content of organic materials in the carbonate samples. This suggests that the burial of organic carbon and the sedimentation rates increased significantly through the environmental change at the beginning of Campbellrand Subgroup deposition. The appearance of abundant microbial communities in Campbellrand Subgroup from the microfacies observations and other works (Beukes, 1987; Altermann and Siegfried, 1997; Eriksson and Altermann, 1998; Johnson et al., 2006; Schroeder et al., 2006) is attributed to the carbon isotopic shift (from about -7‰ to about -0‰) in these carbonate rocks.

The depleted and consistent $\delta^{18}\text{O}$ values in Schmidtsdrif Subgroup can be explained by the higher temperature of seawater and/or diagenetic modification. The depleted $\delta^{18}\text{O}$ values were proposed to reflect formation temperature at depth in the sediment as a result of lesser variation of depositional and diagenetic conditions, as visible from the lithological and depositional facies description (Altermann and Siegfried, 1997). The oxygen isotopic fractionation between carbonate and water ($\Delta^{18}\text{O} = \delta^{18}\text{O}_{\text{carb}} - \delta^{18}\text{O}_{\text{water}}$) depends on temperature according to the equation 5.1. The large range in $\delta^{18}\text{O}$ indicates that a significant fraction of Schmidtsdrif Subgroup

carbonates had their original $\delta^{18}\text{O}$ values lowered by former isotopic exchange with hydrothermal fluids. Thus, Schmidtsdrif Subgroup carbonates precipitated in ^{18}O depleted water masses within a marginal marine and/or deep lagoonal basin from the ocean (Altermann and Siegfried, 1997; Johnson et al., 2006). The more variable and on average higher $\delta^{18}\text{O}$ values in the Campbellrand Subgroup, probably imply that the paleo-environment changed and fluctuated at the beginning and during the carbonate deposition in the Campbellrand sub-basin, due to continuous subsidence and abundant microbial growth (Altermann and Herbig, 1991). This suggests that temperature can be the major controlling factor in the carbonate deposition, and the decreasing $\delta^{18}\text{O}$ values in the upper Campbellrand Subgroup carbonate deposition are mostly controlled by the elevated crystallization temperatures during deep burial diagenesis.

The narrow ranges of $\delta^{13}\text{C}$ values (-1‰ to 0‰) in the Campbellrand Subgroup carbonate rocks indicate that the depletion in $\delta^{13}\text{C}$ values, due to the post-depositional alteration, is not significant. The oxygen isotopic composition of carbonate rocks show a wide $\delta^{18}\text{O}$ values range (-15‰ to -6‰) and two $\delta^{18}\text{O}$ values shifts in the upper Schmidtsdrif Subgroup (from around -14‰ to -8‰, upward) and the upper Campbellrand Subgroup (from around -6‰ to -13‰, upward). The first increasing trend of $\delta^{18}\text{O}$ values during the upper Schmidtsdrif Subgroup is associated with a large shift of $\delta^{13}\text{C}$ values from around -6‰ to -1‰ upward while the second $\delta^{18}\text{O}$ values shift is followed by no apparent $\delta^{13}\text{C}$ values shift. One explanation for the co-variation of $\delta^{18}\text{O}$ and $\delta^{13}\text{C}$ values is that at least two mechanisms controlled the deposition of carbonate rocks in the lower (decreasing of temperature and increasing of microbial productivity) and upper Ghaap Group (deeper water deposition and elevated deep burial diagenetic temperature). Considering the highly temperature-dependent variation of $\delta^{18}\text{O}$ values, while $\delta^{13}\text{C}$ values show little dependence on temperature, the latter $\delta^{18}\text{O}$ values shift, during the upper Campbellrand Subgroup, is interpreted as elevated deep burial temperature and the first isotopic shift of both $\delta^{18}\text{O}$ and $\delta^{13}\text{C}$ values are preferentially interpreted as depleted isotopic composition of seawater. But the excursion of $\delta^{13}\text{C}$ values (-7‰ to -1‰) between the lower Schmidtsdrif Subgroup and the overlying Campbellrand

Subgroup strongly suggests that microbial life began to flourish and the deposition carbonate rocks and burial of organic matter prevailed during and after this transition.

Based on the studies of carbon isotopic composition of selected late Archean marine carbonates of South Africa, strong microbial influence on the carbonate precipitation was active from the beginning of Campbellrand Subgroup sedimentation. The $\delta^{13}\text{C}$ values display a large excursion during the transition time from the predominantly clastic Schmidtsdrif Subgroup sedimentation to the almost pure carbonate ramp sedimentation of the Campbellrand Subgroup (Altermann and Siegfried, 1997). This carbon isotopic excursion, combined with previous microfacies studies, infers a remarkable increase in organic burial rates and in microbial activity.

The Precambrian carbonate rocks, especially the late Archean carbonate rock of South Africa, lack a co-variance between $\delta^{18}\text{O}$ and $\delta^{13}\text{C}$ values, suggesting that the carbon isotopic composition is not strongly affected by the post-alteration and can well reflect the composition and evolution of the seawater carbon cycles. The depleted oxygen composition is probably attributed to higher post-depositional temperatures and post-depositional equilibration with warm basinal waters. Previous studies on oxygen isotopes indicate that the seawater was highly saturated with CaCO_3 (Grotzinger and Kasting, 1993; Sumner and Grotzinger, 2004) and the diagenetic alteration of these carbonate rocks is limited (Knauth, 2005; Kasting et al., 2006). Thus, the observed carbon and oxygen isotopic values in the Ghaap Group reflect the early nature of carbonate rocks precipitation from the involved seawater and the diagenetic history, these rocks experienced.

RELATIONSHIP BETWEEN
MICROFACIES OBSERVATION
AND ISOTOPIC ANALYSES

6. Relationship between Microfacies Observation and Isotopic Analyses

Carbonate precipitation in the Archean was ruled by chemical composition of ocean water and by biogenic processes (Eriksson and Altermann, 1998). Carbonate texture and mineralogy commonly reflect the chemical, physical and biological conditions of their depositional environment. Many studies have concentrated on the history of temperature and isotopic composition of Precambrian seawater (e.g. Knauth, 2005; Kasting et al., 2006; Komiya et al., 2008; Thomazo et al., 2009 and many others). Previous studies of stable isotope signature (C and O) in carbonate rocks show that the free oxygen concentration in late Archean ocean and atmosphere were increasing, controlled by the factors of microbial mechanisms including the production of free oxygen by photosynthesis and the consuming of free oxygen by interaction between oxygen and elements such as nitrogen and molybdenum (Godfrey and Falkowski, 2009; Voegelin et al., 2010; Kendall et al., 2010). The increasing of free oxygen from shallow to deep water columns must have an isotopically stratified effect on the carbonate deposition in late Archean Ghaap Group. The well preserved stromatolites of late Archean time in South Africa, imply that the microbial communities were playing an important role in the formation of these carbonate rocks and possible isotopic depth gradient existed in the carbonate deposition.

Stromatolites are lithified sedimentary structures evoked by microbial growth, often showing trapping and binding of sediments from their direct neighbourhood. The morphology of stromatolites usually shows vertical growth patterns as an expression of lateral facies changes (Altermann, 2008). Before the emergence of metazoans, the stromatolitic growth in the Precambrian probably was restricted by the environmental factors such as: the depth of light or ultraviolet light penetration (depth and turbidity of water), temperature limitations, unfavorable chemical and nutrient condition (salinity), the rate of sediment deposition and the current/wave action. Thus, we firstly observed the microfacies of selected carbonate samples mostly in Kathu borehole and compared it with previous sedimentary facies studies (Beukes, 1987; Altermann and Siegfried, 1997; Altermann and Nelson, 1998; Knoll

and Beukes, 2009; Schröder et al., 2009), and then correlated the microfacies studies and interpretations to the isotopic composition of carbon and oxygen in these marine carbonate rocks.

6.1 Carbon and Oxygen Isotopes Variation in Campbellrand Subgroup Carbonate Rocks

Stromatolites are normally interpreted to have formed in shallow marine environment where sufficient light penetrated the water column within few tens of metres. Various types of stromatolitic morphologies were attributed to different habitats for the growth and development of microbial life (Altermann, 2008).

6.1.1 Intertidal to supratidal carbonates dominated by open space structures

The carbonates dominated by open space structures occur in the entire Ghaap Group, which are related to the fenestral stromatolites in figure 6.4. The open space structures have been recognized as variously sized cavities in carbonate rocks, which are filled with calcite and/or internal sediment. The millimeter-sized, irregularly distributed voids are often associated with microbial bindstones and micrites. This type of carbonate deposition was formed preferentially in shallow water environment of intertidal to supratidal facies (Flügel, 2004; Altermann, 2008). Carbonate samples from undulated laminations, voids and organic matter from these open space structures were tested for the carbon and oxygen isotope differences (Table 6.1, Appendix I). Figure 6.1 shows the drilling sites for each sample.

In this group, the $\delta^{13}\text{C}$ values range from -2.4‰ to +0.4‰ and display a large variation. This is probably because sediment of different origin filled in the voids, such as micritic matrix and blocky calcite cements, during different depositional and diagenetic stages. Thus, the variation of $\delta^{13}\text{C}$ and $\delta^{18}\text{O}$ values in these open space structures dominated carbonate rocks, are interpreted as being affected by heavier post-depositional alteration, such as isotopic exchange between later fluids and carbonate rocks, than the carbonates deposited in deeper water realms of deep subtidal and intertidal facies.

Table 6.1 $\delta^{13}\text{C}$ and $\delta^{18}\text{O}$ values of the open space structures dominated carbonate rocks. Dark matter signifies the dark, C-rich laminae; light matter represents the whitish, blocky calcite cements in the fenestral voids among the microbial laminae.

Formation	Sample No.	Dark matter $\delta^{13}\text{C}$ values	Light matter $\delta^{13}\text{C}$ values	Dark matter $\delta^{18}\text{O}$ values	Light matter $\delta^{18}\text{O}$ values
Kogelbeen	91-41	-0.2	-0.5	-9.5	-9.9
Kogelbeen	91-43	+0.4	-0.3	-8.0	-10.0
Kogelbeen	92-43		+0.1		-13.2
Klippan	92-32	-2.4	-0.3 and -1.1	-11.6	-8.3 and -7.9
Klipfontein	92-28	-0.2	+0.1	-7.1	-6.3
Reivilo	91-63	-0.9	-0.7 and -0.9	-9.9	-7.6 and -8.1
Monteville	91-052	-0.4	-0.4	-10.3	-9.7

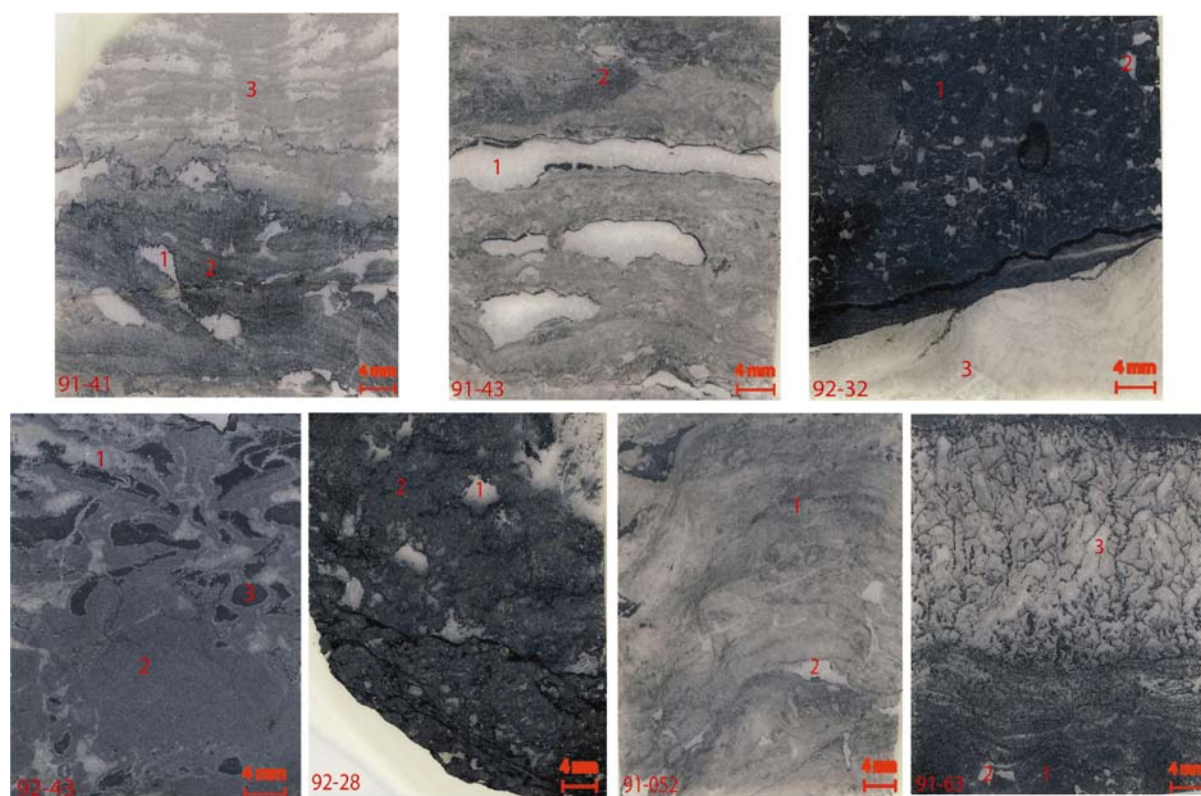


Figure 6.1 The photographs of open space structure stromatolites in thin sections. Sample numbers are given in the left bottom of the photographs and the scale bar in red colour is of 4 mm, right lower corner. Drilling sites are numbered for both dark and light matter.

The carbon isotopic composition of carbonate rocks shows consistent $\delta^{13}\text{C}$ values between microbial lamination and sediment infill in the voids of the lower

Campbellrand Subgroup (Monteville Formation and Reivilo Formation), while the upper Campbellrand Subgroup (>0.2‰ difference in Klipfontein, Klippan and Kogelbeen Formations) shows slightly different $\delta^{13}\text{C}$ values for void sediment and the surrounding microbialite. This suggests that the carbonate minerals, formed in the microbial lamination and the sediment filling the voids, are from the same origin in the lower Campbellrand Subgroup deposition. During the upper Campbellrand Subgroup carbonate deposition, carbonate minerals that were formed in the microbial laminae and sediment filled in the voids are in some cases of different origin and experienced diagenetic alterations.

6.1.2 Shallow subtidal to intertidal carbonates dominated by columnar stromatolites

Table 6.2 $\delta^{13}\text{C}$ and $\delta^{18}\text{O}$ values in the columnar stromatolite dominated carbonate rocks. Dark matter signifies the dark, C-rich microbial laminae, light matter represents the whitish, carbonate sediments trapped in the dark lamination and between the columns.

Formation	Sample No.	Dark matter $\delta^{13}\text{C}$ values	Light matter $\delta^{13}\text{C}$ values	Dark matter $\delta^{18}\text{O}$ values	Light matter $\delta^{18}\text{O}$ values
Kogelbeen	92-45	-0.7	-1.3	-11.7	-11.7
Kogelbeen	92-38	-0.3	-0.2 and -0.3	-9.8	-9.8 and -10.0
Kogelbeen	92-37	-0.2	-1.0	-11.5	-12.3
Papkuil	92-34	-0.5	-0.5	-8.1	-8.0
Fairfield	92-21	-0.6	-0.6	-6.8	-6.5
Reivilo	91-60	-0.7	-0.7	-7.9	-7.4
Monteville	91-55	-0.5	-1.7	-9.5	-11.4

The deposits dominated by columnar stromatolites display varying morphologies of columnar stromatolites, which are exposed in figure 6.4. These morphologies represent a wide range of shallow water environments, from shallow subtidal to intertidal. For each sample, it was tested, whether the $\delta^{13}\text{C}$ and $\delta^{18}\text{O}$ values for the microbial laminae of the columns, the sediment between them and the sediment trapped in the lamination are different (Appendix I). Below, in Table 6.2, the carbon and oxygen isotopic values of these samples are listed. Figure 6.2 shows the drilling sites for each sample.

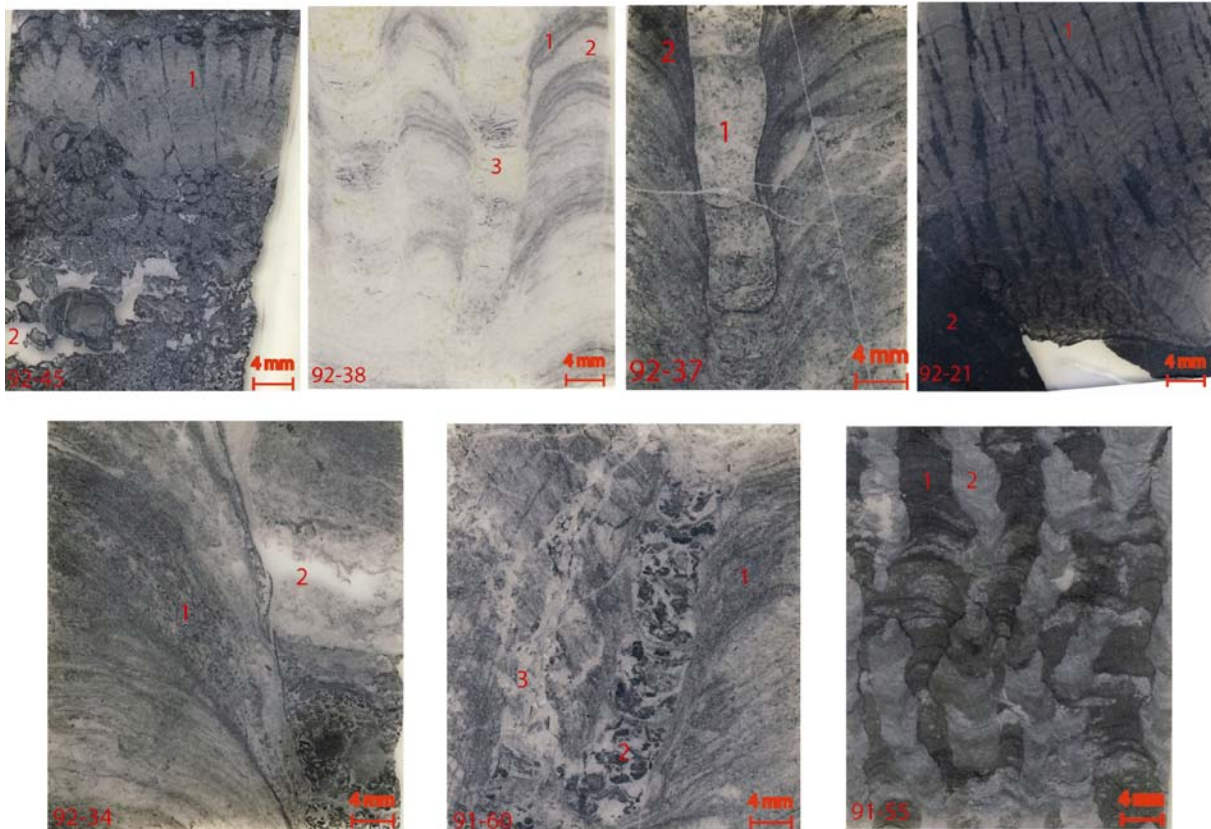


Figure 6.2 The photographs of columnar stromatolites in thin sections. Sample numbers are given in the left bottom of the photographs and the scale bar in red colour is of 4 mm, right lower corner. Drilling sites are numbered for both dark and light matter.

In this group, the values of $\delta^{13}\text{C}$ range from -1.7‰ to -0.2‰ , which is typical for marine carbonate facies. Most of the microbial laminations (dark and light laminae) in stromatolite columns and the sediments trapped and bound between the columns show the same $\delta^{13}\text{C}$ and $\delta^{18}\text{O}$ values. Three samples (91-55, 92-37 and 92-45) have significantly lower $\delta^{13}\text{C}$ values but consistent $\delta^{18}\text{O}$ values (except sample of 91-55) in the sediments trapped between the columns than the microbial laminations themselves. Sediment between the columns in 91-55 is diagenetic calcite cement and shows both lower $\delta^{13}\text{C}$ and $\delta^{18}\text{O}$ values.

The slightly different $\delta^{13}\text{C}$ values between the lower Campbellrand Subgroup and the upper Campbellrand Subgroup imply that carbonate deposition was mostly controlled by the composition of contemporaneous seawater. The carbon isotopic

composition of seawater is gradually increasing in $\delta^{13}\text{C}$ values upward in Campbellrand Subgroup. The carbonate minerals in stromatolitic layers and in the sediments trapped in the lamination show similar $\delta^{13}\text{C}$ values. This indicates that the carbonate minerals in both stromatolitic layers and trapped sediments in the lamination have the same source and were precipitated by equal processes. The samples of 92-38, 92-34, 92-21 and 91-60 also show similar $\delta^{13}\text{C}$ values among the stromatolitic layers, the sediments trapped in the lamination and the sediments trapped between the columns. This implies that the debris trapped between the columns was descended from the stromatolites themselves (Altermann, 2008). However, samples of 92-37, 92-45 and 91-55 show different $\delta^{13}\text{C}$ values in the sediments trapped between the columns. This indicates that the sediments trapped between the columns are diagenetic calcite cements (Altermann, 2008) and/or of different origin.

6.1.3 Deep subtidal carbonates dominated by finely laminated microbial mat

The finely laminated and contorted microbial mats occupy exclusively the uppermost Campbellrand Subgroup (Gamohaam Formation), and are shown in figure 6.4. The fine laminations of these microbial mats are commonly contorted and convoluted by currents and/or storm waves. The fine laminations are thought to be formed in a deeper water environment, below the fair weather wave base and to be disrupted by occasional storm, current or wave action, eroding them and producing an “*in situ debris*” in otherwise barren any clastic input environment (Altermann, 2008). Samples were tested for both carbon and oxygen isotopes from the convoluted fine laminations and the coarse, blocky calcite cements filling the open voids between the fine laminations (Appendix I). Below, in Table 6.3, the carbon and oxygen isotopic values of these samples are listed. Figure 6.3 shows the drilling sites for each sample.

Table 6.3 $\delta^{13}\text{C}$ and $\delta^{18}\text{O}$ values in the finely laminated microbial mats dominated carbonate rocks. Dark matter signifies the dark, C-rich laminae devoid of clastic input; light matter represents the whitish, blocky calcite cements in the voids between the laminae strings.

Formation	Sample No.	Dark matter $\delta^{13}\text{C}$ values	Light matter $\delta^{13}\text{C}$ values	Dark matter $\delta^{18}\text{O}$ values	Light matter $\delta^{18}\text{O}$ values
-----------	------------	--	---	--	---

Relationship between Microfacies Observation and Isotopic Analyses

Gamohaan	GAS1-558	-1.2	-0.5	-9.5	-5.0
Gamohaan	92-60	-0.3	+0.2	-11.7	-9.7
Gamohaan	92-57	-0.3	-0.0	-11.8	-10.8
Gamohaan	92-56	-0.1 and -0.2	-0.0	-12.2 and -12.6	-9.5

In this group, the $\delta^{13}\text{C}$ values range from -1.2‰ to $+0.2\text{‰}$. Carbonate minerals of the fine microbial laminations and cements between the laminations both display differences in their $\delta^{13}\text{C}$ and $\delta^{18}\text{O}$ values. However, the microbial community can change the chemical composition of seawater by their metabolic activity and finally change the isotopic composition of precipitated carbonate rocks which are deposited from the surrounding seawater.

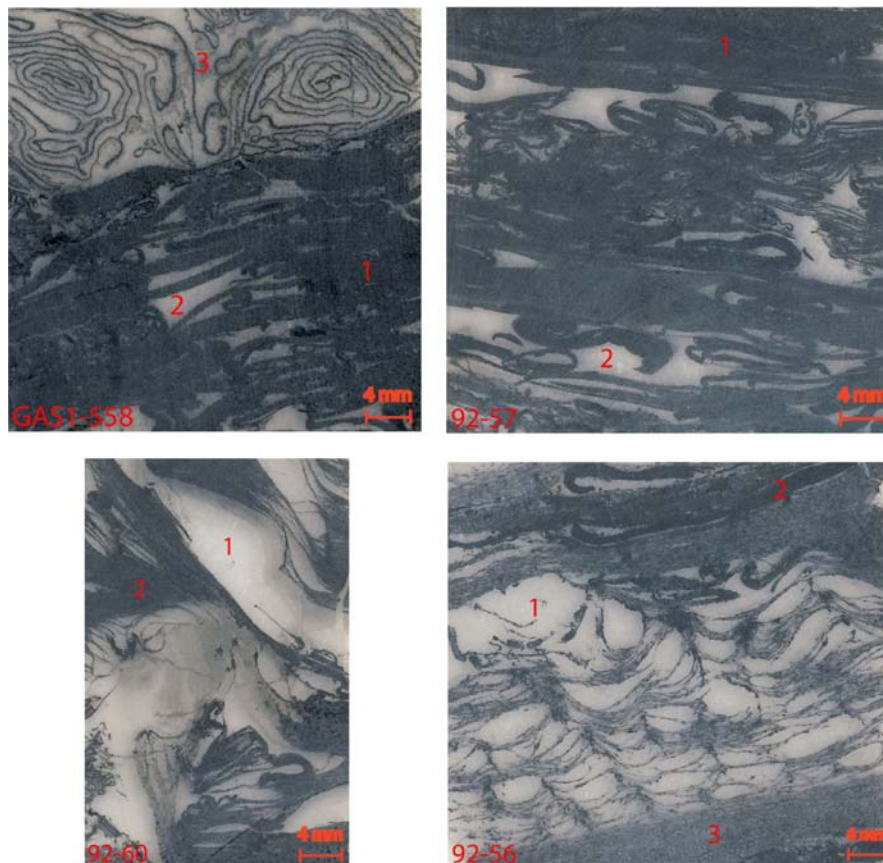


Figure 6.3 The photographs of contorted, finely laminated microbial mats in thin sections. Sample numbers are given in the left bottom of the photographs and the scale bar in red colour is of 4 mm, right lower corner. Drilling sites are numbered for both dark and light matter.

Changes of $\delta^{13}\text{C}$ and $\delta^{18}\text{O}$ values between the fine microbial laminations and the cements in the voids between laminae strings provide evidence for the different

origin of carbonate minerals and mechanisms of post-depositional alterations. The dark, C-rich lamination in these deep subtidal microbial mats is generally isotopically lighter than the clearly diagenetic cement in the voids. This can be probably best explained by increased meteoric water intrusion during burial and cementation (compare discussions above in 6.1.2). The $\delta^{13}\text{C}$ values display a significant difference between fine microbial laminations and cements between them, also implying that the cements are originated from a later, diagenetic carbonate mineral precipitation. Comparing to the above discussed supratidal and intertidal carbonates, the carbon isotopic composition of finely laminated microbial carbonates has higher $\delta^{13}\text{C}$ values, suggesting that the carbon isotopic composition of seawater became gradually heavier upwards, because of fast burial of organic carbon, during the upper Campbellrand Subgroup carbonate deposition.

6.2 Carbon Isotopes and Water Depth

The water depth is important for carbonate deposition, linked to the microbial communities, if the composition of seawater and biological productivity change with water depth (Chester, 2000). Based on the microscopic observation and field occurrence of the carbonate rocks, three main facies realms are present in the Campbellrand Subgroup, namely deep subtidal, intertidal and supratidal. Interpretation and comparison with previous studies of sedimentary facies (Beukes, 1987; Altermann and Herbig, 1991; Eriksson and Altermann, 1998; Wright and Altermann, 2000; Altermann, 2008) and isotopic composition through geological time (Des Marais, 2001; Fischer et al., 2009; Frauenstein et al., 2009) imply a strong relationship between the macro- and microscopic facies interpretation and the isotopic analyses of the late Archean tidal-flat carbonate rocks.

6.2.1 Carbon isotopes of microbialite types

Microbial life plays an important role in biogeochemical cycling of carbon isotopes. During the CO_2 fixation by photosynthetic organisms, ^{12}C is preferentially taken up from the surface water to produce organic matter. Subsequently, a fraction of this biologically derived organic carbon sinks into the deeper water. Any changes in the sedimentation of different water depth would cause an increase or

decrease in the organic carbon burial and thus in the deposition of marine carbonate with heavier C isotopes. It can be therefore expected that there is a systematic correlation between carbon-isotope values and the water depth of the basin, as interpreted from the different stromatolitic morphologies in this study.

The low porosity of carbonate rocks commonly blocks the circulation of fluids once the carbonate rocks are completely solidified. Thus, carbonate rocks tend to preserve the original isotopic composition even if they suffered dolomitization (Banner et al., 1988; Qing and Mountjoy, 1994; Qing, 1998). Post-depositional alteration is often accompanied by textural change such as coarsening (Qing and Mountjoy, 1994; Qing, 1998; Flügel, 2004). Therefore, from the isotope study presented here, we selected the least altered, fine-grained carbonate minerals with primary textures such as stromatolitic laminae from over 100 rock samples based on detailed microscopic observations.

This study focuses on the comparison of microfacies observations with the stable ($\delta^{13}\text{C}_{\text{carb}}$ and $\delta^{18}\text{O}$) isotope analyses of the carbonate rocks of Ghaap Group from Kathu borehole, South Africa. Carbon isotope values of these carbonate rocks have been assigned to three recognized facies realms in figure 6.4: (1) deep subtidal, finely laminated microbial mats, (2) shallow subtidal to intertidal columnar stromatolites, (3) intertidal to supratidal fenestral stromatolites. Carbon and oxygen isotopes values of the three recognized microfacies have been plotted in figure 6.5.

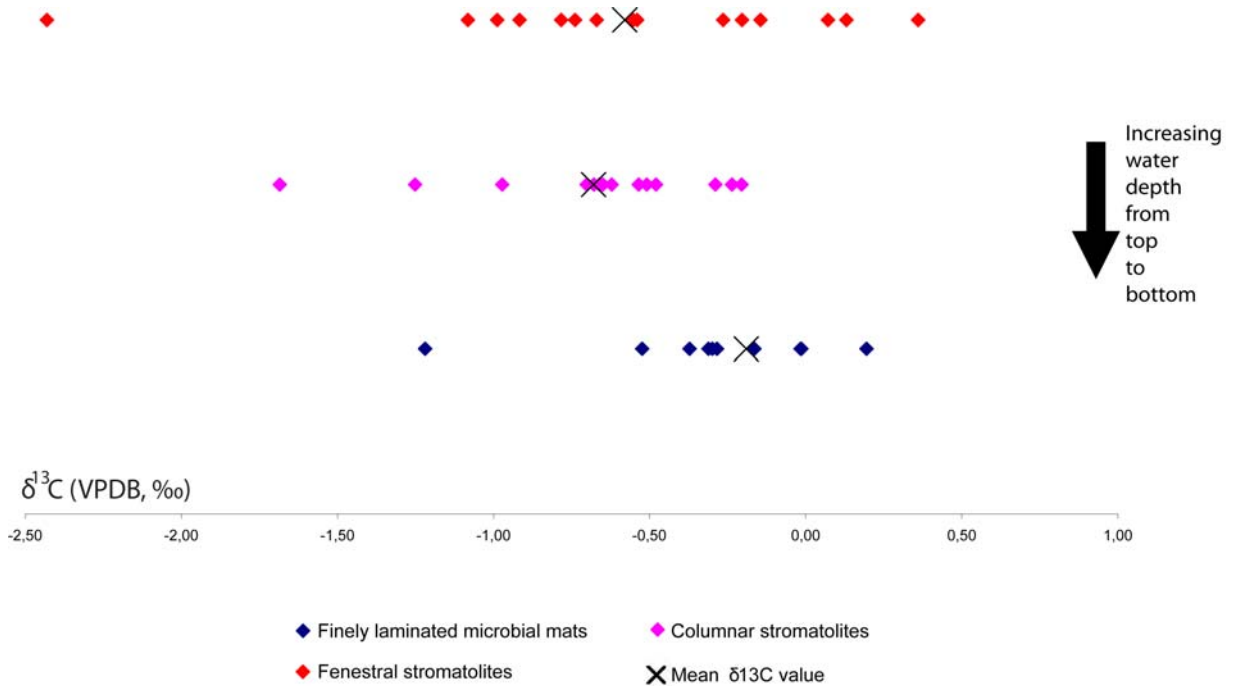


Figure 6.4 Ranges of $\delta^{13}\text{C}$ values for the three lithofacies studies. The mean $\delta^{13}\text{C}$ values are marked as X for the three lithofacies.

The analyses show that $\delta^{13}\text{C}$ values of deep subtidal and intertidal microbial carbonates have nearly 0.5‰ difference (Figure 6.4 and figure 6.5). Deep subtidal finely laminated microbial mats display narrow range of $\delta^{13}\text{C}$ values (-0.5‰ to +0.2‰) and a relatively higher mean $\delta^{13}\text{C}$ value (-0.2‰) when compared to the shallow intertidal and supratidal facies, which were represented by columnar stromatolites and fenestral stromatolites respectively. Sample of GAS1-558 shows an abnormal low $\delta^{13}\text{C}$ value (-1.2‰) in the coiled laminae, which is preferentially interpreted as the different origin of carbonate deposition (probably storm induced). Shallow subtidal and intertidal columnar stromatolites have depleted $\delta^{13}\text{C}$ values ranging from -1.3‰ to -0.2‰, with a mean value of -0.6‰. Supratidal fenestral stromatolites show a wide range of $\delta^{13}\text{C}$ values, ranging from -1.1‰ to +0.4‰, with a mean value of -0.5‰. In the figure 6.4, carbonate deposits from the deep subtidal to intertidal facies show narrow range of $\delta^{13}\text{C}$ values and imply that possible isotopic depth gradient existed between the subtidal to intertidal environments, without significant diagenetic influences. However, carbonate deposits from the supratidal facies have the widest range of $\delta^{13}\text{C}$ values which is preferentially

interpreted as varying diagenetic alterations and possible air-sea exchange with different carbon isotopic source value.

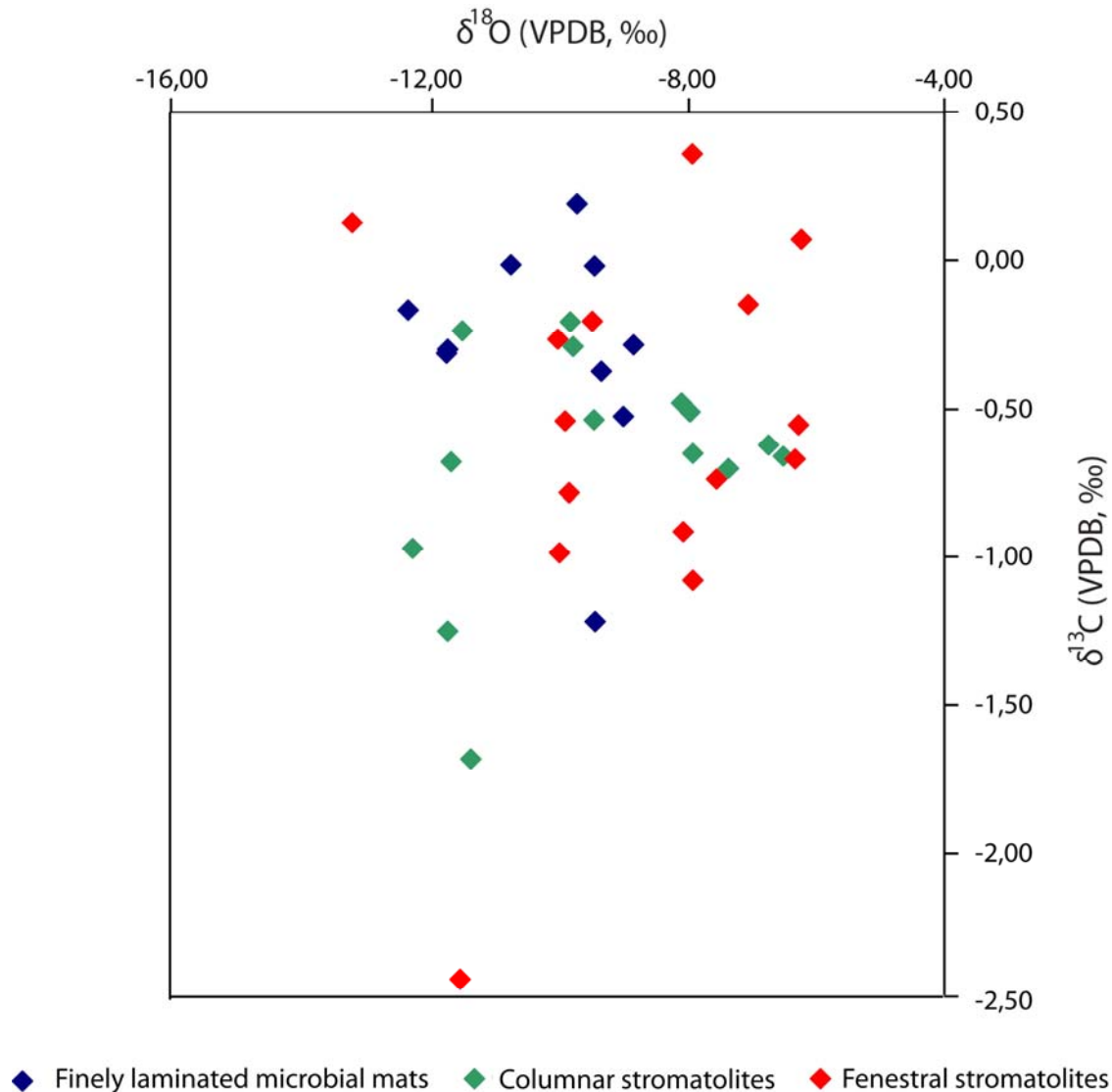


Figure 6.5 Crossplot of $\delta^{13}\text{C}$ and $\delta^{18}\text{O}$ values for the three lithofacies studies.

6.2.2 Interpretation of carbonate isotope variations

The $\delta^{13}\text{C}$ composition of surface water in modern oceans is highly variable, but in general surface water is enriched in ^{13}C (by about 2‰) relative to deep ocean water, because of biological activity and air-sea exchange processes (Kroopnick, 1985; Charles et al., 1993). The differences in $\delta^{13}\text{C}$ values, which were evoked by simple life forms (cyanobacteria) and their photosynthesis, are usually thought to be a cause of $\delta^{13}\text{C}$ shift (Hotinski et al., 2004). This process must have had similar

depth-related variations in $\delta^{13}\text{C}$ values for shallow marine carbonates in the late Archean ocean.

Thus, the facies-dependent variations in C and O isotopes of the studied carbonates could be caused by a depth gradient of DIC consumption in connection with the elevated sedimentation rate and preservation of organic material with greater depth. The columnar stromatolites and finely laminated microbial mats show narrow ranges of $\delta^{13}\text{C}$ values, compared with the fenestral stromatolites, suggesting that their depositional environment (microfacies) was more uniform and less fluctuating, as it is well documented in their carbon isotope composition. Thus, the $\delta^{13}\text{C}$ values of marine carbonate rocks deposited below intertidal environment can be used for the reconstruction of the sedimentary paleo-environment.

Carbonate rocks deposited in deep subtidal and intertidal facies show narrow ranges of $\delta^{13}\text{C}$ values, and have a 0.5‰ difference in their mean $\delta^{13}\text{C}$ values. This suggests that the carbonate rocks deposited in the deep intertidal and subtidal facies have experienced less fluctuating depositional conditions than the shallow supratidal sedimentation. The different ranges of carbon isotope values in Ghaap Group carbonate rocks thus suggests a water depth gradient existed during carbonate deposition between deep subtidal and intertidal environments.

6.3 Carbon and Oxygen Isotopes and Sedimentary Facies

The sedimentary facies of the carbonate rocks sampled from the different formations of the Ghaap Group comprise tidal-flat microbial laminates, microbial mats and columnar stromatolites. Carbonate cements found in thin sections from these different facies, include early fibrous and later blocky cements. Stable isotopic measurements of carbon and oxygen isotopes are described here. The $\delta^{13}\text{C}_{\text{carb}}$ and $\delta^{18}\text{O}$ values are plotted in figure 6.6.

In figure 6.6, the isotopic composition of carbonate rocks in Ghaap Group plots in four domains. There is a systematic co-variation between the isotopic compositions (C and O) and the stratigraphic successions. Carbonate samples from the

Schmidtsdrif Subgroup show both low $\delta^{13}\text{C}$ and low $\delta^{18}\text{O}$ values (from -8.0‰ to -4.2‰ for $\delta^{13}\text{C}$ and from -13.5‰ to -11.5‰ for $\delta^{18}\text{O}$) that all plot in the square of **D**. Carbonate samples from the Campbellrand Subgroup display a narrow range of $\delta^{13}\text{C}$ values (from -2.4‰ to $+0.4\text{‰}$, mostly around 0‰) while the $\delta^{18}\text{O}$ values show a large variation (from -13.5‰ to -6.3‰) in square **A**, **B** and **C**. The carbonates in the lowermost Campbellrand Subgroup (Monteville Formation) and the uppermost Campbellrand Subgroup (Kogelbeen Formation and Gamohaagan Formation) show the lowest $\delta^{18}\text{O}$ values around -12‰ (Square **C**), while the middle Campbellrand Subgroup (from Reivilo Formation to Klippan Formation) displays a wide range and relatively higher $\delta^{18}\text{O}$ values from -10‰ to -6‰ (Square **B**).

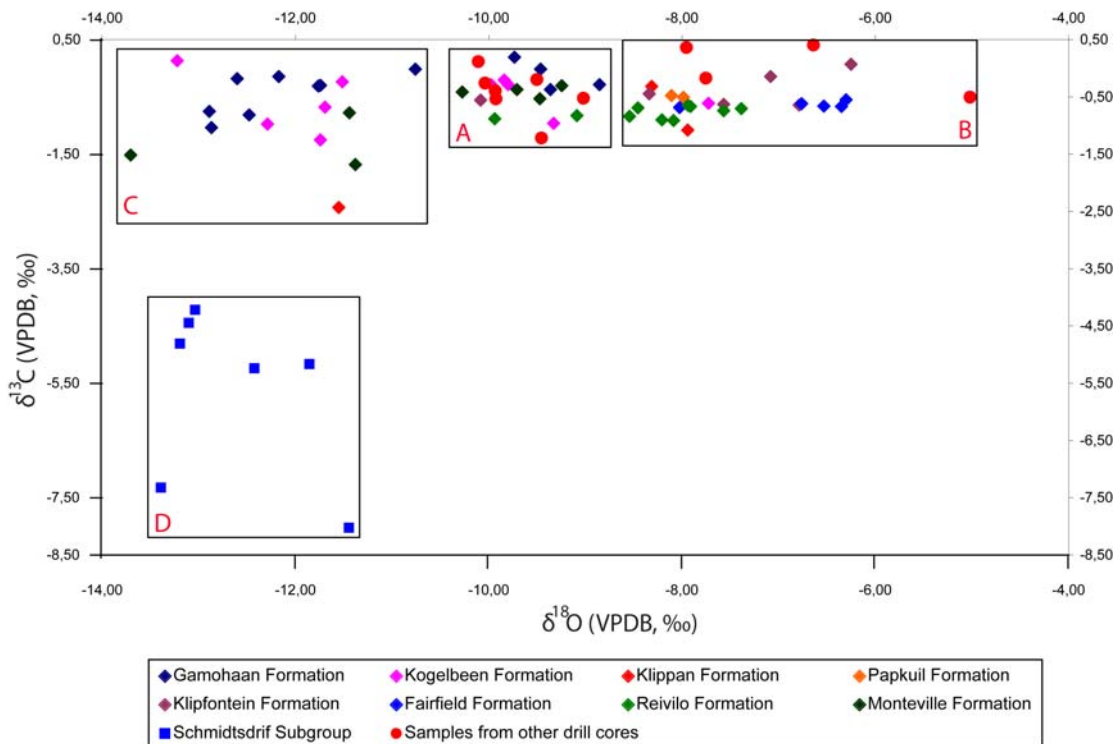


Figure 6.6 Crossplot of $\delta^{13}\text{C}$ and $\delta^{18}\text{O}$ values for carbonate rocks of the Ghaap Group. Note the middle square of typical marine carbonate in area **A**, expanded to include two pathways of probably post-diagenetic marine components (Burdett et al., 1990). There are two diagenetic processes of the isotopic composition for the carbonates in area **A**, which are represented by early stabilization of carbonate minerals on restricted tidal flats (**B**), and late burial cementation under higher burial temperature and/or exposure to meteoric fluids (**C**). The depleted $\delta^{13}\text{C}$ and $\delta^{18}\text{O}$ values in domain **D** represent exclusively the Schmidtsdrif Subgroup carbonate samples. Samples were taken from other drill cores than Kathu borehole are plotted in red colour.

The depleted $\delta^{13}\text{C}$ and $\delta^{18}\text{O}$ values of the Schmidtsdrif Subgroup imply that the carbonate precipitation during this period differed from the times of the somewhat younger Campbellrand Subgroup. The carbon and oxygen isotopic interaction between seawater and atmosphere is associated with the extensive volcanic outgassing and hydrothermal flux during the Archean (from 2.7 Ga to 2.4 Ga, Ernst and Buchan, 2001; Condie, 2001). The extremely low $\delta^{13}\text{C}$ values, which are similar to the original mantle $\delta^{13}\text{C}$ values (-5‰, from Kump and Arthur, 1999; Condie et al., 2001; Des Marais, 2001), suggest that the deposition of Schmidtsdrif Subgroup carbonates may have been mainly influenced by the chemical interaction between late Archean seawater and atmosphere. During the carbonate deposition of Schmidtsdrif Subgroup, the isotopic signatures were possibly overprinted by the volcanic/magmatic activity.

The isotope values (C and O) of Campbellrand Subgroup carbonate rocks can be grouped into three distinct domains according to the co-variation between $\delta^{18}\text{O}$ and $\delta^{13}\text{C}$ values in figure 6.6 as following: **(A)** deposition occurred in normal marine shallow tidal-flat setting, which is represented by restricted and less co-variation between $\delta^{18}\text{O}$ and $\delta^{13}\text{C}$ values (from -1.2‰ to +0.2‰ for $\delta^{13}\text{C}$ and from -10.3‰ to -8.9‰ for $\delta^{18}\text{O}$) in the entire Campbellrand Subgroup carbonates, **(B)** environmentally restricted tidal-flat carbonates are indicated by heavier $\delta^{18}\text{O}$ values and positive linear relationship between $\delta^{18}\text{O}$ and $\delta^{13}\text{C}$ values (from -1.1‰ to +0.4‰ for $\delta^{13}\text{C}$ and from -8.1‰ to -6.3‰ for $\delta^{18}\text{O}$) in the middle Campbellrand Subgroup (from Reivilo Formation to Klippan Formation), and **(C)** the lightest $\delta^{18}\text{O}$ values (from -13.7‰ to -11.4‰) and variable $\delta^{13}\text{C}$ values (from -2.4‰ to +0.1‰) in both lower (Monteville Formation) and upper (Gamohaana Formation) Campbellrand Subgroup carbonates.

The carbonate samples in domain **A** show restricted range of $\delta^{18}\text{O}$ (-10‰ to -8‰) and $\delta^{13}\text{C}$ (-1‰ to +0‰). The less co-variation between $\delta^{18}\text{O}$ and $\delta^{13}\text{C}$ values in domain **A** (Allan and Matthews, 1982; Rollinson, 1993) suggest that the depletion of $\delta^{13}\text{C}$ and $\delta^{18}\text{O}$ values in carbonate rocks due to post-depositional alteration was not significant. The square **B** in figure 6.6, which shows a positive linear

relationship between oxygen and carbon isotopic composition of carbonate rocks, is interpreted as little isotopic exchanges with sediment influx and probably reflects of primary marine oxygen isotopic gradients associated with restricted marine environment. These ^{18}O enriched isotope values are uniquely restricted to the middle Campbellrand Subgroup (from Reivilo Formation to Klippan Formation) (Figure 5.4). This implies that the carbonate rocks had been deposited in a restricted marine environment during the middle Campbellrand Subgroup. Columnar stromatolites and fine laminated microbial mats in both the lowermost (Monteville Formation) and uppermost (Gamohaan Formation) Campbellrand Subgroup, formed in the intertidal and deep subtidal environment, follow the diagenetically influenced isotope value (domain **C** in figure 6.6). The episodic currents and/or storm events, as interpreted from the occurrence of fine microbial laminations and soft-sediment deformation imply the possible elevated deep burial temperatures and isotopic exchange between carbonate minerals and warm basinal water. The average $\delta^{13}\text{C}$ difference between limestone in shallow water (-1.3‰) and iron-formation in deep water (-5.3‰) was suggested that the water must have been isotopically stratified with respect to the total dissolved inorganic C, which was related to the hydrothermal input (Klein and Beukes, 1989; Beukes and Klein, 1990; Beukes et al., 1990). Depleted $\delta^{18}\text{O}$ values in the carbonate rocks of the uppermost Campbellrand Subgroup indicate that the deep subtidal seawater temperature probably had been substantially influenced by hydrothermal inputs (Klein and Beukes, 1989; Beukes and Klein, 1990).

6.4 Discussion

6.4.1 Isotopes (C and O) and water depth

Due to the lower but increasing content of free oxygen in the Archean environment, the decomposition of organic matter would cause a carbon isotopic difference in seawater from where carbonate precipitated. Rising of free oxygen concentration in the late Archean ocean is supported by recent studies of Mo and Re isotopes in black shales (Wille et al., 2007; Kendall et al., 2010), Ce isotopes in

carbonate rocks (Komiya et al., 2008) and review of stable isotopes related to life (C, N, S, Fe) in the rock record (Thomazo et al., 2009).

The oxygenation of burial organic matter could cause a decrease of $\delta^{13}\text{C}$ values in carbonate rocks. It was found in this study that intertidal carbonates have lighter $\delta^{13}\text{C}$ values than the deep subtidal carbonates with $\delta^{13}\text{C}$ values of -0.5‰ . Thus, the rising of oxygen in Archean ocean was probably limited to shallow water environment and then gradually increased into the deeper water environment. Considering the higher organic content of deep subtidal carbonates than in the intertidal carbonates of this study, another interpretation could be an increase in organic carbon burial which would also lead to the isotopically heavier seawater from which carbonate rocks precipitated. Thus, the observed $\delta^{13}\text{C}$ values difference of -0.5‰ in intertidal and deep subtidal carbonate rocks of Ghaap Group is interpreted as both, reflecting the elevated organic preservation and lower content of free oxygen in the deep subtidal environment.

6.4.2 Isotopes (C and O) and sedimentary facies

According to the model, proposed by Altermann and Herbig (1991) and Altermann and Siegfried (1997), the Griqualand West basin experienced several transgression-regression cycles and a high subsidence rate matched by carbonate deposition. Shallow marine conditions prevailed during the carbonate accumulation of Ghaap Group.

The carbon and oxygen isotopes, which are plotted in figure 5.2 and figure 5.4 according to the stratigraphic position, show an increasing trend upward in $\delta^{13}\text{C}$ values and an increasing of $\delta^{18}\text{O}$ values (from the Schmidtsdrif Subgroup to Klippan Formation of Campbellrand Subgroup) and later decreasing of $\delta^{18}\text{O}$ values trend (from the Klippan Formation to the Gamohaam Formation). Combining with the plotted $\delta^{13}\text{C}$ and $\delta^{18}\text{O}$ values in figure 6.6, the isotopic ratios can be altered by elevated deep burial temperature and isotopic exchange with warm basinal water. A possible sedimentary facies change is reflected by both the isotopic composition (C and O) and microfacies of carbonate rocks.

The Schmidtsdrif Subgroup consists mainly of shale, quartzites, and subordinately of oolite beds and crypt-microbial laminates, and it is interpreted as deeper shelf to deep lagoonal deposits in the Kathu borehole (Altermann and Siegfried, 1997). It overlies unconformably the Ventersdorp Supergroup lava. The strong negative $\delta^{13}\text{C}$ and $\delta^{18}\text{O}$ values (domain **D** in figure 6.6) are preferentially interpreted as the extensive volcanic and hydrothermal overprints (Ernst and Buchan, 2001; Condie, 2001) of isotopic signatures and effects on high seawater temperatures.

The overlying Campbellrand Subgroup starts with the Monteville Formation. Several generally shallowing-upward cycles are recognized from the upper Monteville Formation to the uppermost Gamohaam Formation (Altermann and Siegfried, 1997; and Altermann and Nelson, 1998). The $\delta^{13}\text{C}$ values are mostly around -1‰ for the Monteville Formation and display a varying but generally increasing values from -1‰ to +0.4‰ in the later Reivilo, Fairfield, Klipfontein Heuwels, Papkuil, Klippan and Kogelbeen Formations. The upward increasing trend of $\delta^{13}\text{C}$ values in the Campbellrand Subgroup can be explained as the elevated sedimentation rate and burial of organic matter, which is consistent with the proposed model of fast basinal subsidence by Altermann and Herbig (1991). The $\delta^{18}\text{O}$ values show a decrease from Klippan Formation to the uppermost Gamohaam Formation. Such a decrease in $\delta^{18}\text{O}$ values is preferentially interpreted as the isotopic exchanges of different isotope sources between carbonate minerals and fluid water. The sedimentary facies thus changed from a relatively shallower tidal flat environment to a deeper subtidal environment (Gamohaam Formation).

6.4.3 Late Archean environment and carbonate chemistry

Strong controversy characterizes the discussion on the temperature and the timing of oxygenation of Precambrian seawater (Holland and Beukes, 1990; Kasting, 2001; Canfield, 2005; Kendall et al., 2010). Stromatolites are common components of Precambrian carbonate rocks (Grotzinger and Knoll, 1999), and indicate the presence of O_2 -producing microbial life in late Archean oceans. The

photosynthetic production of free oxygen in the oceans and in the atmosphere is thought to have begun at 2.2 and 2.5 billion years ago (e.g. Cloud, 1972; Holland, 1984; Karhu, 1993; Karhu and Holland, 1996), or maybe earlier at 2.7 billion year ago (Kendall et al., 2010).

A variety of isotopic analyses of late Archean carbonate rocks have been discussed for the evolution of late Archean atmosphere and ocean (Kasting and Howard, 2006; Sumner and Grotzinger, 1996; Komiya et al., 2008; Godfrey and Falkowski, 2009; Kendall et al., 2010). Komiya et al., (2008) calculated the oxygen content of seawater based on the analysis of Ce content and Ce anomalies in carbonate minerals through geological time. The Ce anomalies in shallow marine stromatolites and ooids are present in 2.72 Ga Tumbiana Formation, 2.5 Ga Wittenoorn Dolomite and 2.3 Ga Kazput Formation in their study. Thus, Komiya et al., (2008) suggested that oxygen content of shallow water had increased since 2.7 Ga and became very high at the time of 2.5 Ga and 2.3 Ga. Thomazo et al., (2009) compiled the stable isotope signature of elements related to life (C, N, S, Fe) in the carbonate rocks between 2.8 and 2.5 Ga and suggested the atmosphere remained free of oxygen around 2.7 Ga. Both the isotopic studies by Komiya et al., (2008) and Thomazo et al., (2009) imply the oxygenation was likely only limited to shallow water environment before 2.5 Ga.

Late Archean environment

The abundant carbonates in the Ghaap Group (2.6 Ga to 2.5 Ga) especially in the Campbellrand Subgroup have $\delta^{13}\text{C}$ values close to 0‰ (-2.4‰ to +0.4‰) similar to present-day normal marine conditions (Des Marais, 2001; Frauenstein et al., 2009) while the $\delta^{13}\text{C}_{\text{org}}$ values (-21.6‰ to -38.6‰) are slightly ^{13}C -depleted than previously published Archean $\delta^{13}\text{C}_{\text{org}}$ value records (Hayes et al., 1983; Faure and Mensing, 2005). Carbon isotope composition of the carbonate rocks suggests that the CaCO_3 saturation of seawater was still high during the late Archean time, and the concentration of CO_2 in the atmosphere was higher than it is at present. The process of photosynthesis is thought to be the most important mechanism which can change the concentration of CO_2 in the atmosphere and seawater, due to the

primary (fixation) influence by biota and secondary (weathering) processes (Des Marais, 1997; Lowe and Tice, 2004; Raymond, 2005).

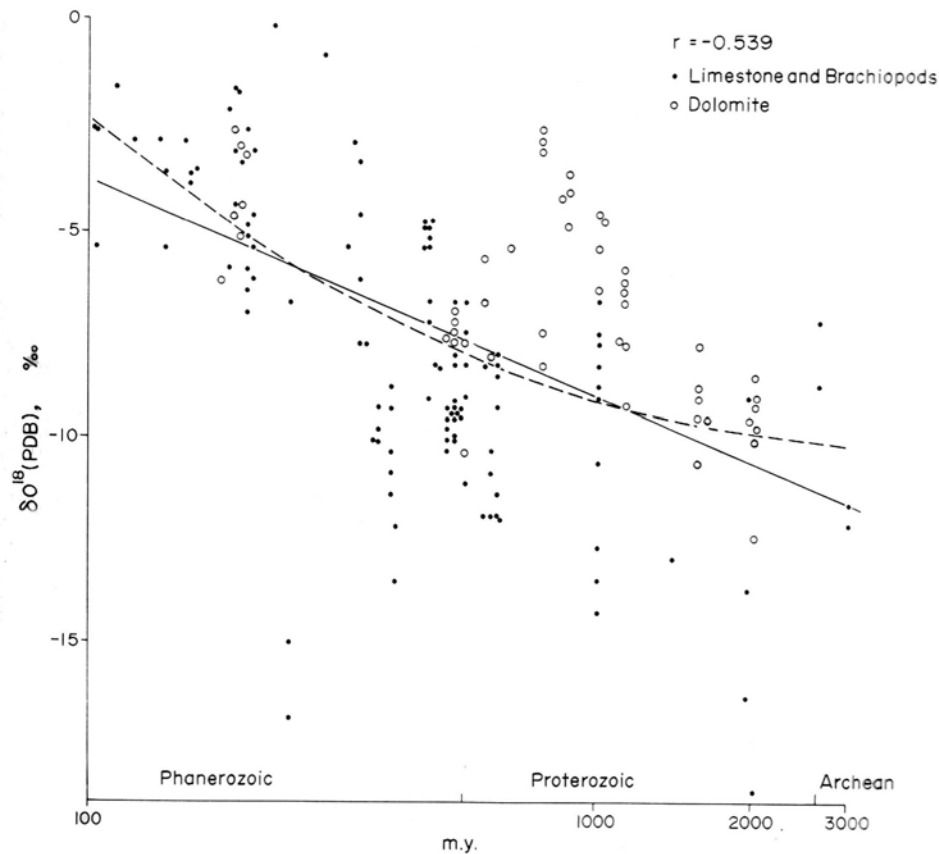


Figure 6.7 Secular trends of $\delta^{18}\text{O}$ values in sedimentary carbonate rocks (Veizer and Hoefs, 1976, the statistical distribution on the time axis is log normal).

The lack of systematic co-variation between $\delta^{13}\text{C}$ and $\delta^{18}\text{O}$ values is commonly used as evidence that the carbon isotope signal is not controlled by post-depositional alterations (Allan and Matthews, 1982; Kaufman and Knoll, 1995; Xiao et al., 1997). Carbonate samples from Ghaap Group in figure 6.6 (domain **A**) have restricted ranges in $\delta^{13}\text{C}$ (-0.5 ± 1 ‰) and $\delta^{18}\text{O}$ (-9.5 ± 1 ‰) values and lacks of co-variation. This indicates that the depletion in $\delta^{18}\text{O}$ values of these carbonate rocks, probably caused by the interaction with high temperature fluids, which has a limited effect on the $\delta^{13}\text{C}$ values. Thus it is possible to use the carbonate $\delta^{18}\text{O}$ values of domain **A** and **B** in figure 6.6 as primary (or near-primary) isotopic signatures for constraining the paleo-temperature of the water from which carbonate precipitated.

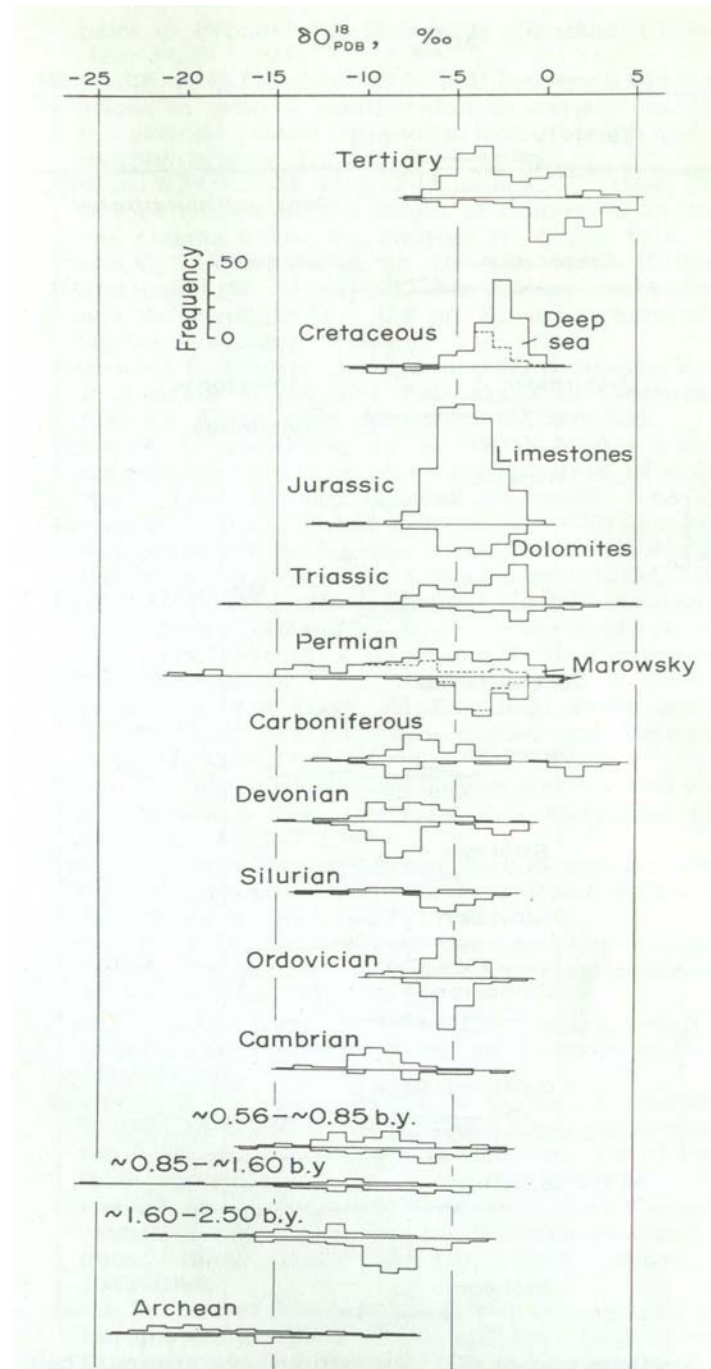


Figure 6.8 Histograms of compiled carbonate $\delta^{18}\text{O}$ values for different geological age group. The top histogram is for limestones and the 'upside down' one for dolomites (Veizer and Hoefs, 1976).

Systematic decreasing of $\delta^{18}\text{O}$ values in carbonate rocks with increasing geological age back to the Archean (Figure 6.7 and 6.8) has been widely discussed (Clayton and Degens, 1959; Keith and Weber, 1964; Veizer and Hoefs, 1976; Veizer et al., 1992b; Shields and Veizer, 2002; Knauth, 2005; Kasting et al., 2006).

Three main factors may account for this: (1) a continuous post-depositional diagenetic process through geological time (Veizer and Hoefs, 1976; Choquette and James, 1987; Fu et al., 2006; Fairchild and Kennedy, 2007); (2) a progressive increasing of the oxygen isotopic composition of seawater with time (Veizer and Hoefs, 1976; Knauth and Epstein, 1976; Kasting et al., 2006); (3) a progressive decreasing of the average temperatures of seawater with time (Karhu and Epstein, 1986; Burdett et al., 1990; Knauth and Lowe, 2003).

The $\delta^{18}\text{O}$ values of Archean seawater were suggested to be between 0.0‰ to +1.0‰ SMOW according to the model of isotopic exchange between seawater and mid-ocean ridge basalts (Holland, 1984). Thus, we use the constant seawater $\delta^{18}\text{O}$ values of 0‰ in the course of geological time (Allègre, C.J., 2008) and well preserved stromatolitic carbonate samples (pure calcite) for the calculation of average seawater temperature during the Ghaap Group carbonate deposition. The heaviest $\delta^{18}\text{O}$ values of the carbonates in figure 6.6 (-8 ± 2 ‰, domain **A** and **B**) are assumed to reflect the least altered isotopic signatures and imply the average seawater temperature of 55 ± 10 °C ($10^3 \ln \alpha_{\text{Cc-H}_2\text{O}} = 18.03 (10^3 \text{T}^{-1}) - 32.42$, Friedman and O'Neil, 1977; Kim and O'Neil, 1997; Kim et al., 2007).

Compared with modern marine depositions, depleted $\delta^{18}\text{O}$ values (-16 ‰ to -6 ‰) of carbonate rocks in the entire Ghaap Group suggest that the mean surface ocean temperature in late Archean is estimated to have been up to 70°C when little diagenetic alteration is assumed. Such temperature, although discussed by Knauth and Lowe (2003) and by Robert and Chaussidon (2006), seem very questionable and would signify an extremely warm, “super-tropical” environment for the Ghaap Group deposition and unusually hot atmosphere of the Earth, that could lead to an atmospheric “run away” scenario (Kasting, 1988). It can thus be rather assumed that either the O isotopy system has been disturbed during diagenesis as temperatures of around 70 °C are not realistic for oceanic surface water and thus must be diagenetic or evaporative, restricted basin temperatures, or a mixture of both conditions and processes.

Knauth and Lowe (2003) used the $\delta^{18}\text{O}$ values of chert samples from the Onverwacht Group (3.4 billion years) in South Africa and calculated the near surface temperature on the order of 55-85°C. Knauth (2005), Kasting and Howard (2006) and Robert and Chaussidon (2006) reviewed chert and carbonate samples through geological time and suggested that seawater temperature changes from about 70°C 3.5 billion year ago to about 20°C 800 million years ago. Early Proterozoic marine carbonates of the Rocknest Formation (1.93-1.89 Ga) have been studied by Burdett et al., (1990) with the carbon and oxygen isotopic analysis. The depleted $\delta^{18}\text{O}$ values (about 8‰) relative to younger marine carbonate suggest that the surface water temperature may still have been 30-35°C at 1.9 Ga, significantly higher than modern marine environments. Although some of the cherts investigation (Robert and Chaussidon, 2006) were proven to be hydrothermal alteration products of original sea bottom sediments (Hofmann and Bolhar, 2007; De Vries and Touret, 2007), the overall increase in both chert and carbonate $\delta^{18}\text{O}$ values with time (Figure 6.7 and figure 6.8) is interpreted as global cooling through geological time. The oxygen isotopic evidences offered a significantly warmer estimated seawater temperature during the Ghaap Group carbonate deposition than the carbonate deposition in modern oceans.

Late Archean Carbonate Chemistry

Carbon isotopic composition of carbonate rocks in Ghaap Group shows a large excursion in the transition from lower Schmidtsdrif Subgroup to the upper Campbellrand Subgroup. This excursion (-7‰ to -1‰) in $\delta^{13}\text{C}$ values is interpreted as two different isotopic fractionation mechanisms dominating the Schmidtsdrif Subgroup and Campbellrand Subgroup respectively. The Schmidtsdrif Subgroup carbonate deposition was controlled by the stronger carbon and oxygen isotopic interactions in the system of $\text{CO}_2 + \text{CH}_4$, between seawater and atmosphere during the earlier extensive volcanic outgassing and hydrothermal flux. The Campbellrand Subgroup carbonate deposition was mostly influenced by the exchange of carbon isotope in the system of $\text{CO}_2 + \text{HCO}_3^-$, and showed heavier but normal marine $\delta^{13}\text{C}$ values. This $\delta^{13}\text{C}$ excursion possibly represents the compositional changes in both ocean and atmosphere at late Archean time. During the Schmidtsdrif Subgroup,

carbonate rocks were deposited in a deep water environment where the isotopic signatures exchanged between carbonate minerals and basinal seawater. The Campbellrand Subgroup carbonate deposition was mostly in a shallower environment where isotopic exchange was possible between carbonate minerals and open marine seawater. The biological fixation of CO₂ and production of O₂ in shallow marine environment raise the pH values by removing carbonic acid from the system, subsequently increases the saturation state of CaCO₃ and the concentration of free oxygen both in the shallow marine and atmosphere (Grotzinger and Kasting, 1993). Thus, the increasing trend of δ¹³C values in the entire Ghaap Group is preferentially interpreted as the consequence of continuously and gradually increasing biological activity.

Carbonate rocks underwent a remarkable carbon and oxygen isotopic evolution during late Archean, reflecting the changes of environmental and compositional conditions in atmosphere and ocean. The emergence of microbial life and their activities greatly changed the concentration of free oxygen and other redox sensitive element such as Fe²⁺, Re²⁺ and Mo²⁺ in atmosphere and seawater (Grotzinger and Knoll, 1995; Sumner and Grotzinger, 2004; Wille et al., 2007; Voegelin et al., 2010; Kendall et al., 2010). Many factors control the δ¹³C_{org} values, including the isotopic composition of source DIC, the kinetic effects of biological photosynthesis and the kinetic effects of carbon recycling among biosphere, seawater and sediments. When the isotopic composition of carbon is recorded in the carbonate rocks, the difference between δ¹³C_{org} and δ¹³C_{carb} ($\Delta\delta^{13}\text{C}_{\text{org-carb}} = \delta^{13}\text{C}_{\text{org}} - \delta^{13}\text{C}_{\text{carb}}$) can be used as a proxy for life in sedimentary rocks. A systematic difference in the isotope composition of organic and carbonate C (with $\Delta\delta^{13}\text{C}_{\text{org-carb}} \sim -30\text{‰}$ in figure 5.2) has been observed in this study and most organic-rich sedimentary rocks through geological history (Schidlowski, 2001; Thomazo et al., 2009). This carbon isotopic difference between organic-rich and carbonate-rich reservoirs would support the interpretation of the presence of increasing biological activities such as photosynthesis (Schidlowski, 2001; Thomazo et al., 2009).

CONCLUSIONS

7. Conclusions

Carbonate samples were selected from the continuous stratigraphic succession through the Ghaap Plateau carbonates of the 3600-m deep Kathu drillcore. Microfacies analysis of these samples supports former facies interpretations (Beukes, 1987; Altermann and Siegfried, 1997, Schröder et al., 2009). In this study, selected stromatolitic carbonate samples show various stromatolitic morphologies and carbonate sediments which precipitated in their direct neighbourhood. Microfacies studies on these carbonate rocks reveal a possible depositional depth difference for the different microbial mats and stromatolites. Stable isotope analysis (C and O isotopes) of the same samples document the environmental changes in carbonate deposition and provide valuable information for the chemical and physical conditions of ancient atmosphere and ocean. Stratigraphic profiles of carbonate $\delta^{13}\text{C}_{\text{carb}}$, $\delta^{13}\text{C}_{\text{org}}$ and $\delta^{18}\text{O}$ were obtained through the Ghaap Group from the Kathu borehole of South Africa.

Three morphological types of stromatolites were distinguished and analysed for their carbon isotopic composition. The differences among the three types of finely laminated microbial mats, columnar stromatolites and fenestral stromatolites, which have been interpreted as deep subtidal, shallow subtidal to intertidal and intertidal to supratidal environments respectively, show a general 0.5‰ difference in the mean $\delta^{13}\text{C}$ values (Figure 6.1 and 6.2). The finely laminated microbial mats dominated deep subtidal carbonate rocks show a narrow range of $\delta^{13}\text{C}$ values (from -0.5‰ to +0.2‰) with a mean $\delta^{13}\text{C}$ values of -0.2‰. The columnar stromatolites dominated shallow subtidal to intertidal carbonate rocks show a narrow range of $\delta^{13}\text{C}$ values (from -1.3‰ to -0.2‰) with a mean $\delta^{13}\text{C}$ values of -0.6‰. The fenestral stromatolites dominated intertidal to supratidal carbonate rocks display a wide range of $\delta^{13}\text{C}$ values (from -1.1‰ to +0.4‰) with a mean $\delta^{13}\text{C}$ values of -0.5‰. The variable $\delta^{13}\text{C}$ values in the supratidal carbonate rocks are thought to be influenced by air-sea exchange processes. The relatively narrow range of $\delta^{13}\text{C}$ values in deep subtidal to intertidal are thought to be well preserved in carbonate rocks without such carbon isotopic exchanges. Possible explanation for the difference of $\delta^{13}\text{C}$ values between deep subtidal and intertidal are

interpreted as changes in the composition of seawater with the depth during the carbonate deposition in Ghaap Group. The rise of free oxygen is only confined in the shallower water facies and its affect on the redox state and chemical characteristics of surface seawater is limited.

Determined stratigraphic variation in carbon isotopic composition of Ghaap Group carbonate rocks reveals a distinctive carbon isotope pattern: $\delta^{13}\text{C}$ values of carbonate rocks in Ghaap Group are fluctuating, but in general they are slightly negative and show an increasing trend from the lower to upper formations. This indicates that biological activity was playing an important role in the carbonate isotopic composition in Campbellrand Subgroup. A $\delta^{13}\text{C}$ values excursion (from around -7‰ to -0‰) is observed in the transition stage from the lower Schmidtsdrif Subgroup to the upper Campbellrand Subgroup. This implies a possible chemical change in the seawater from a relatively restricted environment which was highly influenced by the volcanic outgassing and hydrothermal influx to a more open environment where biological activity play a significant role on carbonate deposition.

Determined stratigraphic variation in oxygen isotopic composition of Ghaap Group carbonate rocks reveals two distinctive oxygen isotope variations: (1) $\delta^{18}\text{O}$ values of carbonate rocks show progressive increase from the lower Schmidtsdrif Subgroup (around -15‰) to the middle Campbellrand Subgroup of Klippan Formation (around -5‰). The most depleted $\delta^{18}\text{O}$ values in the Schimidtsdrif Subgroup carbonates are though to be influenced by the volcanic outgassing and hydrothermal influx overprints with depleted $\delta^{13}\text{C}$ values. The high temperature mostly controls the deposition of these carbonate rocks. As the $\delta^{18}\text{O}$ values display a progressive increase upward until the Klippan Formation, the surface oceanic temperature is though to decrease as the carbonate deposition continues. (2) $\delta^{18}\text{O}$ values of carbonate rocks show a negative shift from the middle Campbellrand Subgroup of Klippan Formation (around -5‰) to the uppermost Gamohaan Formation (around -13‰). This decrease of $\delta^{18}\text{O}$ values in carbonate rocks is

preferentially interpreted as an elevated deep burial temperature in deeper water column with possible hydrothermal influence.

A systematic difference in the isotope composition between organic C and carbonate C (with $\Delta\delta^{13}\text{C}_{\text{org-carb}} \sim -30\text{‰}$ in Figure 5.3) has been observed in most available organic-rich carbonate rocks in this study. The differences between $\delta^{13}\text{C}_{\text{carb}}$ values and $\delta^{13}\text{C}_{\text{org}}$ values provide an evidence for the presence of biological activity, and the overall decreasing trend of $\delta^{13}\text{C}_{\text{org}}$ values in the stratigraphic profile suggests that the compositional change in ancient atmosphere and seawater is a gradual process.

Combining the observation of carbon isotopes with the oxygen isotopes offers a new insight to the paleo-environmental settings of the Ghaap Group sedimentary deposits (Figure 6.3). The $\delta^{13}\text{C}$ and $\delta^{18}\text{O}$ values are plotted in four domains. The four distinct domains of $\delta^{13}\text{C}$ and $\delta^{18}\text{O}$ values confirm previous sedimentary facies studies (Beukes, 1987; Altermann and Siegfried, 1997; Eriksson and Altermann, 1998; Knoll and Beukes, 2009). Due to the $\delta^{13}\text{C}$ values shift from -7‰ (Schmidtsdrif Subgroup) to -0.8‰ (Campbellrand Subgroup), carbonate formation was probably precipitated in a basin isolated from the ocean (marginal marine and/or deep lagoonal environment) without significant dilution by a large oceanic reservoir. Schmidtsdrif Subgroup carbonate involves precipitation from ^{13}C depleted water masses which were highly overprinted by early volcanic degassing and hydrothermal influx.

Compared with modern marine depositions, depleted $\delta^{18}\text{O}$ values (-16‰ to -6‰) of carbonate rocks in the entire Ghaap Group suggest that the mean surface ocean temperature in late Archean is estimated to have been up to $55 \pm 10 \text{ }^\circ\text{C}$ when little diagenetic alteration is assumed. Such estimated temperature seems very questionable because O isotopy system usually has been disturbed during diagenetic process and possible hydrothermal influence. Thus, the calculated temperature of $55 \pm 10 \text{ }^\circ\text{C}$ Ghaap Group carbonate deposition may be not the realistic for oceanic surface water but diagenesis, restricted basinal temperatures

and/or a mixture of both conditions and processes. But the overall increases in both chert and carbonate $\delta^{18}\text{O}$ values with time (Figure 6.7 and figure 6.8) are interpreted as global cooling through geological time. Finally, the oxygen isotopic evidences in this study offer a significantly warmer estimated seawater temperature during the Ghaap Group carbonate deposition than the carbonate deposition in modern oceans.

Biological activity in marine environment exert a great influence on the later Campbellrand Subgroup carbonate deposition than the former Schmidtsdrif Subgroup, subsequently change the chemical composition of surface seawater and carbonate minerals. The environmental change including water depth, diagenetic fluids input and surface oceanic temperature can be recorded in the isotopic composition (C and O) of carbonate rocks. Therefore, we can use the plotted $\delta^{13}\text{C}$ and $\delta^{18}\text{O}$ values for the sedimentary facies comparisons and paleo-environmental reconstructions.

8. References

- Allan, J.R. and Matthews, R.K., 1982. Isotope signatures associated with early meteoric diagenesis. *Sedimentology* 29, 797-817.
- Allègre, C.J., 2008. *Isotope Geology*. Cambridge University Press, 512pp.
- Altermann, W., 1996. Sedimentology, geochemistry and palaeogeographic implications of volcanic rocks in the upper Archaean Campbell Group, western Kaapvaal craton, South Africa. *Precambrian Research* 79, 73-100.
- Altermann, W., 1997. Sedimentological evaluation of Pb–Zn exploration potential of the Precambrian Griquatown Fault Zone in the Northern Cape Province, South Africa. *Mineralium Deposita* 32, 382–391.
- Altermann, W., 2004. Chapter 6.5. Precambrian stromatolites: Problems in definition, classification, morphology and stratigraphy. In: Eriksson, P.G., Altermann, W., Nelson, D.R., Mueller, W. and Catuneanu, O. (Eds.): *The Precambrian Earth: Tempos and Events*. *Developments in Precambrian Geology*, Elsevier, 564-574.
- Altermann, W., 2008. Accretion, trapping and binding of sediment in Archean stromatolites -- morphological expression of the antiquity of life. *Space Science Review* 135, 55-79.
- Altermann, W. and Hålbich, I.W., 1990. Thrusting, folding and stratigraphy of the Ghaap Group along the south-western margin of the Kaapvaal Craton. *South African Journal of Geology* 93, 553-556.
- Altermann, W. and Hålbich, I.W., 1991. Structural history of the southwestern corner of the Kaapvaal Craton and the adjacent Namaqua realm: new observations and a reappraisal. *Precambrian Research* 52, 133-166.
- Altermann, W. and Herbig, H.-G., 1991. Tidal flat deposits of the Lower Proterozoic Campbell Group along the southwestern margin of the Kaapvaal Craton, Northern Cape Province, South Africa. *Journal of African Earth Sciences* 13, 415-435.
- Altermann, W. and Nelson, D.R., 1996. Neoproterozoic carbonate platform development: an example from the Kaapvaal craton, South Africa. 17th Regional African-European Meeting of Sedimentology, Sfax, Tunisia, 1996. IAS Abstract Volume, 8-9.
- Altermann, W. and Nelson, D.R., 1998. Sedimentation rates, basin analysis and regional correlations of three Neoproterozoic and Palaeoproterozoic sub-basins of the Kaapvaal craton as inferred from precise U–Pb zircon ages from volcanoclastic sediments. *Sedimentary Geology* 120, 225–256.

- Altermann, W. and Schopf, J.W., 1995. Microfossils from the Neoproterozoic Campbell Group, Griqualand West Sequence of the Transvaal Supergroup, and their paleoenvironmental and evolutionary implications. *Precambrian Research* 75, 65-90.
- Altermann, W. and Siegfried, H.P., 1997. Sedimentology and facies development of an Archean shelf: carbonate platform transition in the Kaapvaal Craton, as deduced from a deep borehole at Kathu, South Africa. *Journal of African Earth Science* 24, 391-410.
- Altermann, W. and Wotherspoon, J.M., 1995. The carbonates of the Transvaal and Griqualand West Sequences of the Kaapvaal Craton, with special reference to the Lime Acres limestone deposit. In: Eriksson, P.G. and Altermann, W., Editors, 1995. *The Mineral Deposits of the Transvaal Sequence and the Upper Bushveld Igneous Complex*. *Mineralium Deposita* 30, 124-134.
- Altermann, W., Kazmierczak, J., Oren, A. and Wright, D., 2006. Cyanobacterial calcification and its rock-building potential during 3.5 billion years of Earth history. *Geobiology* 4, 147-166.
- Altermann, W., Hälbig, I.W., Horstmann, U.E., Ahrendt, H., Fitch, F.J. and Miller, J.A., 1992. The age of tectogenesis and metamorphism of the south-western Kaapvaal Craton. Abstract 29th International Geological Congress, Kyoto, Japan, 2-3, 261.
- Atherstone, 1896. Kimberley and its diamonds. *Transactions of the Geological Society of South Africa* 1, 76-89.
- Awramik, S.M. and Grey, K., 2005. Stromatolites: Biogenicity, biosignatures, and bioconfusion. *Proc. SPIE*, 5906: 5906P-1—5906P-9.
- Awramik, S.M. and Riding, R., 1988. Role of algal eukaryotes in subtidal columnar stromatolite formation. *Proceedings of the National Academy of Sciences of the United States of America* 85, 1327-1329.
- Banner, J.L., Hanson, G.N. and Meyers, W.J., 1988. Water-rock interaction history of regionally extensive dolomites of the Burlington-Keokuk Formation (Mississippian): Isotopic evidence. *Sedimentology and Geochemistry of Dolostones*, SEPM Special Publication 43, 97-113.
- Bekker, A., Holland, H.D., Wang, P.-L., Rumble III, D., Stein, H.J., Hannah, J.L., Coetzee, L.L. and Beukes, N.J., 2004. Dating the rise of atmospheric oxygen. *Nature* 427, 117-120.

- Berkner, L.V. and Marshall, L.C., 1965. On the origin and rise of oxygen concentration in the Earth's atmosphere. *Journal of Atmospheric Science* 22, 225-261.
- Beukes, N.J., 1977. Stratigraphy and structure of the Transvaal dolomites in the Northern Cape Province – control on lead mineralization in the Griquatown area and iron-manganese mineralization in the Sishen Postmasburg area. In: Abstracts Geocongress 77, Geological Society of South Africa, 14-19.
- Beukes, N.J., 1979. Litostratigrafiese onderverdeling van die Schmidtsdrif-Subgroep van die Ghaap-Groep in Noord-Kaapland. *Transactions of the Geological Society of South Africa* 82, 313-327.
- Beukes, N.J., 1980. Stratigrafie en litofasies van die Campbellrand-Subgroep van die Proterofitiese Ghaap-Groep, Noord-Kaapland. *Transactions of the Geological Society of South Africa* 83, 141-170.
- Beukes, N.J., 1983. Paleoenvironmental setting of iron-formations in the depositional basin of the Transvaal Supergroup, South Africa. In: Trendall, A.F. and Morris, R.C. (Eds.), *Iron-Formation: Facts and Problems*. Elsevier, New York, 131-209.
- Beukes, N.J., 1986. The Transvaal sequence in Griqualand West. In: Anhaeusser, C.R. and Maske, S. (Eds.), *Mineral Deposits of Southern Africa, Volume 1*. Geological Society of South Africa, Johannesburg, 819-828.
- Beukes, N.J., 1987. Facies relations, depositional environments and diagenesis in a major early Proterozoic stromatolitic carbonate platform to basinal sequence, Campbellrand Subgroup, Transvaal Supergroup, South Africa. *Sedimentary Geology* 54, 1-46.
- Beukes, N. and Klein, C., 1990. Geochemistry and sedimentology of a facies transition – from microbanded to granular iron-formation – in the early Proterozoic Transvaal Supergroup, South Africa. *Precambrian Research* 47, 99-139.
- Beukes, N.J., Klein, C., Kaufman, A.J. and Hayes, J.M., 1990. Carbonate petrography, kerogen distribution, and carbon and oxygen isotope variations in an early Proterozoic transition from limestone to iron-formation deposition, Transvaal Supergroup, South Africa. *Economic Geology* 85, 663–690.
- Brown, J.S., 1943. Suggested use of the word microfacies. *Economic Geology* 38, 325.
- Brown, N., 1896. The succession of the rocks in the Pilgrim's Rest Goldfield. *Transactions of the Geological Society of South Africa* 2, 3-4.

- Burdett, J.W., Grotzinger, J.P. and Arthur, M.A., 1990. Did major changes in the stable isotope composition of Proterozoic seawater occur? *Geology* 18, 227-230.
- Button, A., 1973. The stratigraphic history of the Malmani dolomite in the eastern and north-eastern Transvaal. *Transactions of the Geological Society of South Africa* 76, 229-247.
- Canfield, D.E., 2005. The early history of atmospheric oxygen: Homage to Robert M. Garrels. *Annual Reviews Earth and Planetary Sciences* 33, 1-36.
- Charles, C.D., Wright, J.D. and Fairbanks, R.G., 1993. Thermodynamic influences on the marine carbon isotope record. *Paleoceanography* 8, 691-697.
- Chester, R., 2000. *Marine Geochemistry*, 2nd Edition. Blackwell Science Ltd, Oxford, UK. 506pp.
- Choquette, P.W. and James, N.P., 1987. Diagenesis in limestones, 3. The deep burial environment. *Geoscience Canada* 14, 3-35.
- Clayton, R.N. and Degens, E.T., 1959. Use of carbon-isotope analyses of carbonates for differentiating fresh-water and marine sediments: GEOLOGICAL NOTES. *Bulletin American Association of Petroleum Geologists* 43, 890-897.
- Clendenin, C.W., 1989. Tectonic influence on the evolution of the early Proterozoic Transvaal Sea, Southern Africa. PhD thesis, University of the Witwatersrand, Johannesburg.
- Cloud, P., 1972. A working model of the primitive Earth. *American Journal of Science* 272, 537-548.
- Condie, K.C., 2001. Continental growth during formation of Rodinia at 1.35-0.9 Ga. *Gondwana Research* 4, 5-16.
- Condie, K.C., Des Marais, D.J. and Abbott, D., 2001. Precambrian superplumes and supercontinents: a record in black shales, carbon isotopes, and paleoclimates? *Precambrian Research* 106, 239-260.
- Craig, H., 1965. The measurement of oxygen isotope paleotemperatures. *Proc. Spoleto Conference on Stable Isotopes in Oceanographical Studies and Paleotemperatures* 3, 9-130.
- De Vries, S.T. and Touret, J.L.R., 2007. Early Archaean hydrothermal fluids; a study of inclusions from the ~3.4 Ga Buck Ridge Chert, Barberton Greenstone Belt, South Africa. *Chemical Geology* 237, 289-302.
- Des Marais, D.J., 1994. Tectonic control of the crustal organic carbon reservoir during the Precambrian. *Chemical Geology* 114, 303-314.

- Des Marais, D.J., 1997. Isotopic evolution of the biogeochemical carbon cycle during the Proterozoic Eon. *Organic Geochemistry* 27, 185-193.
- Des Marais, D.J., 2001. Isotopic evolution of the biogeochemical carbon cycle during the Precambrian. *Reviews in Mineralogy and Geochemistry* 43, 555-578.
- Eriksson, K.A., 1972. Cyclic sedimentation in the Malmani Dolomite, Potchefstroom Synclinorium. *Transactions of the Geological Society of South Africa* 75, 85-97.
- Eriksson, K.A., 1977. Tidal flat and subtidal sedimentation in the 2250 M.Y. Malmani dolomite, Transvaal, South Africa. *Sedimentary Geology* 18, 223-244.
- Eriksson, K.A., McCarthy, T.S. and Truswell, J.F., 1975. Limestone formation and dolomitization in a lower Proterozoic succession from South Africa. *Journal of Sedimentary Research* 45, 604-614.
- Eriksson, K.A., Truswell, J.F. and Button, A., 1976. Palaeoenvironmental and geochemical models from an early Proterozoic carbonate succession in South Africa. *Developments in Sedimentology* 20, 635-643.
- Eriksson, P.G. and Altermann, W., 1998. An overview of the geology of the Transvaal Supergroup dolomites (South Africa). *Environmental Geology* 36, 179-188.
- Eriksson, P.G., Altermann, W. and Hartzler, F.J., 2006. The Transvaal Supergroup and its precursors. In: Johnson, M.R., Anhaeusser, C.R. and Thomas, R.J., *The geology of South Africa*. Geological Society of South Africa, Johannesburg/Council for Geoscience, Pretoria, 237-260.
- Eriksson, P.G., Catuneanu, O., Nelson, D.R., Mueller, W.U. and Altermann, W. Towards a synthesis, 2004. In: Eriksson, P.G., Altermann, W., Nelson, D.R., Mueller, W.U. and Catuneanu, O., editors. *The Precambrian Earth: tempos and events*. Amsterdam: Elsevier, 739-769.
- Eriksson, P.G., Catuneanu, O., Sarkar, S. and Tirsgaard, H., 2005. Patterns of sedimentation in the Precambrian. *Sedimentary Geology* 176, 17-42.
- Ernst, R.E. and Buchan, K.L., 2001. Large mafic magmatic events through time and links to mantle-plume heads. In: Ernst, R.E. and Buchan, K.L., (Eds.) *Mantle Plumes: Their Identification through Time*. Geological Society of America Special Paper 352, 483-575.
- Fairchild, I.J. and Kennedy, M.J., 2007. Neoproterozoic glaciation in the Earth System. *Journal of the Geological Society* 164, 895-921.
- Farquhar, J., Bao, H. and Thiemens, M., 2000. Atmospheric influence of Earth's earliest sulfur cycle. *Science* 289, 756-758.

- Faure, G. and Mensing, T.M., 2005. *Isotopes: Principles and Applications*, 3rd Edition. John Wiley & Sons Ed., 897pp.
- Fischer, W.W., Schroeder, S., Lacassie, J.P., Beukes, N.J., Goldberg, T., Strauss, H., Horstmann, U.E., Schrag, D.P. and Knoll, A.H., 2009. Isotopic constraints on the Late Archean carbon cycle from the Transvaal Supergroup along the western margin of the Kaapvaal Craton, South Africa. *Precambrian Research* 169, 15-27.
- Flügel, E., 2004. *Microfacies of carbonate rocks-analysis, interpretation and application*. Springer Press, Germany, 190-203.
- Frauenstein, F., Veizer, J., Beukes, N., Van Niekerk, H.S. and Coetzee, L.L., 2009. Transvaal Supergroup carbonates: Implications for Paleoproterozoic $\delta^{18}\text{O}$ and $\delta^{13}\text{C}$ records. *Precambrian Research* 175, 149-160.
- Friedman, I. and O'Neil, J.R., 1977. *Compilation of stable isotope fractionation factors of geochemical interest*. USGS Prof. Paper, 440-KK.
- Fu, Q., Qing, H. and Bergman, K.M., 2006. Early dolomitization and recrystallization of carbonate in an evaporite basin: the Middle Devonian Ratner laminite in southern Saskatchewan, Canada. *Journal of the Geological Society* 163, 937-948.
- Gandin, A., Wright, D.T. and Melezhik, V., 2005. Vanished evaporites and carbonate formation in the Neoarchaeon Kogelbeen and Gamohaam formations of the Campbellrand Subgroup, South Africa. *Journal of African Earth Sciences* 41, 1-23.
- Garde, A.A., 1979. Strontium geochemistry and carbon and oxygen isotopic compositions of lower proterozoic dolomite and calcite marbles from the Marmorilik Formation, West Greenland. *Precambrian Research* 8, 183-199.
- Godderis, Y. and Veizer, J., 2000. Tectonic control of chemical and isotopic composition of ancient oceans: the impact of continental growth. *American Journal of Science* 300, 434-461.
- Godfrey, L.V. and Falkowski, P.G., 2009. The cycling and redox state of nitrogen in the Archaean ocean. *Nature Geoscience* 2, 725-729.
- Grotzinger, J.P. and Kasting, J.F., 1993. New constraints on Precambrian ocean composition. *The Journal of Geology* 101, 235-243.
- Grotzinger, J.P. and Knoll, A.H., 1995. Anomalous carbonate precipitates: Is the Precambrian the key to the Permian? *Palaios* 10, 578-596.
- Grotzinger, J.P. and Knoll, A.H., 1999. Stromatolites: Evolutionary mileposts or environmental dipsticks? *Annual Reviews of Earth and Planetary Science* 27, 313-358.

- Grover, G. and Read, J.F., 1978. Fenestral and associated vadose diagenetic fabrics of tidal flat carbonates, middle Ordovician new market limestone, southwestern Virginia. *Journal of Sedimentary Petrology* 48, 453-473.
- Hatch, F. H., 1904. The oldest sedimentary rocks of the Transvaal. *Transactions of the Geological Society of South Africa* 7, 147-150.
- Hayes, J.M., Kaplan, I.R. and Wedeking, K.W., 1983. Precambrian organic geochemistry, preservation of the record. In: Schopf, J.W. (Ed.), *The Earth's Earliest Biosphere: Its Origin and Evolution*, Princeton University Press, Princeton, 93-134.
- Hoefs J., 2009. *Stable Isotope Geochemistry*. 6th Edition, Springer-Verlag, Berlin, 208pp.
- Hofmann, A. and Bolhar, R., 2007. Carbonaceous cherts in the Barberton greenstone belt and their significance for the study of early life in the Archean record. *Astrobiology* 7, 355-388.
- Hofmann, H.J., Pearson, D.A.B. and Wilson, B.H., 1980. Stromatolites and fenestral fabric in Early Proterozoic Huronian Supergroup, Ontario. *Canadian Journal of Earth Sciences* 17, 1351-1357.
- Holland, H.D., 1984. *The chemical evolution of the atmosphere and oceans*. Princeton University Press, 598pp.
- Holland, H.D. and Beukes, N.J., 1990. A paleoweathering profile from Griqualand West, South Africa: Evidence for a dramatic rise in atmospheric oxygen between 2.2 and 1.9 BYBP. *American Journal of Science* 290-A, 1-34.
- Hotinski, R.M., Kump, L.R. and Arthur, M.A., 2004. The effectiveness of the Paleoproterozoic biological pump: A $\delta^{13}\text{C}$ gradient from platform carbonates of the Pethei Group (Great Slave Lake Supergroup, NWT). *Geological Society of America Bulletin* 116, 539-554.
- Hunt, J.M., 1995. *Petroleum geochemistry and geology*. 2nd edition, W.H. Freeman, New York, Oxford. 743pp.
- IAPWS—the International Association for the Properties of Water and Steam, 2002. *Guidelines for the use of fundamental physical constants and basic constants of water*. Revision of September 2001 guidelines, Gaithersburg, MA. Available at <http://www.iapws.org>. Accessed March 15, 2007.
- Johnson, M.R., Anhaeusser, C.R. and Thomas, R.J. (Eds.), 2006. *The Geology of South Africa*. Geological Society of South Africa, Johannesburg/Council for Geoscience, Pretoria, 691pp.

- Karhu, J.A., 1993. Palaeoproterozoic evolution of the carbon isotope ratios of sedimentary carbonates in the Fennoscandian Shield. *Geological Survey of Finland Bulletin* 371, 1-87.
- Karhu, J. and Epstein, S., 1986. The implication of the oxygen isotope records in coexisting cherts and phosphates. *Geochimica et Cosmochimica Acta* 50, 1745-1756.
- Karhu, J. and Holland, H.D., 1996. Carbon isotopes and the rise of atmospheric oxygen. *Geology* 24, 867–870.
- Kasting, J.F., 1988. Runaway and moist greenhouse atmospheres and the evolution of Earth and Venus. *ICARUS* 74, 472-494.
- Kasting, J.F., 2001. The rise of atmospheric oxygen. *Science* 293, 819-820.
- Kasting, J.F. and Howard, M.T., 2006. Atmospheric composition and climate on the early Earth. *Philosophical Transactions of the Royal Society B* 361, 1733-1742.
- Kasting, J.F., Howard, M.T., Wallmann, K., Veizer, J., Shields, G. and Jaffrés, J., 2006. Paleoclimates, ocean depth, and the oxygen isotopic composition of seawater. *Earth and Planetary Science Letters* 252, 82-93.
- Kaufman, A.J. and Knoll, A.H., 1995. Neoproterozoic variations in the C-isotopic composition of seawater: stratigraphic and biogeochemical implications. *Precambrian Research* 73, 27-49.
- Kaufman, A.J., Hayes, J.M. and Klein, C., 1990. Primary and diagenetic controls of isotopic compositions of iron-formation carbonates. *Geochimica et Cosmochimica Acta* 54, 3461-3473.
- Kazmierczak, J. and Altermann, W., 2002. Neoproterozoic biomineralization by benthic cyanobacteria. *Science* 298, 2351.
- Kazmierczak, J. Kempe, S. and Altermann, W. 2004: Chapter 6.4: Microbial origin of Precambrian carbonates: Lessons from modern analogues. In: Eriksson, P.G., Altermann, W., Nelson, D.R., Mueller, W. & Catuneanu, O. (Eds.): *The Precambrian Earth: Tempos and Events. Developments in Precambrian Geology*, Elsevier, 545-563.
- Keith, M.L. and Weber, J.N., 1964. Carbon and oxygen isotopic composition of selected limestones and fossils. *Geochimica et Cosmochimica Acta* 28, 1787-1816.
- Kendall, B., Reinhard, C.T., Lyons, T.W., Kaufman, A.J., Poulton, S.W. and Anbar, A.D., 2010. Pervasive oxygenation along late Archaean ocean margins. *Nature Geoscience* 3, 647-652.

- Killingley, J.S., 1983. Effects of diagenetic recrystallization on $^{18}\text{O}/^{16}\text{O}$ values of deep-sea sediments. *Nature* 301, 594-597.
- Kim, S.-T. and O'Neil, J. R., 1997. Equilibrium and nonequilibrium oxygen isotope effects in synthetic carbonates. *Geochimica et Cosmochimica Acta* 61, 3461-3475.
- Kim, S.-T., O'Neil, J. R., Hillaire-Marcel, C. and Mucci, A., 2007. Oxygen isotope fractionation between synthetic aragonite and water: Influence of temperature and Mg^{2+} concentration. *Geochimica et Cosmochimica Acta* 71, 4704-4715.
- Klein, C. and Beukes, N.J., 1989. Geochemistry and sedimentology of a facies transition from limestone to iron-formation deposition in the early Proterozoic Transvaal Supergroup, South Africa. *Economic Geology* 84, 1733-1774.
- Klein, C. and Beukes, N.J., 1993. Sedimentology and geochemistry of the glaciogenic late Proterozoic Rapitan Iron-Formation in Canada. *Economic Geology* 88, 542-565.
- Klein, C., Beukes, N.J. and Schopf, J.W., 1987. Filamentous microfossils in the early Proterozoic Transvaal Supergroup: Their morphology, significance and paleoenvironmental setting. *Precambrian Research* 36, 81-94.
- Knauth, L.P., 2005. Temperature and salinity history of the Precambrian ocean: implications for the course of microbial evolution. *Palaeogeography, Palaeoclimatology, Palaeoecology* 219, 53-69.
- Knauth, L.P. and Epstein, E., 1976. Hydrogen and oxygen isotope ratios in nodular and bedded cherts. *Geochimica et Cosmochimica Acta* 40, 1095-1108.
- Knauth, L.P. and Kennedy, M.J., 2009. The late Precambrian greening of the Earth. *Nature* 460, 728-732.
- Knauth, L.P. and Lowe, D.R., 2003. High Archean climatic temperature inferred from oxygen isotope geochemistry of cherts in the 3.5 Ga Swaziland Supergroup, South Africa. *Geological Society of America Bulletin* 115, 566-580.
- Knoll, A.H. and Beukes, N.J., 2009. Introduction: Initial investigations of a Neoproterozoic shelf margin-basin transition (Transvaal Supergroup, South Africa). *Precambrian Research* 169, 1-14.
- Komiya, T., Hirata, T., Kitajima, K., Yamamoto, S., Shibuya, T., Sawaki, Y., Ishikawa, T., Shu, D., Li, Y. and Han, J., 2008. Evolution of the composition of seawater through geological time, and its influence on the evolution of life. *Gondwana Research* 14, 159-174.
- Kroopnick, P., 1985. The distribution of ^{13}C of ΣCO_2 in the world oceans. *Deep Sea Research Part A. Oceanographic Research Papers* 32, 57-84.

- Kump, L.R. and Arthur, M.A., 1999. Interpreting carbon-isotope excursions: carbonates and organic matter. *Chemical Geology* 161, 181-198.
- Logan, B.W., 1974. Inventory of diagenesis in Holocene-Recent carbonate sediments, Shark Bay, Western Australia. *American Association of Petroleum Geologists Memoir* 22, 195-249.
- Lohmann, K.C. and Walker, J.C.G., 1989. The $\delta^{18}\text{O}$ record of Phanerozoic abiotic marine calcite cements. *Geophysical Research Letters* 16, 319-322.
- Lowe, D.R. and Tice, M.M., 2004. Geologic evidence for Archean atmospheric and climatic evolution: Fluctuating levels of CO_2 , CH_4 , and O_2 with an overriding tectonic control. *Geology* 32, 493-496.
- Mabrouk, A., Belayouni, H., Jarvis, I. and Moody, R.T.J., 2006. Strontium, $\delta^{18}\text{O}$ and $\delta^{13}\text{C}$ as palaeo-indicators of unconformities: Case of the Aleg and Abiod formations (Upper Cretaceous) in the Miskar Field, southeastern Tunisia. *Geochemical Journal* 40, 405-424.
- Mayr, C., Fey, M., Haberzettl, T., Janssen, S., Lücke, A.S, Maidana, N. I., Ohlendorf, C., Schäbitz, F., Schleser, G. H., Struck, U., Wille M. and Zolitschka. B., 2005. Palaeoenvironmental changes in southern Patagonia during the last millennium recorded in lake sediments from Laguna Azul (Argentina). *Palaeogeography, Palaeoclimatology, Palaeoecology* 228, 203-227.
- Moore, C.H., 1997. Carbonate diagenesis and porosity. *Developments in Sedimentology* 46, Elsevier Publishing Company, 338pp.
- Morse, J.W. and Mackenzie, F.T., 1990. Geochemistry of sedimentary carbonates. *Developments in sedimentology* 48, Elsevier, 707pp.
- Ohmoto, H., Watanabe, Y., Ikemi, H., Poulson, S.R. and Taylor, B.E., 2006. Sulphur isotope evidence for an oxic Archean atmosphere. *Nature* 442, 908-911.
- O'Neil, J.R., Clayton, R.N. and Mayeda, T.K., 1969. Oxygen isotope fractionation in divalent metal carbonates. *Journal of Chemical Physics* 51, 5547-5558.
- Ono, S., Eigenbrode, J.L., Pavlov, A.A., Kharecha, P., Rumble III, D., Kasting, J.F. and Freeman, K.H., 2003. New insights into Archean sulphur cycle from mass-independent sulphur isotope records from the Hamersley Basin, Australia. *Earth and Planetary Science Letters* 213, 15-30.
- Ono, S., Wing, B., Johnston, D., Farquhar, J. and Rumble III, D., 2006. Mass-dependent fractionation of quadruple stable sulphur isotope system as a new

- tracer of sulfur biogeochemical cycles. *Geochimica et Cosmochimica Acta* 70, 2238-2252.
- Pavlov, A.A., Brown, L.L. and Kasting, J.F., 2001. UV shielding of NH₃ and O₂ by organic hazes in the Archean atmosphere. *Journal of Geophysical Research* 106, 23267-23287.
- Polteau, S., Moore, J.M. and Tsikos, H., 2006. The geology and geochemistry of the Palaeoproterozoic Makganyene diamictite. *Precambrian Research* 148, 257-274.
- Preuss, A., Schauder, R., Fuchs, G. and Stichler, W., 1989. Carbon isotope fractionation by autotrophic bacteria with three different carbon dioxide fixation pathways. *Zeitschrift fuer Naturforschung C: A Journal of Biosciences* 44, 397-402.
- Qing, H., 1998. Petrology and geochemistry of early-stage, fine- and medium-crystalline dolomites in the Middle Devonian Presqu'ile Barrier at Pine Point, Canada. *Sedimentology* 45, 433-446.
- Qing, H. and Mountjoy, E.W., 1994. Rare-earth element geochemistry of dolomites in the Middle Devonian Presqu'ile barrier, Western Canada Sedimentary Basin: Implications for water/rock ratios during dolomitization. *Sedimentology* 41, 787-804.
- Raaben, M.E., 2006. Dimensional parameters of columnar stromatolites as a result of stromatolite ecosystem evolution. *Stratigraphy and Geological Correlation* 14, 150-163.
- Raymond, J., 2005. The evolution of biological carbon and nitrogen cycling -- a genomic perspective. *Reviews in Mineralogy and Geochemistry* 59, 211-231.
- Reinhold, C., 1998. Multiple episodes of dolomitization and dolomite recrystallization during shallow burial in Upper Jurassic shelf carbonates: eastern Swabian Alb, southern Germany. *Sedimentary Geology* 121, 71-95.
- Riding, R.E. and Awramik, S.M., Editors, 2000. *Microbial Sediments*. Springer-Verlag, Berlin, 331pp.
- Ripperdan, R.L., 2001. Stratigraphic variation in marine carbonate carbon isotope ratios. *Reviews in Mineralogy and Geochemistry* 43, 637-662.
- Robert, F. and Chaussidon, M., 2006. A palaeotemperature curve for the Precambrian oceans based on silicon isotopes in cherts. *Nature* 443, 969-972.
- Roeske, C.A. and O'Leary, M., 1984. Carbon isotope effects on the enzyme-catalyzed carboxylation of ribulose biphosphate. *Biochemistry* 23, 6275-6284.
- Rogers, A. W., 1933. Calcareous sediments in the Witwatersrand Formation. *Transactions of the Geological Society of South Africa* 36, 65-68.

- Rollinson, H.R., 1993. Using geochemical data: Evaluation, Presentation, Interpretation. Longman, UK, 352pp.
- S.A.C.S.: South African Committee for Stratigraphy, 1980. Stratigraphy of South Africa. Part I (Comp. Kent, L.E.), Lithostratigraphy of the Republic of South Africa, South West Africa/Namibia, and the Republics of Bophuthatswana, Transkei and Venda. Handbook Geological Survey of South Africa 8, 690pp.
- Schidlowski, M., 1995. Isotope fractionations in the terrestrial carbon cycle: A brief overview. *Advances in Space Research* 15, 441-449.
- Schidlowski, M., 2001. Carbon isotopes as biogeochemical recorders of life over 3.8 Ga of Earth history: evolution of a concept. *Precambrian Research* 106, 117-134.
- Schidlowski, M., Hayes, J.M. and Kaplan, I.R., 1983. Isotopic inferences of ancient biochemistries: Carbon, sulphur, hydrogen and nitrogen. In: Schopf, J.W., Editor, *Earth's Earliest Biosphere: Its Origin and Evolution*, Princeton University Press, Princeton, N.J., 149-186.
- Schröder, S., Lacassie, J.P. and Beukes, N.J., 2006. Stratigraphic and geochemical framework of the Agouron drill cores, Transvaal Supergroup (Neoproterozoic-Paleoproterozoic, South Africa). *South African Journal of Geology* 109, 23-54.
- Schröder, S., Beukes, N.J. and Sumner, D.Y., 2009. Microbialite-sediment interactions on the slope of the Campbellrand carbonate platform (Neoproterozoic, South Africa). *Precambrian Research* 169, 68-79.
- Sharpe, J. W. N., 1949. The economic auriferous bankets of the Upper Witwatersrand Beds and their relationship to sedimentation features. *Transactions of the Geological Society of South Africa* 52, 256-300.
- Shaw, G.H., 2008. Earth's atmosphere—Hadean to early Proterozoic. *Chemie der Erde - Geochemistry* 68, 235–264.
- Shields, G. and Veizer, J., 2002. Precambrian marine carbonate isotope database: version 1.1. *Geochemistry, Geophysics, Geosystems* 3, 1-12.
- Shields, G., Carden, G.A.F., Veizer, J., Meidla, T., Rong, J.Y. and Li, R.Y., 2003. Sr, C, and O isotope geochemistry of Ordovician brachiopods: a major isotopic event around the Middle-Late Ordovician transition. *Geochimica et Cosmochimica Acta* 67, 2005-2025.
- Shinn, E.A., 1968. Practical significance of birdseyes structures in carbonate rocks. *Journal of Sedimentary Petrology* 38, 215-223.

- Simonson, B.M., Sumner, D.Y., Beukes, N.J., Johnson, S. and Gutzmer, J., 2009. Correlating multiple Neoproterozoic-Paleoproterozoic impact spherule layers between South Africa and Western Australia. *Precambrian Research* 169, 100-111.
- Sreenivas, B., Das Sharma, S., Kumar, B., Patil, D.J., Roy, A.B. and Srinivasan, R., 2001. Positive $\delta^{13}\text{C}$ excursion in carbonate and organic fractions from the Paleoproterozoic Aravalli Supergroup, Northwestern India. *Precambrian Research* 106, 277-290.
- Sumner, D.Y., 1997. Carbonate precipitation and oxygen stratification in late Archean seawater as deduced from facies and stratigraphy of the Gamohaam and Frisco formations, Transvaal Supergroup, South Africa. *American Journal of Science* 297, 455-487.
- Sumner, D.Y. and Beukes, N.J., 2006. Sequence stratigraphic development of the Neoproterozoic Transvaal carbonate platform, Kaapvaal Craton, South Africa. *South African Journal of Geology* 109, 11-22.
- Sumner, D.Y. and Grotzinger J.P., 1996. Were kinetics of Archean calcium carbonate precipitation related to oxygen concentration? *Geology* 24, 119-122.
- Sumner, D.Y. and Grotzinger J.P., 2004. Implications for Neoproterozoic ocean chemistry from primary carbonate mineralogy of the Campbellrand-Malmani Platform, South Africa. *Sedimentology* 51, 1273-1299.
- Sundquist, E.T., 1985. Geological perspectives on carbon dioxide and the carbon cycle. In Sundquist, E.T., Broecker, W.S., (Eds.). *The carbon cycle and atmospheric CO₂: Natural Variations Archean to Present*. American Geophysical Union Monography 32, 5-59.
- Thomazo, C., Pinti, D.L., Busigny, V., Ader, M., Hashizume, K. and Philippot, P., 2009. Biological activity and the Earth's surface evolution: Insights from carbon, sulfur, nitrogen and iron stable isotopes in the rock record. *Comptes Rendus Palevol* 8, 665-678.
- Trendall, A.F., Compston, W., Williams, I.S., Armstrong, R.A., Arndt, N.T., McNaughton, N.J., Nelson, D.R., Barley, M.E., Beukes, N.J., de Laeter, J.R., Retief, E.A. and Thorne, A.M., 1990. Precise zircon U-Pb chronological comparison of the volcano-sedimentary sequences of the Kaapvaal and Pilbara cratons between about 3.1 and 2.4 Ga. In: Glover, J.E. and Ho, S.E., Editors, 3rd International Archean Symposium, Perth, 1990, Extended Abstracts Volume, 81-84.

- Truswell, J.F. and Eriksson, K.A., 1972. The morphology of stromatolites from the Transvaal Dolomite north-west of Johannesburg, South Africa. *Transactions of the Geological Society of South Africa* 75, 99-110.
- Truswell, J.F. and Eriksson, K.A., 1973. Stromatolitic associations and their palaeo-environmental significance: A re-appraisal of a lower Proterozoic locality from the Northern Cape Province, South Africa. *Sedimentary Geology* 10, 1-23.
- Truswell, J.F. and Eriksson, K.A., 1975. A palaeoenvironmental interpretation of the early Proterozoic Malmani dolomite from Zwartkops, South Africa. *Precambrian Research* 2, 277-303.
- Tsikos, H., Beukes, N.J., Moore, J.M. and Harris, C., 2003. Deposition, diagenesis, and secondary enrichment of metals in the Paleoproterozoic Hotazel Iron-Formation, Kalahari Manganese Field, South Africa. *Economic Geology* 98, 1449-1462.
- Urey, H.C., 1947. The thermodynamic properties of isotopic substances. *Journal of the Chemical Society (London)* 1947, 562-581.
- Veizer, J. and Compston, W., 1976. $^{87}\text{Sr}/^{86}\text{Sr}$ in Precambrian carbonates as an index of crustal evolution. *Geochimica et Cosmochimica Acta* 40, 905-914.
- Veizer, J. and Hoefs, J., 1976. The nature of $\text{O}^{18}/\text{O}^{16}$ and $\text{C}^{13}/\text{C}^{12}$ secular trends in sedimentary carbonate rocks. In: *Geochimica et Cosmochimica Acta* 40, 1387-1395.
- Veizer, J., Ala, D., Azmy, K., Bruckschen, P., Buhl, D., Bruhn, F., Carden, G.A.F., Diener, A., Ebner, S., Godderis, Y., Jasper, T., Korte, C., Pawellek, F., Podlaha, O. and Strauss, H., 1999. $^{87}\text{Sr}/^{86}\text{Sr}$, $\delta^{13}\text{C}$, and $\delta^{18}\text{O}$ evolution of Phanerozoic seawater. *Chemical Geology* 161, 59-88.
- Veizer, J., Clayton, R.N. and Hinton, R.W., 1992a. Geochemistry of Precambrian carbonates: IV. Early paleoproterozoic (2.25 ± 0.25 Ga) seawater. *Geochimica et Cosmochimica Acta* 56, 875-885.
- Veizer, J., Clayton, R.N., Hinton, R.W., Von Brunn, V., Mason, T.R., Buck, S.G. and Hoefs, J., 1990. Geochemistry of Precambrian carbonates: 3-shelf seas and non-marine environments of the Archean. *Geochimica et Cosmochimica Acta* 54, 2717-2729.
- Veizer, J., Plumb, K.A., Clayton, R.N., Hinton, R.W. and Grotzinger, J.P., 1992b. Geochemistry of Precambrian carbonates: V. Late Paleoproterozoic seawater. *Geochimica et Cosmochimica Acta* 56, 2487-2501.

- Visser, J., and Grobler, N.J., 1972. The transition beds at the base of the Dolomite Series in the northern Cape Province. *Transactions of the Geological Society of South Africa* 75, 265-274.
- Voegelin, A.R., Nägler, T.F., Beukes, N.J. and Lacassie, J.P., 2010. Molybdenum isotopes in late Archean carbonate rocks: Implications for early Earth oxygenation. *Precambrian Research* 182, 70-82.
- Walker, J.C.G., 1979. The Early history of oxygen and ozone in the atmosphere. *Pure and Applied Geophysics* 117, 498-512.
- Walraven, F. and Martini, J., 1995. Zircon Pb evaporation age determinations of the Oak tree Formation, Chuniesport Group, Transvaal Sequence: implications for Transvaal-Griqualand West basin correlations. *South African Journal of Geology* 98, 58-67.
- Watanabe, Y., Naraoka, H., Wronkiewicz, D.J., Condie, K.C. and Ohmoto, H., 1997. Carbon, nitrogen, and sulphur geochemistry of Archean and Proterozoic shales from the Kaapvaal Craton, South Africa. *Geochimica et Cosmochimica Acta* 61, 3441-3459.
- Wille, M., Kramers, J.D., Nägler, T.F., Beukes, N.J., Schröder, S., Meisel, Th., Lacassie, J.P. and Voegelin, A.R., 2007. Evidence for a gradual rise of oxygen between 2.6 and 2.5 Ga from Mo isotopes and Re-PGE signatures in shales. *Geochimica et Cosmochimica Acta* 71, 2417-2435.
- Wilson-Moore, C., 1896. The economic importance of the Murchison Range. *Transactions of the Geological Society of South Africa* 1, 51-75.
- Winter, H. de la R., 1963. Algal structures in the sediments of the Ventersdorp System. *Transactions of the Geological Society of South Africa* 66, 115-121.
- Winter, B.L. and Knauth, L.P., 1992. Stable isotope geochemistry of early Proterozoic carbonate concretions in the Animikie Group of the Lake Superior region: evidence for anaerobic bacterial processes. *Precambrian Research* 54, 131-151.
- Wright, D.T. and Altermann, W., 2000. Microfacies development in Late Archaean stromatolites and oolites of the Ghaap Group of South Africa. *Geological Society, London, Special Publications* 178, 51-70.
- Xiao, S.H., Knoll, A.H., Kaufmann, A.J., Yin, L.M. and Zhang, Y., 1997. Neoproterozoic fossils in Mesoproterozoic rocks: Chemostratigraphic resolution of a biostratigraphic conundrum from the North China Platform. *Precambrian Research* 84, 197-220.

- Young, R.B., 1928. Pressure phenomena in the dolomitic limestones of the Campbell Rand Series in Griqualand West. Transactions of the Geological Society of South Africa 31, 157-165.
- Young, R.B., 1933. Conditions of deposition at the Dolomite basin. Transactions of the Geological Society of South Africa 36, 121-135.
- Young, R.B., 1934. A comparison of certain stromatolitic rocks in the Dolomite Series of South Africa with modern algal sediments in the Bahamas. Transactions of the Geological Society of South Africa 37, 153-162.

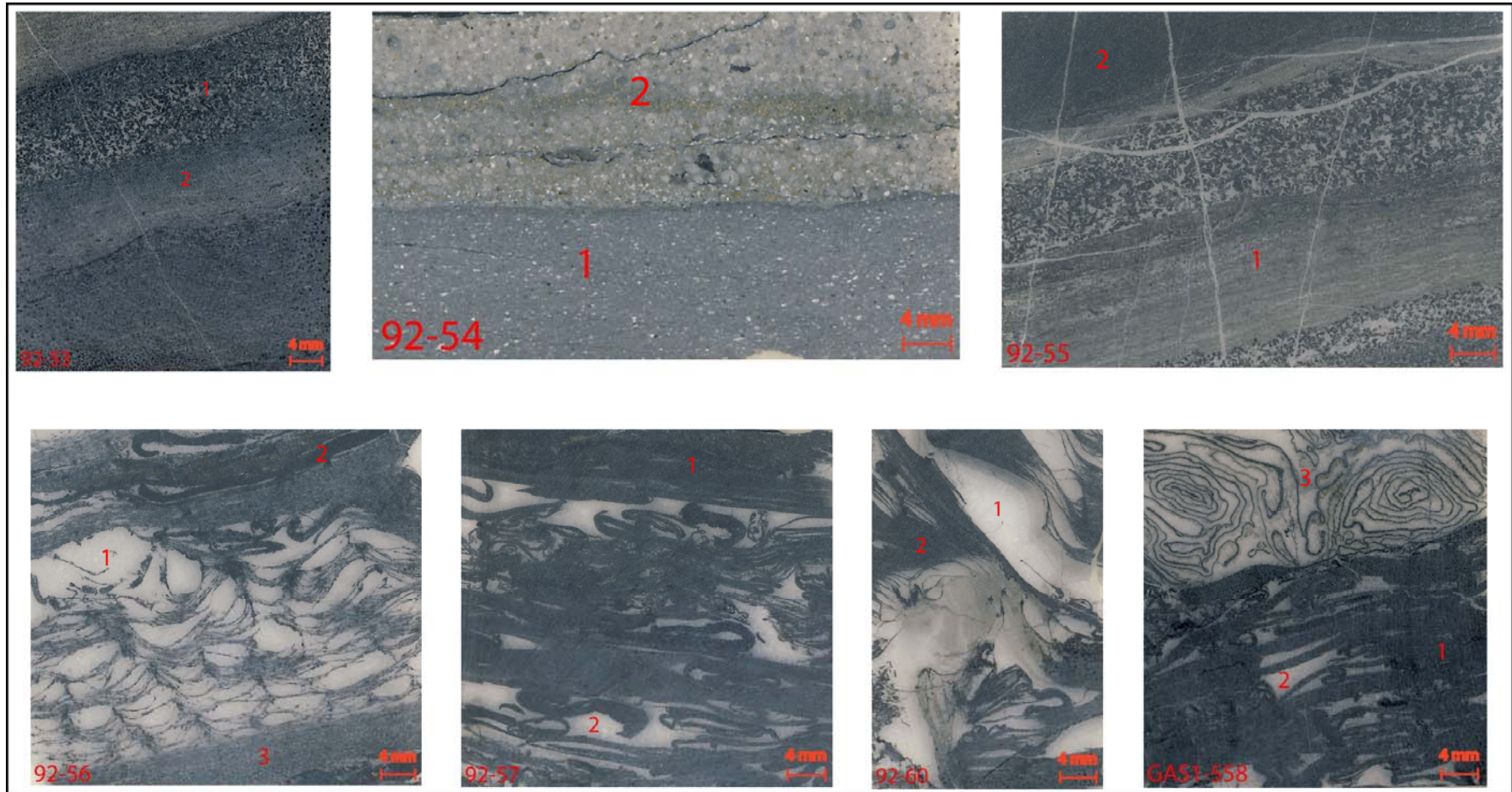
APPENDIX

Carbon and Oxygen Isotopes Measurements

Gamohaan Formation:

Depth in the Kathu Cores (m)	Sample No.	Lithology	$\delta^{13}\text{C}_{\text{carb}}$ (VPDB, ‰)	$\delta^{18}\text{O}$ (VPDB, ‰)	$\delta^{13}\text{C}_{\text{org}}$ (VPDB, ‰)	Remarks
558 (Hotazel core)	GAS1-558-1	Dark contorted finely microbial mats	-1,22	-9,45	-38,63	Sample has been drilled in three points. Organic-rich microbial mats (GAS1-558-1) and carbonate-rich cement between contorted laminates (GAS1-558-2) and coiled laminae (GAS1-558-3).
	GAS1-558-2	Cements between contorted microbial mats	-0,52	-9,02		
	GAS1-558-3	Cements between coiled laminae	-0,51	-5,02		
336	92-60-1	Calcite cements between microbial mats	+0,19	-9,73		Sample has been drilled in two points. Organic-rich microbial mats (92-60-2) and carbonate-rich cement between contorted laminates (92-60-1).
	92-60-2	Dark contorted finely microbial mats	-0,30	-11,74	-30,26	
341	92-57-1	Dark contorted finely microbial mats	-0,31	-11,76	-33,35	Sample has been drilled in two points. Organic-rich microbial mats (92-57-1) and carbonate-rich cement between contorted laminates (92-57-2).
	92-57-2	Cements between contorted microbial mats	-0,01	-10,76		
358	92-56-1	Calcite cements between microbial mats	-0,02	-9,46		Sample has been drilled in three points. Organic-rich microbial mats (92-56-2,3) and carbonate-rich cement between contorted laminates (92-56-1).
	92-56-2	Upper dark contorted microbial mats	-0,14	-12,17	Low organic carbon	
	92-56-3	Lower dark contorted microbial mats	-0,18	-12,60		
368	92-55-1	Dark bio-clastic dolarenite	-0,28	-8,86		Sample has been drilled in two points. Organic-rich bio-clasts (92-55-1) and laminates (92-55-2).
	92-55-2	Dark organic-rich laminites	-0,37	-9,36		
372	92-53-1	Dark bio-clastic dolarenite	-0,81	-12,48		Sample has been drilled in two points. Organic-rich bio-clasts (92-53-1) and laminates (92-53-2).
	92-53-2	Dark organic-rich laminites	-1,04	-12,87	-31,39	

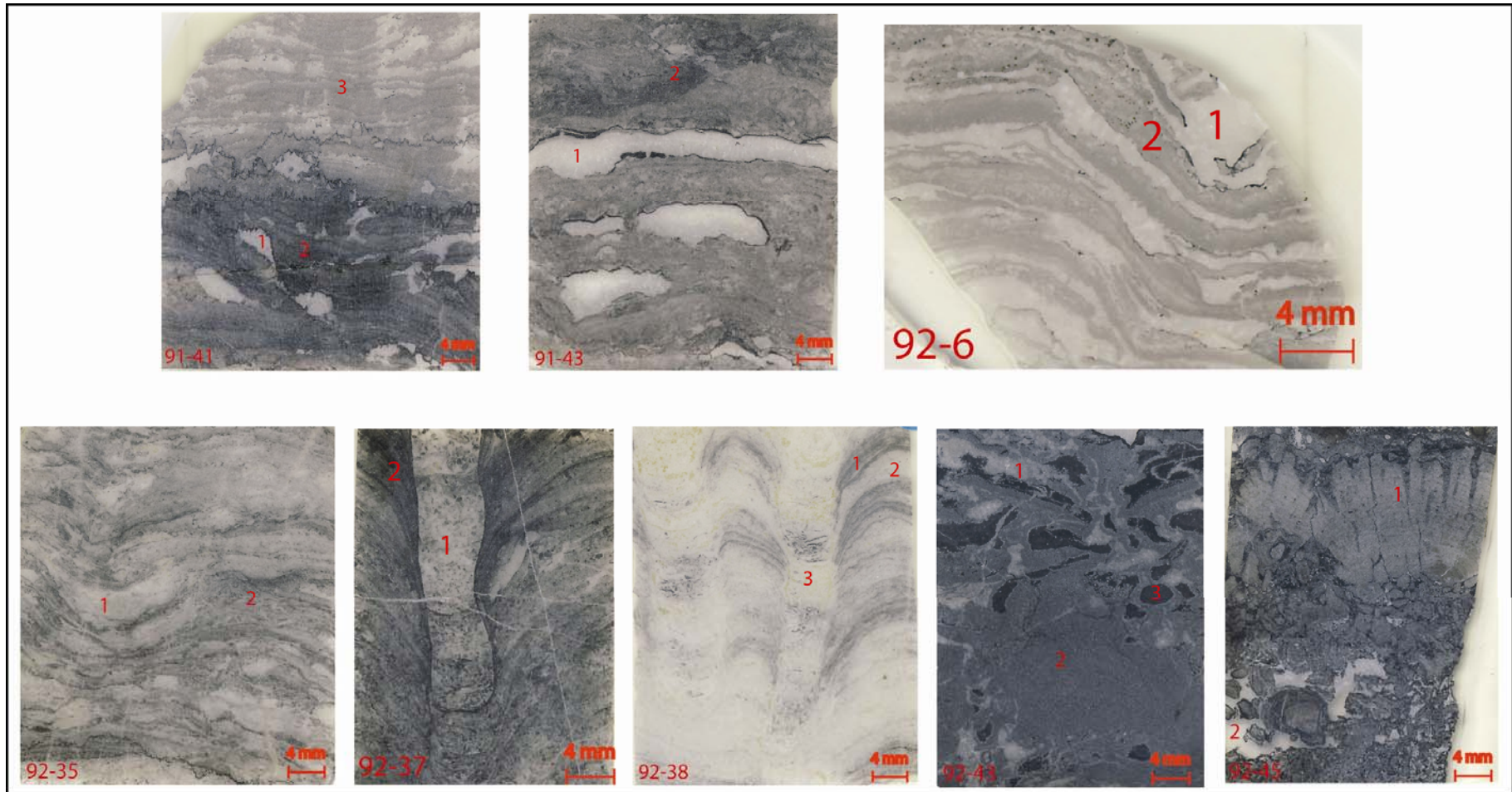
Gamohaan Formation drilling points on thin sections:



Kogelbeen Formation:

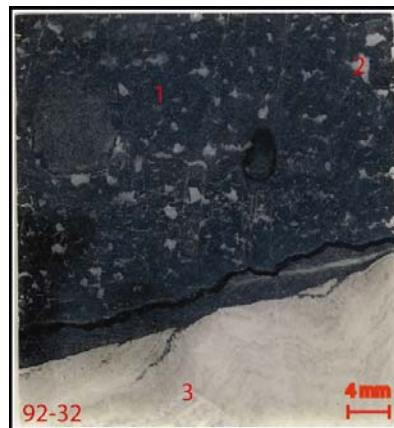
Depth in the Kathu Core (m) or locality	Sample No.	Lithology	$\delta^{13}\text{C}_{\text{carb}}$ (VPDB, ‰)	$\delta^{18}\text{O}$ (VPDB, ‰)	$\delta^{13}\text{C}_{\text{org}}$ (VPDB, ‰)	Remarks
Lime Acres	91-41-1	Calcite in the fenestral voids	-0,54	-9,92	Low organic carbon	Sample has been drilled in three points. Organic-rich microbial laminates (91-41-2), carbonate-rich laminates (91-41-3) and calcite in the voids (91-41-1).
	91-41-2	Dark organic-rich laminites	-0,20	-9,50		
	91-41-3	Carbonate-rich laminites	-0,40	-9,93		
Lime Acres	91-43-1	Dolomite in the voids	-0,27	-10,04	-26,07	Sample has been drilled in two points. Organic-rich carbonates (91-43-2) and dolomites in the voids (91-43-1).
	91-43-2	Dark organic-rich carbonates	+0,36	-7,95		
Finsch	92-6-1	Silicified laminated carbonates	+0,11	-10,11	Low organic carbon	Sample has been drilled in two silicified carbonate points.
	92-6-2	Silicified laminated carbonates	Low carbonate	Low carbonate		
540	92-45-1	Dark silicified columnar stromatolites	-0,68	-11,69	Low organic carbon	Sample has been drilled in two points. Organic-rich columnar laminates (92-45-1) and carbonate-rich cement between columns (92-45-2).
	92-45-2	Carbonate-rich cement between columns	-1,25	-11,74		
587	92-43-1	Cherts breccia with carbonate	+0,13	-13,22	Low organic carbon	Sample has been drilled in three carbonate-rich points.
	92-43-2	Cherts breccia with carbonate	Low carbonate	Low carbonate		
	92-43-3	Cherts breccia with carbonate	Low carbonate	Low carbonate		
822	92-38-1	Dark organic-rich columnar stromatolites	-0,29	-9,80	Low organic carbon	Sample has been drilled in three points. Organic-rich columnar laminates (92-38-1) and carbonate-rich cement between organic-rich laminates (92-38-2) and columns (92-38-3).
	92-38-2	Carbonate-rich columnar stromatolites	-0,20	-9,84		
	92-38-3	Carbonate-rich sediment between columns	-0,29	-9,97		
847	92-37-1	Carbonate-rich sediments between columns	-0,97	-12,29	-24,33	Sample has been drilled in two points. Organic-rich columnar laminates (92-37-2) and carbonates between columns (92-37-1).
	92-37-2	Dark organic-rich columnar stromatolites	-0,24	-11,52		
855	92-35-1	Carbonate-rich laminites	-0,97	-9,33	-22,93	Sample has been drilled in two points. Organic-rich laminates (92-35-2) and carbonate-rich laminates (92-35-1).
	92-35-2	Dark organic-rich laminites	-0,61	-7,73		

Kogelbeen Formation drilling points on thin sections:



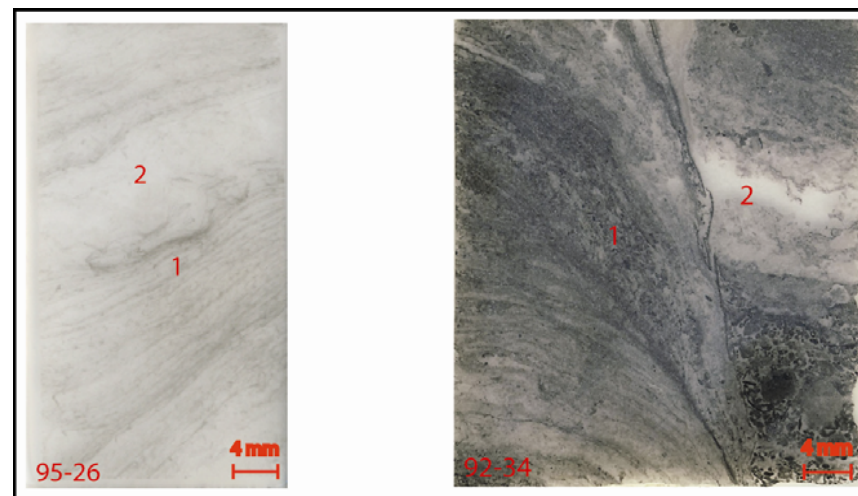
Klippan Formation:

Depth in the Kathu Core (m)	Sample No.	Lithology	$\delta^{13}\text{C}_{\text{carb}}$ (VPDB, ‰)	$\delta^{18}\text{O}$ (VPDB, ‰)	$\delta^{13}\text{C}_{\text{org}}$ (VPDB, ‰)	Remarks
1232	92-32-1	Dark organic-rich carbonates	-2,43	-11,55	-21,63	Sample has been drilled in three points. Organic-rich laminates (92-32-1), calcite in the voids (92-32-2, two measures) and carbonate-rich laminates (92-32-3).
	92-32-2	Calcite filled in the birds eyes	-1.12	-7.92		
	92-32-2	Calcite filled in the birds eyes	-1,03	-7,96		
	92-32-3	Carbonate-rich laminites	-0,32	-8,31		

Klippan Formation drilling points on thin sections:

Papkuil Formation:

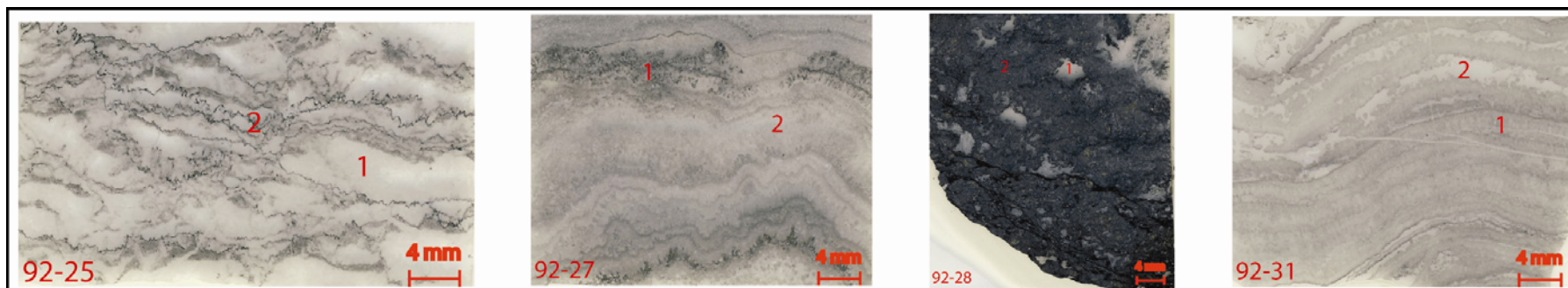
Depth in the Kathu Core (m) or locality	Sample No.	Lithology	$\delta^{13}\text{C}_{\text{carb}}$ (VPDB, ‰)	$\delta^{18}\text{O}$ (VPDB, ‰)	$\delta^{13}\text{C}_{\text{org}}$ (VPDB, ‰)	Remarks
1357	92-34-1	Dark organic-rich laminates	-0,48	-8,11	-27,09	Sample has been drilled in two points. Organic-rich laminates (92-34-1), calcite between the columns (92-34-2).
	92-34-2	Sediments between columns	-0,51	-7,98		
YSKOR GH6-7 102m	95-26-1	Dark organic-rich laminites	-0,18	-7,75	Low organic carbon	Sample has been drilled in two points. Organic-rich laminates (95-26-1), calcite between laminates (95-26-2).
	95-26-2	Calcite between laminites	+0,40	-6,64		

Papkuil Formation drilling points on thin sections:

Klipfontein Heuwel Formation:

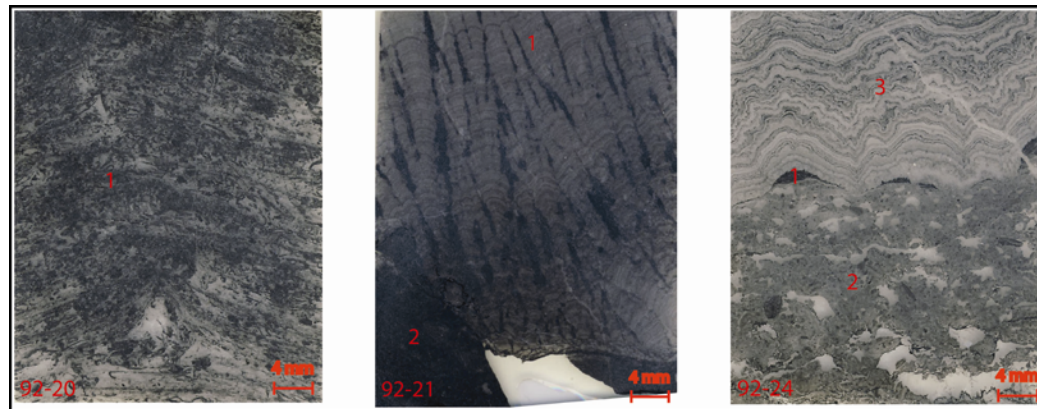
Depth in the Kathu Core (m)	Sample No.	Lithology	$\delta^{13}\text{C}_{\text{carb}}$ (VPDB, ‰)	$\delta^{18}\text{O}$ (VPDB, ‰)	$\delta^{13}\text{C}_{\text{org}}$ (VPDB, ‰)	Remarks
1502	92-31-1	Chert seams with silicified carbonates	Low carbonate	Low carbonate		Sample has been drilled in two points. Little carbonate in the sample, values are probably imprecise and not useable.
	92-31-2	Chert seams with silicified carbonates	-9.95	-10.68		
1553	92-28-1	Calcite filled in the voids	+0,07	-6,25		Sample has been drilled in two points. Calcite filled in the voids (92-28-1), organic-rich microbial mats (92-28-2).
	92-28-2	Dark organic-rich microbial mats	-0,15	-7,08	-35,35	
1553	92-27-1	Dark organic-rich microbial laminates	-0,64	-6,79	Low organic carbon	Sample has been drilled in two points. Organic-rich laminates (92-27-1) and dolomites between the laminates (92-27-2).
	92-27-2	Dolomites between microbial laminites	-0,56	-10,09		
1611	92-25-1	Dolomites between wavy laminites	-0,45	-8,34	-29,96	Sample has been drilled in two points. Dolomites between the columns (92-25-1), organic-rich laminates (92-25-2).
	92-25-2	Dark organic-rich wavy laminates	-0,63	-7,57		

Klipfontein Heuwel Formation drilling points on thin sections:



Fairfield Formation:

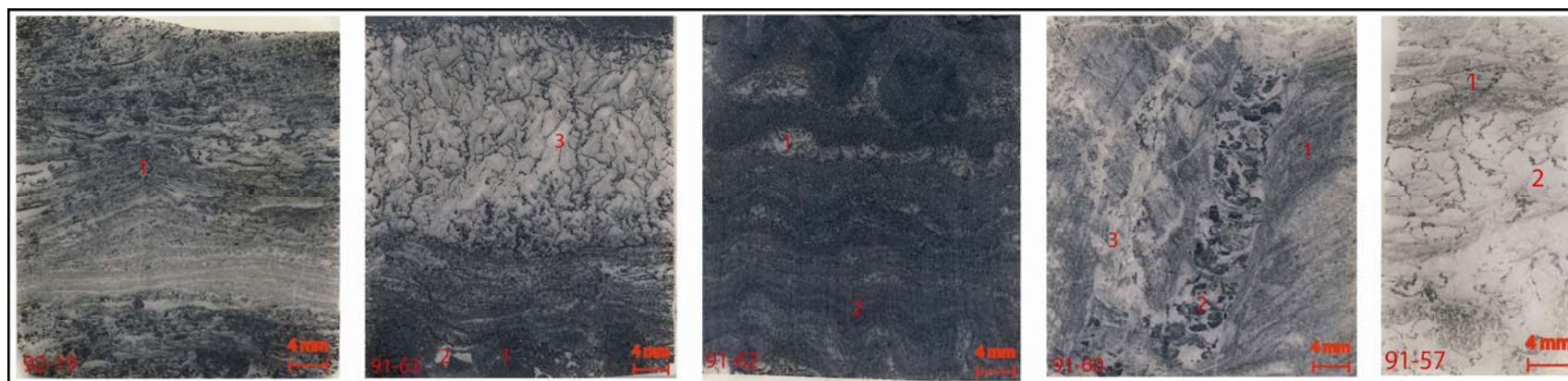
Depth in the Kathu Core (m)	Sample No.	Lithology	$\delta^{13}\text{C}_{\text{carb}}$ (VPDB, ‰)	$\delta^{18}\text{O}$ (VPDB, ‰)	$\delta^{13}\text{C}_{\text{org}}$ (VPDB, ‰)	Remarks
1644	92-24-1	Dark organic-rich carbonates	-0,55	-6,30	Low organic carbon	Sample has been drilled in three points. Organic-rich microbial remains (92-24-1), carbonate muds (92-34-2) and wavy silicified laminates (92-34-3).
	92-24-2	Carbonate muds	-0,67	-6,35		
	92-24-3	Wavy silicified laminites	Low carbonate	Low carbonate		
1693	92-21-1	Columnar stromatolites	-0,66	-6,53	-35,79	Sample has been drilled in two points. Organic-rich carbonates (92-21-2) and columnar stromatolites (92-21-1).
	92-21-2	Dark organic-rich carbonates	-0,62	-6,76		
1769	92-20	Dark microbial clastic dolarenite	-0,69	-8,02	-29,00	Sample has been drilled in one point of organic-rich carbonates.

Fairfield Formation drilling points on thin sections:

Reivilo Formation:

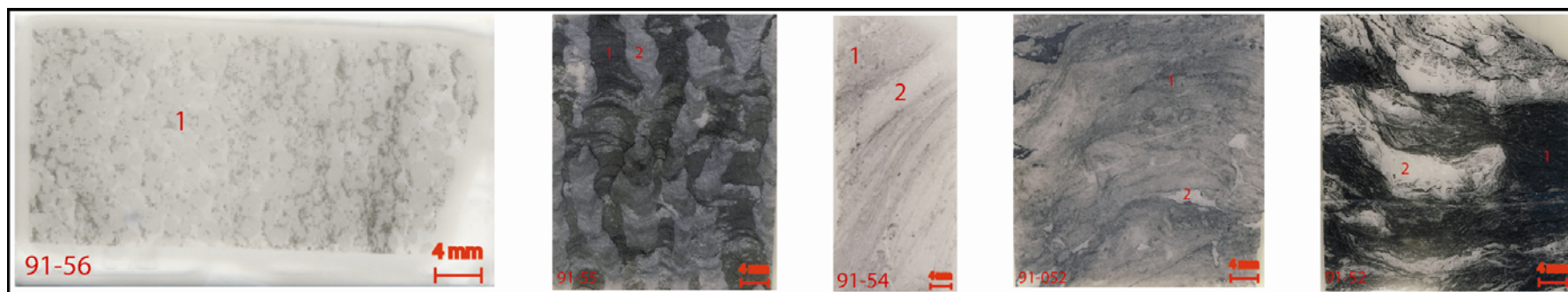
Depth in the Kathu Core (m)	Sample No.	Lithology	$\delta^{13}\text{C}_{\text{carb}}$ (VPDB, ‰)	$\delta^{18}\text{O}$ (VPDB, ‰)	$\delta^{13}\text{C}_{\text{org}}$ (VPDB, ‰)	Remarks
1803	92-19	Dark organic-rich clastic dolarenite	-0,67	-7,91	-28,23	Sample has been drilled in one point of organic-rich carbonates.
2090	91-63-1	Dark organic-rich laminates	-0,88	-9,94	-29,54	Sample has been drilled in three points. Organic-rich carbonates (91-63-1), calcite filled in the voids (91-63-2) and calcite in the cusped stromatolites (91-63-3).
	91-63-2	Calcite filled in the voids	-0,74	-7,57		
	91-63-3	Calcite in the cusped stromatolites	-0,92	-8,09		
2130	91-62-1	Dolomite between the laminates	-0,90	-8,21		Sample has been drilled in two points. Organic-rich laminates (91-62-2) and dolomites in the wavy laminates (91-62-1).
	91-62-2	Dark organic-rich laminites	-0,84	-8,54	-29,01	
	91-60-1	Dark organic-rich laminites	-0,70	-7,39	-28,82	
2280	91-60-2	Bio-clasts between the columns	-0,65	-7,94		Sample has been drilled in three points. Organic-rich laminates (91-60-1), bio-clasts between the columns (91-60-2) and dolomites in the carbonate-rich laminates (91-60-3).
	91-60-3	Dolomites between the dark laminates	-0,88	-15,94		
	91-57-1	Dark organic-rich laminites	-0,70	-8,45	-29,60	
2547	91-57-2	Calcite in the cusped stromatolites	-0,83	-9,09		Sample has been drilled in two points. Organic-rich laminates (91-57-1) and calcite in the cusped stromatolites (91-57-2).

Reivilo Formation drilling points on thin sections:



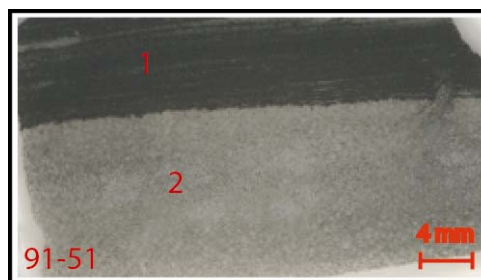
Monteville Formation:

Depth in the Kathu Core (m)	Sample No.	Lithology	$\delta^{13}\text{C}_{\text{carb}}$ (VPDB, ‰)	$\delta^{18}\text{O}$ (VPDB, ‰)	$\delta^{13}\text{C}_{\text{org}}$ (VPDB, ‰)	Remarks
2638	91-56	Pelletal carbonate	-1,52	-13,70		Sample has been drilled in one point of pelletal carbonate.
2685	91-55-1	Dark columnar stromatolites	-0,54	-9,47	-27,76	Sample has been drilled in two points. Organic-rich laminates (91-55-1) and dolomites between the columns (91-55-2).
	91-55-2	Dolomites between columns	-1,68	-11,38		
2796	91-54-1	Dark columnar stromatolites	-0,30	-9,24	-29,13	Sample has been drilled in two points. Organic-rich laminates (91-54-1) and carbonate-rich laminates (91-54-2).
	91-54-2	Carbonate-rich laminates	-0,78	-11,44		
2892	91-052-1	Dark organic-rich carbonates	-0,37	-9,71	Low organic carbon	Sample has been drilled in two points. Organic-rich carbonates (91-052-1) and calcite in the voids (91-052-2).
	91-052-2	Calcite filled in the voids	-0,42	-10,27		
	91-52-1	Recrystallized laminates	Low carbonates	Low carbonate		
2890	91-52-2	Recrystallized carbonates	-14,67	-14,14		Sample has been drilled in two points. Strongly recrystallized laminates (91-52-1) and recrystallized carbonate (91-52-2, measured for three times).
	91-52-2	Recrystallized carbonates	-14,87	-14,32		
	91-52-2	Recrystallized carbonates	-14,81	-14,29		

Monteville Formation drilling points on thin sections:

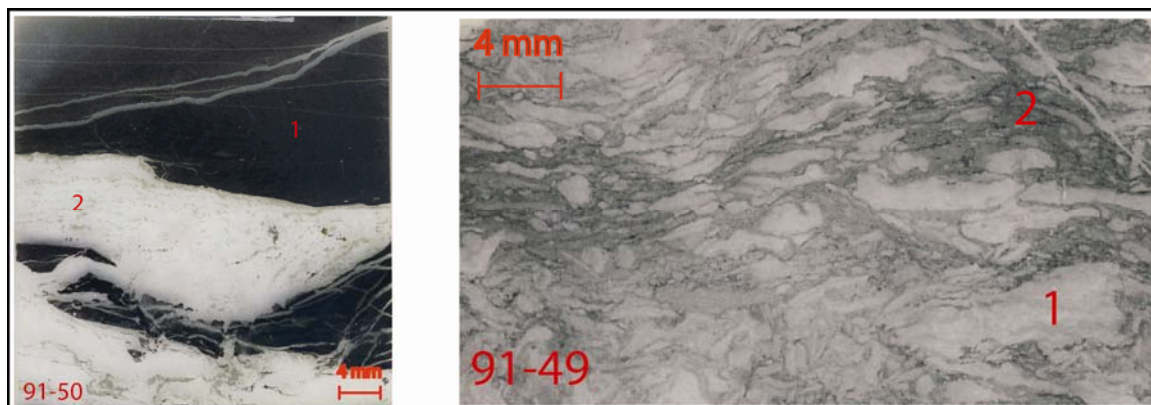
Lokammona Formation:

Depth in the Kathu Core (m)	Sample No.	Lithology	$\delta^{13}\text{C}_{\text{carb}}$ (VPDB, ‰)	$\delta^{18}\text{O}$ (VPDB, ‰)	$\delta^{13}\text{C}_{\text{org}}$ (VPDB, ‰)	Remarks
3199	91-51-1	Dark organic-rich laminated micrites	-5,17	-11,85	Low organic carbon	Sample has been drilled in two points. Organic-rich laminates (91-51-1) and carbonate micrites (91-51-2).
3199	91-51-2	Carbonate micrites	-8,03	-11,45		

Lokammona Formation drilling points on thin sections:

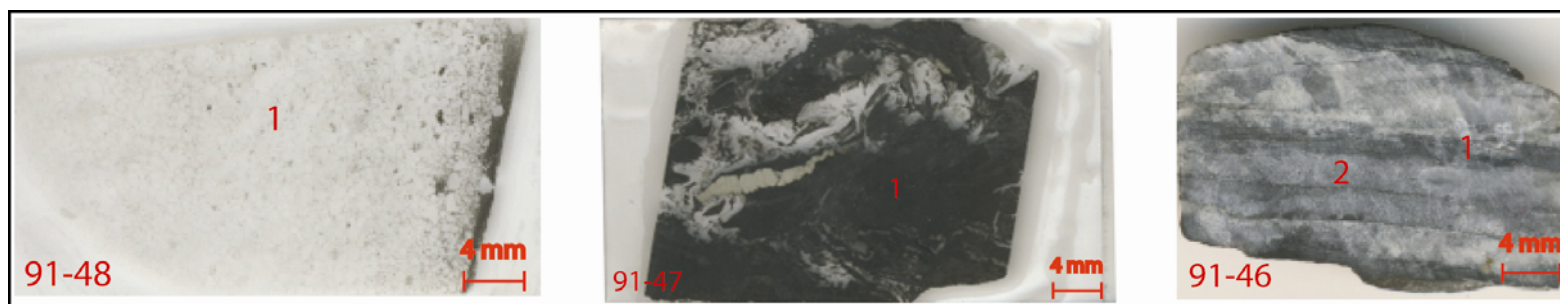
Boomplaas Formation:

Depth in the Kathu Core (m)	Sample No.	Lithology	$\delta^{13}\text{C}_{\text{carb}}$ (VPDB, ‰)	$\delta^{18}\text{O}$ (VPDB, ‰)	$\delta^{13}\text{C}_{\text{org}}$ (VPDB, ‰)	Remarks
3242	91-50-1	Dark carbonate micrites	-4,81	-13,19	Low organic carbon	Sample has been drilled in two points. Dark carbonate micrites (91-50-1) and gray carbonate micrites (91-50-2).
	91-50-2	Gray carbonate micrites	-5,24	-12,42		
3327	91-49-1	Gray irregular laminated carbonate	-4,45	-13,10	Low organic carbon	Sample has been drilled in two points. Gray irregular laminated carbonate (91-49-1) and dark irregular laminated carbonate (91-49-2).
	91-49-2	Dark irregular laminated carbonate	-4,22	-13,03		

Boomplaas Formation drilling points on thin sections:

Vryburg Formation:

Depth in the Kathu Core (m)	Sample No.	Lithology	$\delta^{13}\text{C}_{\text{carb}}$ (VPDB, ‰)	$\delta^{18}\text{O}$ (VPDB, ‰)	$\delta^{13}\text{C}_{\text{org}}$ (VPDB, ‰)	Remarks
3586	91-48	Graded oolite	-7,41	-13,46	No organic carbon	Sample has been drilled in one point of oolite. Isotopic measurement has been carried out for two times.
	91-48	Graded oolite	-7,27	-13,35		
3647	91-47	Dark silicified carbonates	Low carbonate	Low carbonate		Sample has been drilled in one point of dark silicified carbonate. Isotopic measurement has been carried out for two times, but no results.
3656	91-46-1	Dark silicified carbonate micrites	Low carbonate	Low carbonate	No organic carbon	Sample has been drilled in two points. Dark silicified carbonate micrites (91-46-1) and gray silicified carbonate micrites (91-46-2).
	91-46-2	Gray silicified carbonate micrites	-34,01	0,24		

Vryburg Formation drilling points on thin sections:

CURRICULUM VITAE

Baiquan Xu

Born: 27 September 1981

Jiaozuo, Henan, China

Education

- 2007-2011 Department für Geo- und Umweltwissenschaften, Ludwig-Maximilians-Universität München: Ph.D. 7/2011, Geology.
- 2004-2007 Department for Geological Science and Engineering, Shandong University of Science and Technology: M.S. 7/2007, Geology
- 2000-2004 Department for Geological Science and Engineering, Shandong University of Science and Technology: B.S. 7/2004, Geology

Awards

- 2007 Awarded the first price in China University Contest in the 4th Supermap GIS Application
- 2007-2011 China Scholarship Council Scholarship

Research Experience

- 2007-2011 Analysis of the Ghaap Group carbonate rocks in South Africa, through microfacies observation and stable isotopic analysis. (with Prof. W. Altermann)
- 2004-2007 Analysis of the coexistence of a variety of energy resources into the reservoir (ore) mechanism and the distribution of enrichment. (with Prof. Fengjie Yang)
- 2000-2004 Analysis of the fault zone in coal mine through transient electromagnetic method. (with Lectors Peihe Zhai)

Publications

1. Baiquan Xu, 2007. The ring structure characteristics of South Ordos Basin and its deep control factors. Shandong University of Science and Technology, In Chinese. CNKI: CDMD: 2.2008.013363
2. Yang Fengjie, Xu Baiquan, Li Hongkui and Yang Zhenyi, 2008. Ring structure characteristics of South Ordos basin and its control factors in the deep, SPIE Proceedings 7110-44 2008.9 Cardiff UK
3. Baiquan Xu, Christoph Mayr and Wladyslaw Altermann, 2010. Carbon and oxygen isotope variations in late Archean carbonate rocks in South Africa. Geophysical Research Abstracts Vol.12, EGU2010-3651-5, 2010.
4. Baiquan Xu, Christoph Mayr and Wladyslaw Altermann, 2011. C- and O-isotopy of late Archean carbonate rocks, Kathu Borehole, SA. 23rd Colloquium of African Geology, 2011.